MEDRC Series of R & D Reports
MEDRC Project: 17-JD-002

Coupling Magnetite Nanoparticles with Sorbent Material(S) for Olive Mill Wastewater Remediation

M.Sc. Thesis By

Jehad Walid Abdelnabi

Supervisors

Prof. Muna Abu-Dalo

Applied Chemistry Department
Jordan University of Science and Technology

Prof. Abeer Al-Bawab

Chemistry Department
University of Jordan

A Thesis Submitted in Partial Fulfillment of the Requirements for the **Degree of Master** in Applied Chemistry

MEDRC Water Research
Muscat
Sultanate of Oman

28th July, 201

COUPLING MAGNETITE NANOPARTICLES WITH SORBENT MATERIAL(S) FOR OLIVE MILL WASTEWATER REMEDIATION

COUPLING MAGNETITE NANOPARTICLES WITH SORBENT MATERIAL(S) FOR OLIVE MILL WASTEWATER REMEDIATION

By

Jehad Walid Abdelnabi

Advisor

Prof. Muna Abu-Dalo

Co-Advisor

Prof. Abeer Al-Bawab

Thesis submitted in partial fulfillment of the requirements for the degree of
M.Sc. in Chemistry

At

The Faculty of Graduate Studies

Jordan University of Science and Technology

July, 2019

COUPLING MAGNETITE NANOPARTICLES WITH SORBENT MATERIAL(S) FOR OLIVE MILL WASTEWATER REMEDIATION

By

Jehad Walid Abdelnabi

Signature of Author	…….
Committee Member	Signature and Date
Prof. Muna Ahmad Abu-Dalo (Chairman)	…….
Prof. Abeer Fayez Al-Bawab (Co-Advisor)	…….
Prof. Nathir Ahmad Al-Rawashdeh (Member)	…….
Dr. Fadwa Mohammad Odeh (External Examiner)	…….

July, 2019

تفويض

نحن الموقعين أدناه، نتعهد بمنح جامعة العلوم والتكنولوجيا الأردنية حرية التصـرف في نشـر محتوى الرســالة الجامعية، بحيث تعود حقوق الملكية الفكرية لرســالة الماجســتير الى الجامعة وفق القوانين والأنظمة والتعليمات المتعلقة بالملكية الفكرية وبراءة الاختراع.

المشرف الرئيس	المشرف المشارك	الطالب
أ. د. منى احمد ابو دلو	**أ. د. عبير فايز البواب**	**جهاد وليد عبد النبي**
التوقيع والتاريخ	التوقيع والتاريخ	الرقم الجامعي والتوقيع
.....	.....	**116210**
.....	.....	.....

DEDICATION

This thesis is dedicated

To the most ambitious person I know: me

To my great father **Mr. Walid Abdelnabi** for being my first teacher

To my potent mother **Mrs. Asma'a Ishkokani**, for being my greatest inspiration

To my son **Zead,** the best gift from Allah, who will forever be a source of pride

To my husband **Tareq** who always supported me emotionally

To my brothers **Nasser**, **Abdulrahman**, **Yahiya** and **yamen**, and my sisters **Saja** and **Mariam** each of whom has a distinctive place in my heart

ACKNOWLEDGMENT

Above all, I pay my reverence to the merciful Lord for all graces and gifts He bestowed upon me. I am absolutely sure that without His volition and guidance this thesis would have been just a dream.

I owe my heartfelt gratitude to my marvelous supervisor, **Prof. Muna Abu Dalo** who afforded me the room to work in my own way, while guiding me in the right direction whenever she thought I needed it. Her comprehensive and creative advices, insightful comments, rational suggestions and challenging questions added extremely to my experience. Throughout the trails and struggles of this thesis her warm embraces with immense love have been a constant source of optimism and enthusiasm. One simply could not wish for a better supervisor.

I extend my thanks to my role model, **Prof. Abeer Al-Bawab** who encouraged me continuously and inspired me to accomplish this research by charming me with novel ideas and demanding a skillful work in all my endeavors. I am lucky to have you as a co-supervisor.

I revere the great attention, patience and moral support accompanied with profound love and appreciation by my parents whom guidance, unwavering encouragement and prayers gave me the power to complete this study. Thank you for permanently wishing the best for your daughter. What I have accomplished, I have accomplished to make you proud.

I am immensely indebted to my affectionate sisters and brothers for cooperation and creation of right studying atmosphere throughout my years of study and research.

I feel a deep senses of gratitude to my beloved and supportive husband for extending his persistent support, unfailing help, continuous encouragement and understanding.

Special thanks to **Dr. Fadwa Odeh** and **Prof. Nathir Al-Rawashdeh** for being members of my examination committee and for their recommendations and healthy criticism.

I would like to acknowledge **Prof. Borhan Albiss** for his kind guidance and suggestion to make this thesis better.

It is a great pleasure to acknowledge all the staff members of Hamdi Mango Center particularly **Dr. Ayat Bozeya**, **Eng. Saida Abu Malloh** and **Aya Khalaf** for responding honestly and mutually to all questions arises in this work, sharing their knowledge and stimulating discussion which made my laboratory work more delightful.

A message of thanks is also conveyed to the chemists **Ismaeel Mheidate** and **Heba Kanaan** for introducing me to the topic and assisting me incessantly during this study.

Gratitude goes to the **Middle East Desalination Research Centre** (MEDRC) and the **Scientific Research and Support Fund** for their financial support that pushed me to improve my performance in my courses and thesis.

Finally, thanks to all of my friends, particularly **Bayan Al-Tbakhi**, **Nour Al-nairat** and **Doa'a Abu Dalo**.

Jehad Abdelnabi

TABLE OF CONTENTS

Title **Page**

LIST OF FIGURES

LIST OF TABLES

LIST OF APPENDICES

LIST OF ABBREVIATIONS

Abbreviation	Description
BET	Brunauer, Emmett and Teller
COD	Chemical oxygen demand
DLS	Dynamic light scattering
FC Reagent	Folin ciocalteau reagent
GAC	Granular activated carbon
GAE	Gallic acid equivalents
OMW	Olive mill wastewater
pH	Negative logarithm of the effective hydrogen ion concentration
SEM	Scanning electron microscope
TEM	Transmission electron microscope
TPC	Total phenolic content
TSS	Total suspended solids
VT	Volcanic tuff
VTA24C	Volcanic tuff sample that was activated by successive acid impregnation for 24h and calcination
VTA2C	Volcanic tuff sample that was activated by successive acid impregnation for 2h and calcination
VTA48C	Volcanic tuff sample that was activated by successive acid impregnation for 48h and calcination
VTA72C	Volcanic tuff sample that was activated by successive acid impregnation for 72h and calcination
VTB2C	Volcanic tuff sample that was activated by successive base impregnation for 2h and calcination
VTC	Volcanic tuff sample that was activated by calcination
XRD	X-ray diffraction

ABSTRACT

COUPLING MAGNETITE NANOPARTICLES WITH SORBENT MATERIAL(S) FOR OLIVE MILL WASTEWATER REMEDIATION

By

Jehad Walid Abdelnabi

The generated olive mill wastewater (OMW) from olive milling industry is considered as a source of critical environmental problem in the Mediterranean region, due to its high load of harmful organic compounds such as phenol and its derivatives. They can contaminate ground water resources upon improper disposal methods and harm the human and animal's health upon direct exposure. The management of OMW represents a critical environmental problem, where huge quantities are generated annually in very short period (October to December) making its storage impossible in small mills. A reliable OMW remediation approach that congregates public needs in a cost effective manner is an essential need particularly for Jordan, in which it challenges a crucial problem related to the water resources and environmental quality. In this study, two types of sorbent materials were used for decontamination of OMW, these are volcanic tuff (VT) and granular activated carbon (GAC). VT was activated through calcination alone, acid impregnation followed by calcination and base impregnation followed by calcination. VT samples were characterized by scanning electron microscopy (SEM), X-ray diffraction pattern (XRD), X-ray fluorescence (XRF) and point of zero charge (pH_{PZC}). The surface area was obtained by Brunauer-Emmett-Teller (BET) isotherm. GAC was subjected to chemical oxidation and reduction. Then untreated, oxidized and reduced samples were characterized for pH_{PZC}. Magnetite nanoparticles were prepared by coprecipitation method then characterized by transmission electron microscopy (TEM), XRD, $pH_{PZC,}$ magnetization test, dynamic light scattering (DLS) and zeta potential. Each treated and untreated sorbent material i.e. VT or GAC was coupled with magnetite nanoparticles through three different scenarios (mixing, layering and nanocomposites) and tested their chemical oxygen demand (COD) and total phenolic content (TPC) removal efficiencies through batch and column approaches. OMW was pretreated with coagulation/flocculation/sedimentation processes before it was subjected to sorbent media, to remove the suspended solids. The results obtained from this study revealed that the VT activated by acid impregnation for 48 hr followed by calcination and coupled with 0.5% by weight of magnetite nanoparticles was the best adsorbent for COD with maximum removal of 76% after 24 hr for pretreated OMW at pH 8. On the other hand, VT activated by calcination alone and coupled with 0.5% by weight of magnetite nanoparticles was the best adsorbent for TPC with 73% removal after 48 hr for pretreated OMW at pH 10. On the other hand, the removal efficiency of reduced GAC attained highest COD and TPC removal efficiencies of 88% and 82%, respectively after 24 hr for pretreated OMW at pH 5.3.

Chapter One: Introduction

1.1 Olive Mill Wastewater

Olives are considered one of the most cultivated crops in the world (FAOSTAT database, January 18, 2019). These evergreen blessed trees are the major contributor for economics, heritage and environment throughout the Mediterranean region, which remains the highest provider of the total surface area for olive trees production (Blatchly et al., 2017). More than 850 million productive olive trees are planted worldwide on a surface area of about 1.1×10^{8} Dunums in 2017 (FAOSTAT database, January 18, 2019). It is estimated that each olive tree produces between 15 - 45 kg olives per year (Paraskeva et al., 2006 and Souilem et al., 2017). The annual production of black and green table olives worldwide is 20.8 million tons (FAOSTAT database, January 18, 2019). However, olive milling process produce in addition to olive oil a liquid waste known as olive mill wastewater (OMW) (Niaounakis et al., 2006).

OMW is generated during olive oil production, specifically from the water used for olives washing, vegetation water and the water added to assist centrifugation. OMW is characterized by its dark color as shown in Figure 1, undesirable smell, acidic pH value between 3 and 6, high capacity of suspended solids, organic compounds (polyphenols), and high percent of inorganic compounds (e.g. potassium salts and phosphates). So it is considered as an environmental problem as its pollution load is very high (Niaounakis et al., 2006; Gharaibeh et al., 2008; Ruiz-Méndez et al., 2012; Aly et al., 2014, and Speltini et al., 2016).

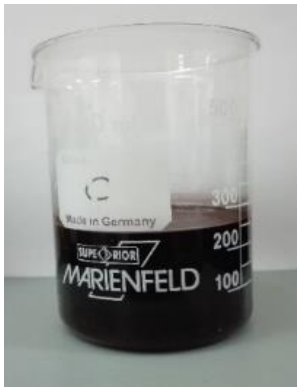

Figure 1: Jordanian olive mill wastewater that was used in this study

1.2 Olive Oil Production

1.2.1 History of Olive Oil Production

The production of olive oil in ancient times, as today, comprised three essential steps: crushing, pressing and oil /water separation processes (Niaounakis et al., 2006).

1.2.1.1 Crushing

In antiquity, olives have been crushed by large pestles or just processed under the foot in the beginnings. A great development in the production technologies has occurred upon invention of trapetum round crushing basin that presented in Figure 2. Trapetum was designated based on rotational motion that allows the use of animal power (Drachmann, 1932 and Niaounakis et al., 2006).

1.2.1.2 Pressing

Simple combination comprising a sloping crushing base coupled with a lower collecting tank was the first device used to join olives crushing and pressing processes (Hadjisavvas et al., 1992). After that, in the Iron Age, a huge advancement in olive pressing techniques was attributed to the invention of lever and weights press shown in Figure 2. The ability of lever and weights press to perform its work lies in the presence of an elongated woody lever that is immovable in one end while the other might be dragged down to apply compression on a sack of olive paste (Hadjisavvas et al., 1992). After a sequence of

developments in the pressing process, the screw presented in Figure 2 was introduced to lever press, which consequently increased its strength (Hadjisavvas et al., 1992).

1.2.1.3 Oil/Water Separation

Water was obligatory in oil production system. Initially, water was used to wash olives before crushing. After the first press, boiling water was added on the sack of olive paste, to extract any residual oil stuck on them or on the press surface. Moreover, the press surface was washed with boiling water before and after each pressing process to remove timeworn stagnant oil that may affect the taste of new oil to be depraved (Niaounakis et al., 2006).

Oil/water separation had been accomplished via different procedures that based on gravity force. The humblest procedure was the scanning of the oily floated layer manually. While withdrawing water over a controllable dump after settling period assumed to be more challenging procedure (Hadjisavvas et al., 1992). Figure 2 shows a graphical representation of the sequence steps of oil production in antiquity.

Until the middle of the 18^{th} century, the processing of olives was founded on such simple technologies used in ancient times. The contemporary golden period of olive oil initiated in 1750s. Many factors led to increase the price of olive oil due to its demand increase especially in food and industry, which involved lubrication, illumination and synthesis of soap. The quantity and the quality was also a main concern of olive oil manufacturers and traders (Niaounakis et al., 2006).

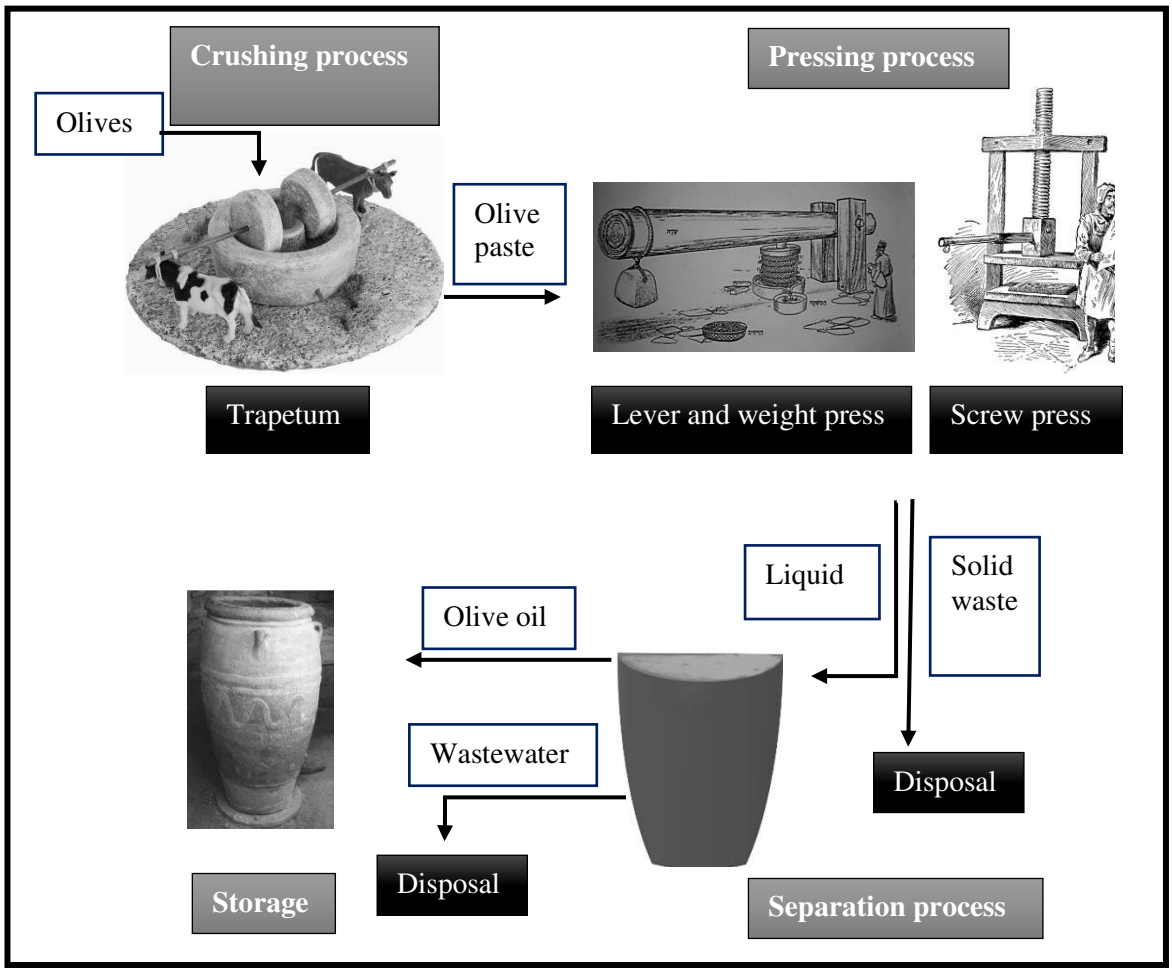

Figure 2: Steps of olive oil production in antiquity

1.2.2 Modern Olive Oil Production Techniques

In modern olive mills, the process of manufacturing olive oil can be comprehended as: a production of homogeneous paste that includes leaves and feed eliminating, olives washing, crushing and mixing, followed by Oil / water separation process as presented in Figure 3 (Niaounakis et al., 2006).

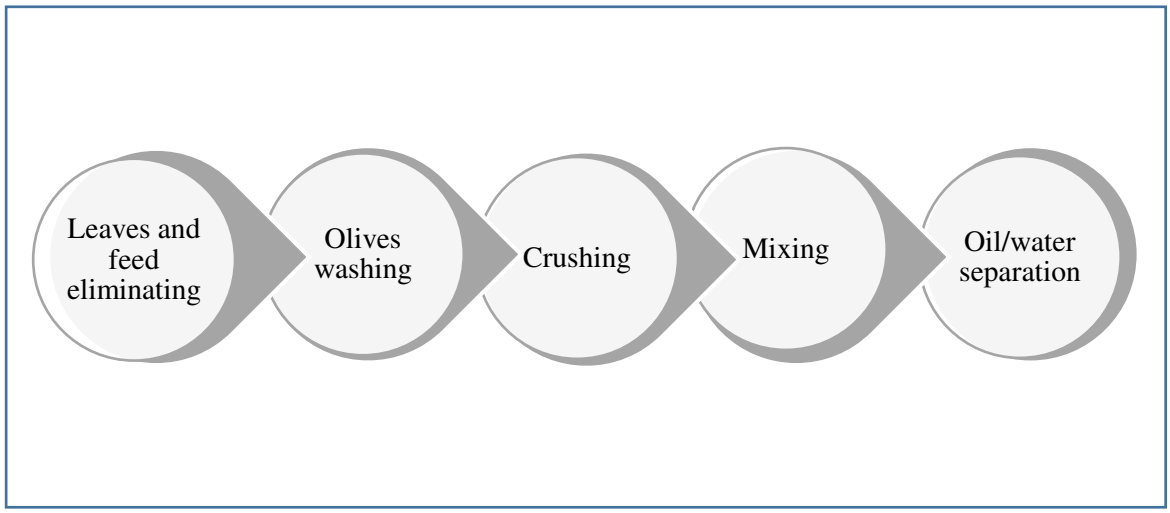

Figure 3: Schematic diagram for olives milling process in modern olive mills

Olives are placed in a large hopper connected to a movable belt as shown in Figure 4. In this step leaves and twigs that could damage machines and introduce an acrid flavour to the oil are removed. This task is achieved by a machine that remove the olive leaves automatically via fans. Olives then are sprayed with water to wash any foreign substance attached to olives such as soil and dust (Kapellakis et al., 2008).

Subsequently, the washed olives are entered crusher in order to permit the oil escape from the vacuoles by ripping the flesh cells. Accordingly, larger oil drops can be formed and separated from other phases. Olives crushing unit presented in Figure 4 is a steel cylinder, comprising hammers fixed on a rotor that revolved at a high speed as olives are fed into the hopper. Olive is compressed by the hammer shafts and is thereby pulled apart and flushed out through a controllable size holes in the cylinder (TDC-OLIVE project, 2004).

Mixing process is essential to increase the size of oil droplet in the produced olive paste. It has been proved that mixing for about 1 hr at 30-35ºC are the optimun conditions to increase the production yield of oil and to decrease its phenolic content. Olive mills required two or three mixing units (Figure 4) built-in with an external chamber that desinated to circulate heated water (TDC-OLIVE project, 2004).

The second stage that is oil purification and extraction can be run via different methods such as: pressing, electrophoresis, chemical separation and percolation which are scarcely used nowadays. On the other hand, centrifugation either two-phase or three-phase are abundantly used methods in recent olive mills (Niaounakis et al., 2006).

Centrifugation principle for oil/ water extraction started nearly in 1890s. Decanters (Figure 4) which are centrifugal separators aligned horizontally are used for this purpose. In this method different phases are separated by the power of centrifugation, which led to separate OMW, oil and olive cake according to their specific densities. Two modes of centrifugation are utilized in olive mills; two phase and three phase, which operate with similar decanters with higher rotational speed and higher inner diameter of the two phase rotor. Moreover, in two phase process there is no need to add boiling water to achieve better extraction (TDC-OLIVE project, 2004 and Niaounakis et al., 2006). Table 1 summarizes the differences between two phase and three phase extraction processes.

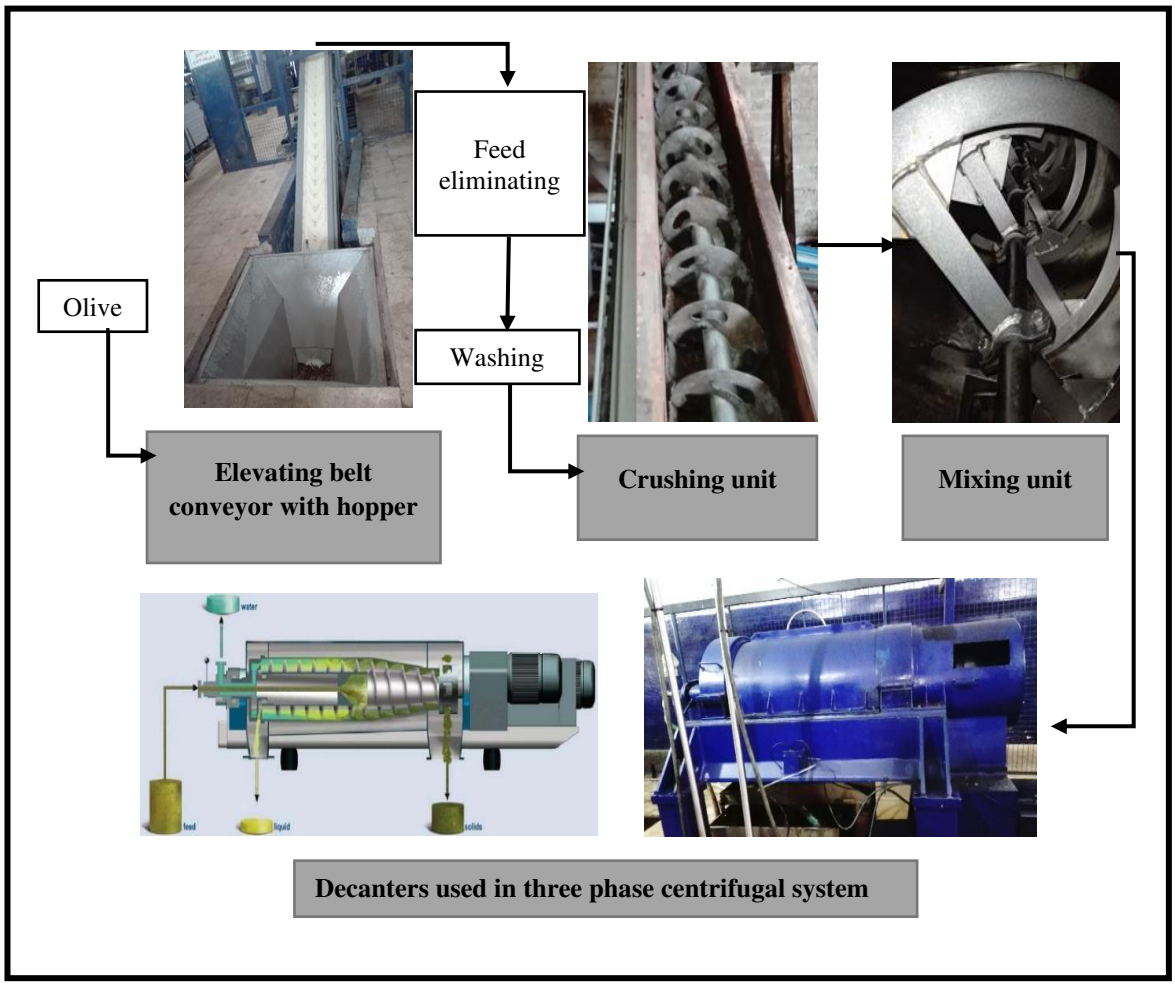

Figure 4: Production of olive oil steps in modern olive mills (Abuatheih factory)

Table 1: Differences between two phase and three phase extraction processes

Characteristic	Three phase	Two phase	Reference
Amount of added water	0.7-1.4 m^3/ton olives	0.1-0.12 m^3/ton olives	(Alburquerque et al., 2004)
Amount of produced wastewater	1-1.6 m^3/ton olives	0.2 m^3/ton olives	(Alburquerque et al., 2004)
Temperature	High temperature	Low temperature	(Niaounakis et al., 2006)
Types of wastes	1- Solid byproduct known as olive cake. 2- Liquid byproduct known as OMW.	A semi solid byproduct known as Thick Paste Olive Mill Waste.	(Niaounakis et al., 2006)
***G value**	Low (2000-2600)×g	High (3000-3600)×g	(TDC-OLIVE project, 2004)
Decanter design	Lower internal diameter	Higher internal diameter	(TDC-OLIVE project, 2004)
Cost	Lower cost	Higher cost	(Niaounakis et al., 2006)

***G value:** acceleration of the sample in the rotor times the acceleration of gravity.

1.3 OMW Problems

1.3.1 Environmental Effect

The emanated gases from the olive mills engender an offensive odor that leads to substantial pollution by odors especially throughout the oil production season. Naturally, OMW undergoes fermentation upon discharging on the land or into natural water bodies and/ or storing in open ponds. Consequently, pungent gases such as methane, hydrogen sulfide, phenols and sulfur dioxide are emitted then contaminate soil or waters (Niaounakis et al., 2006 and Souilem et al., 2017). This environmental impact can be diminished by acidification of fresh OMW (pH between 2 and 3) to prevent the formation of 4- ethylphenol the main contributor for the bad odor. The proposed reason for 4-ethylphenol formation was the degradation of p- coumaric acid (Souilem et al., 2017 and Ruiz-Méndez et al., 2012) as presented in Figure 5.

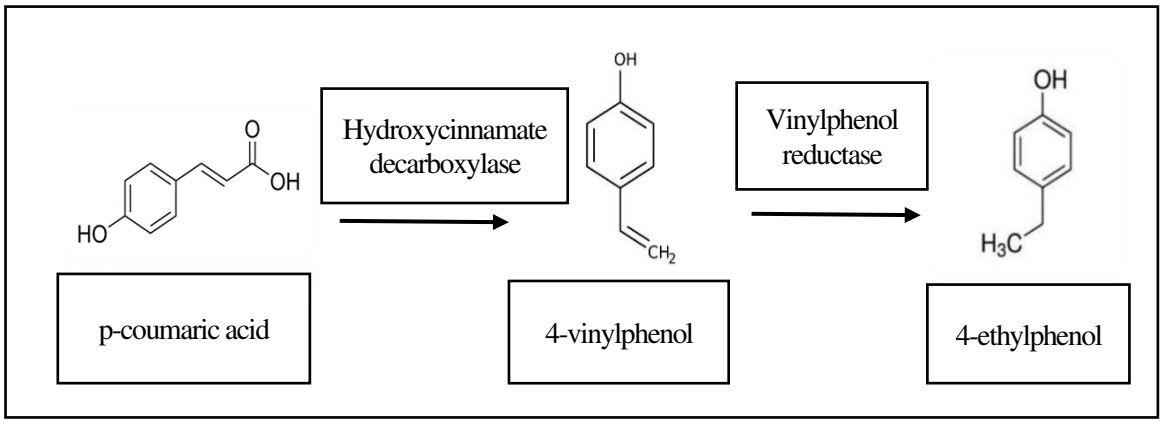

Figure 5: The chemical reaction scheme of degradation of p-coumaric acid to 4-ethylphenol (Suárez et al., 2007)

The discharge of OMW in the natural water bodies adversely affects the water resources and aquatic life. Changing in the color of water is the main visible effect that caused by tannins oxidation then polymerization creating darkly colored phenols. The presence of a high content of reduced sugars motivates the growth of microorganisms, and reduces the concentration of dissolved oxygen that is necessary for aquatic life. Eutrophication phenomena is another deteriorating effect arises from the high load of phosphorous that stimulates algae growth disturbing the ecological balance in natural waters (Niaounakis et al., 2006 and Souilem et al., 2017).

1.3.2 Health Effect

OMW containing harmful organic compounds -such as phenol and its derivatives- that can contaminate ground water resources upon improper disposal methods and thus lead to a serious ground water pollution problem. Moreover, exposure to such toxic chemicals has a direct effect on human and animals; it can damage the central nervous system, respiratory system, kidney, liver, pancreas, blood system and immune system. So it is important to remove phenols and aromatic compounds from contaminated water before discharge (Rui et al., 2012; John et al., 2014 and Leouifoudi et al., 2015).

1.3.3 OMW Management and Limitations

The management of OMW represents a critical environmental problem, where huge quantities -exceeds 30 million m^3 of OMW- are generated annually in the Mediterranean basin (Haddad et al., 2017) in annual seasons of less than one hundred days (October to December) making its storage impossible in small mills. In addition, the OMW is not involved in any waste management causing a great challenge in its remediation (Niaounakis et al., 2006).

Jordan, is the top fourteenth producer of olives on the world. It was estimated that 56×10^4 Dunums of olives were harvested and 14.5×10^4 tons of olives were produced in 2017 (FAOSTAT database, December 20, 2018). There are 130 olive mills produce around 4×10^4 m^3 of OMW annually (Ministry of Agriculture, Annual Report, 2017). Regrettably, these mills discharge OMW without any processing as a result of lack in legislations and national policy that regulate the management of OMW, lack of awareness, in addition to the high cost and sophisticated techniques for treatment processes. The single disposal procedure for OMW used in Jordan is transporting to dumpsites which is also considers as a very high cost approach with serious environmental impact (Ayoub, 2017). Therefore, it is essential to improve a green and cost effective method to treat OMW on site.

1.4 OMW Treatment Processes

Many methods were used for decontamination of OMW, for instance biological, thermal and physical processes which improve the quality of wastewater.

1.4.1 Biological Processes

Biological approach for OMW treatment is the employment of microorganisms to degrade toxic chemicals existing in OMW to methane (CH_4) and carbon dioxide (CO_2). Microorganisms' selection affected by the treatment conditions namely aerobic or anaerobic conditions (Niaounakis et al., 2006).

1.4.1.1 Aerobic Digestion

Aerobic treatment process depends on varieties of microorganisms booming only in the presence of sufficient amount of oxygen and food. It is applied to get rid of organics from wastewater with lower COD concentration, or just as enhancing step to remove remaining organics and nutrients (Niaounakis et al., 2006).

1.4.1.2 Anaerobic Digestion

Anaerobic digestion driven mainly by bacteria booming in the absence of oxygen (Koyama, 1963). It is utilized for removing organics from wastewater with higher COD concentrations (Niaounakis et al., 2006).

Unfortunately, biological treatment process demands deep understanding of the catabolic approach employed by microorganisms to digest each compound in OMW, with the purpose of selecting the most suitable categories of microorganisms that successfully digest the varieties of these compounds. Furthermore, biological approach is more expensive than other treating methods (Niaounakis et al., 2006).

1.4.2 Thermal Processes

Thermal process such as evaporation/distillation, combustion/pyrolysis and lagooning were investigated for OMW treatment. The principle of thermal treatment is decreasing the water content of OMW thus reducing the total volume of the waste (Di Giacomoet al., 1991).

1.4.2.1 Evaporation/Distillation Processes

High reduction of COD concentration was obtained upon utilizing evaporation and distillation as treatment approach of OMW. These techniques generated concentrated residue compressing mineral salts and nonvolatile organics in addition to volatile flux comprising water vapor and volatile ingredients. Unfortunately, these techniques require

high energy and produce a considerable portion of volatile contaminates during the treatment process (Di Giacomoet al., 1991).

1.4.2.2 Combustion/Pyrolysis Processes

Combustion and pyrolysis as rapid, exothermic chemical reactions are widely used to remove the wastes found in highly concentrated OMW. Nevertheless, toxic gases are emitted upon combusting or pyrolyzing OMW causing environmental problems. They also require very expensive equipment and high amount of energy (Petarca et al., 1997).

1.4.2.3 Lagooning

Using lagoons or evaporation ponds allows OMW to be evaporated and dried by the sun's energy. Throughout long periods natural biological degradation occurs for OMW. Lagooning is one of the first treatment processes that was proposed for OMW with low finance and maintenance cost. On the other hand, OMW leakage across the soil may lead to groundwater contamination and produce bad smell water that is unsuitable for irrigation or fertilizer due to anaerobic fermentation (Kasirga, 1988).

1.4.3 Physical Processes

Physical approach involves separation of different phases by sedimentation, flotation, dilution, centrifugation, filtration and membrane technology.

1.4.3.1 Sedimentation

Sedimentation method is extensively used pretreatment process. The suspended organics in OMW can be separated naturally by gravity after a couple of days by sedimentation. After sedimentation, OMW can be viewed as two separate layers, upper layer with a low COD concentration and settled sludge with a high COD concentration (Georgacakis et al., 2002).

1.4.3.2 Air Floatation

Flotation process on the other hand, removes oil droplets and suspended particles from OMW via adding a gas (commonly air) that enables separation, upon adhering to the particle structure, thus the specific gravity is decreased and the suspended particles float. Floatation is relatively inefficient technique for OMW pretreatment due to high content of suspended solids making the ratio of the air to the solid out of the standard working range (Schwoyer, 1981).

1.4.3.3 Dilution

Dilution is capable of reducing the concentration of OMW, consequently, final effluent can simply accomplish the obligatory standards. Nevertheless, in restricted water resources areas, this way seems to be inappropriate, particularly when large water quantities are required for dilution (Fiestas De Ursinos and Padilla, 1992).

1.4.3.4 Centrifugation

Centrifugation technique implies the usage of centrifugal power to separate different phases depending on their density. When OMW is exposed to centrifugation, three isolated phases are produced: olive oil layer, aqueous layer holding the soluble substances, and deposited layer comprising colloidal and suspended particles. Although it was verified that centrifugation technique is capable of completely separating suspended and colloidal materials, and considerably enhancing oil recovery and COD removal, it is considered to be an expensive process and requires a periodic maintenance (Al-Malah et al., 2000) and (Niaounakis et al., 2006).

1.4.3.5 Filtration

Filtration is a process based on using pressure to remove colloidal and suspended solids from OMW. Unfortunately, it was proved that the physico-chemical features of

OMW i.e. the presence of oil, suspended solids and fats blocked the filter and made this technique impractical (Bradley and Baruchello, 1980), (Mitrakas et al., 1996) and (Niaounakis et al., 2006).

1.4.3.6 Membrane Technology

Separation of a very small particles from OMW was conducted using membrane technology. Four different membrane methods including nanofiltration, microfiltration, ultrafiltration and reverse osmosis were investigated for OMW treatment. Unfortunately, membrane fouling caused decrease in membrane permeability and selectivity which led to decrease in its efficiency and increase the cost upon frequent plant closure for washing and cleaning the membranes (Iniotakis et al., 1993).

1.4.4 Physico-chemical Processes

Coupling between physical and chemical processes leads to a more powerful technology known as physico-chemical processes. As an example, adding chemicals for coagulation, flocculation and adsorption that upgrade the quality of OMW (Shammas et al., 2005).

1.4.4.1 Coagulation, Flocculation

Coagulation and flocculation represent the backbone processes in superior wastewater treatment plants. The idea behind using these techniques is to improve suspended or colloidal particles removal in downstream processes such as filtration and sedimentation (Shammas et al., 2005).

Coagulation process is based on addition of organic and/or inorganic coagulants (iron salts or aluminum salts). These coagulant cations serve as destabilizers for the negatively charged suspended or colloidal particles. This step is typically fast and occur in a rapid mixing container. Aggregation of the destabilized particles achieved by slow mixing

process in the flocculation tank with assistance of ionic or non-ionic polymers serve as flocculants (Shammas et al., 2005).

Coupling between coagulation, flocculation and sedimentation processes may lead to more powerful pretreatment technique that reduces the total suspended solid content (TSS) efficiently in wastewater, thus facilitates the main treatment process or may be utilized as post treatment process. The OMW treatment by means of coagulation, flocculation, and sedimentation was investigated by Pelendridou et al. in 2014. This technology was tested as a single treatment process and as a post treatment succeeding aerobic biological treatment. It was found that the use of a combined biological and physicochemical process was the optimum treatment with COD, total phenols (TPC) and TSS removal efficiencies of 65.5%, 66%, and 99.2%, respectively (Pelendridou et al., 2014). Moreover, Hodaifa et al. in 2015 studied the effect of pretreatment by coagulation flocculation sedimentation of OMW, and the results showed a high removal percent of turbidity (27.9 - 61.4%), while organics was removed partially with COD removal of (5.6 - 20.4%) and TPC removal of (11.3 - 25.1%) (Hodaifa et al., 2015). Another study was conducted on OMW treatment by Ozan Eskikaya et al. in 2017 through successive acid cracking then coagulation-flocculation using ferrous sulfate as coagulant. The results demonstrated that 3000 mg /L was the optimum coagulant dose with total COD removal of 79% (Ozan Eskikaya et al., 2017).

1.4.4.2 Adsorption

Adsorption process is believed to be an effective technology for wastewater treatment owing to its design simplicity, low space requirements, low cost, and odor free emissions. This technique is based on bonding dissolved material (adsorbate) present in wastewater to the surface and pores of a solid matter (adsorbent) (Mskay and Calvert, 1990).

Granular activated carbon (GAC) is considered as effective adsorbent, since it has a very high surface area per unit weigh. Nonetheless the high cost of commercial GAC

restricted its use and applications in wastewater treatment (Saravanakumar et al., 2013). On the other hand, locally available materials such as zeolites and VT can also be used as adsorbents. These natural materials in many instances are relatively inexpensive, abundant in supply and have significant potential for modification and enhancement of their adsorption capabilities (Rashed, 2013).

1.5 Adsorbents used in OMW Treatment

1.5.1 Granular Activated Carbon (GAC)

Granular activated carbon (GAC) is a widespread adsorbent due to its high surface area (El-Geundi et al., 1997). Its capability to adsorb various types of pollutants makes it an attractive adsorptive material for OMW treatment (Lakshmanan, 2013).

In 2004 Azzam *et al* tested the capability of using adsorption by GAC as a post treatment step in OMW remediation. OMW was treated by successive settling, centrifugation, and filtration. The filtrate was then exposed to a post-treatment process i.e. adsorption using GAC. It was found that the removal of TPC was approximately 94%, while it achieved approximately 83% for COD (Azzam et al., 2004). Another study was conducted by Azzam et al. in 2010 to investigate the effect of using GAC, as adsorption medium, on the concentrations of phenols and COD of pretreated OMW. The results exhibited that three-stage countercurrent adsorption treatment procedure using GAC (24 g/L OMW) was capable of reducing phenols from 450 mg/L to 15 mg/L. While COD was reduced from 60000 to 22300 mg/L (Azzam et al., 2010). Moreover, Hattab et al. investigated the adsorption capacity of the GAC for COD and TPC reduction by batch process. It was found that GAC led to removal percentage of 91% and 74% of TPC and COD respectively (Hattab et al., 2016). Column experiments were conducted to investigate the treatment of OMW over sand filtration followed by GAC adsorption. Sand filtration was responsible for 64% and 69% COD and TPC removal percentage, respectively. While Adsorption tests with

GAC proved the high capability of GAC in COD and TPC removal percentage to non-detected levels (Mkadem et al., 2014). Actually, GAC was verified to be an effective adsorbent for COD and TPC by many researchers. But, its high cost and the requirement for a high cost regeneration techniques make it less economically feasible as an adsorbent. So, the requirement for available and cost effective adsorption media has led many researchers to search for more efficient and naturally available materials to use (Achak et al., 2019).

1.5.2 Natural Volcanic Tuff (VT)

Volcanic tuff (VT) is the rock shaped mainly from volcanic ash expelled throughout volcanic eruption (Li et al., 1981). Volcanic tuff were formed in Jordan throughout Neogene and Pleistocene periods from basaltic volcanism in Jordan Graben and northeast areas. The Rift of Dead Sea was the main originator for the eruption of volcanos in Jordan. Harrat Ash-Shaam in northeast Jordan is the largest volcanic field which is responsible for production of 5×10^5 ton of the black VT which have a potential for future research. The process of VT formation in Jordan was investigated minutely by Ibrahim et al. (Ibrahim et al., 1995 and Ibrahim, 1996).

Many studies on VT declares the presence of zeolites associated with the VT (Al Dwairi, 1987; Ibrahim, 1996; Al Dwairi et al., 2009; Ibrahim, 2014 and Khoury et al., 2015). In alkaline hydrological systems, thick layers of VT alter slowly to three mineralogical zones that can be characterized in the field by their color to (Ministry of energy and mineral resources, 2015):

1. **Sideromelane zone** appears at the surface, comprises a fresh sideromelane as well as it has black to light grey color.
2. **Palagonite zone** appears as intermediate zone, which is virtually free of zeolite and it has dark brown to reddish brown color.

3. **Zeolite zone** full of zeolite with yellow to light brown color and characterized by the presence of chapazite, phillipsite and faujasite minerals.

Temperature and hydrological environment are the major directors for zeolitization process (Al Dwairi et al., 2014). Volcanoes are usually erupting in tectonic plates regions that generally found close to an ocean or within an island. Upon flowing of the hot lava into the sea a chemical reaction occurs between water, lava and salt from the sea. This reaction over passage of thousand years produce zeolitic VT (de'Gennaro et al., 2000; Harpel et al., 2008; Weckhuysen and Yu, 2015 and Moshoeshoe et al., 2017).

Studies were conducted for investigating zeolitic VT and non zeolitic VT in OMW treatment. Njoum in 2014 tested the feasibility of using zeolitic VT in TPC removal from OMW through column approach. Three columns packed with 5 cm zeolitic VT of different particle sizes showed good removal percentage with average reduction of 37%, 33.8 % and 12% from the first, second and third column, respectively (Njoum, 2014). Kannan in 2017 proved that zeolitic VT is not capable of removing phenols from OMW even after 14 days although OMW was mixed with non-ionic surfactants (Kannan, 2017). Al-Tabbal et al. investigated the effect of using non zeolitic volcanic tuff for treating OMW. It was found that COD decreased from 81000 to 53000 mg/L with 35% removal percent while TPC from 2300 to 1700 mg/L with 26% removal percent (Al-Tabbal et al., 2015). Reddish non zeolitic VT with a particle size < 63 μm was utilized by Gharaibeh et al. to remove COD and turbidity from OMW. The results revealed that reddish VT is not able to remove COD and turbidity from OMW (Gharaibeh et al., 2008). The same conclusion was achieved by Azzam in 2018 after studying the possibility of using VT as adsorbent for phenols and COD removal. Though VT was activated either by calcination or by acid washing, the removal percentage for COD and phenols did not exceed 14% and 21% respectively (Azzam, 2018). To the best of our knowledge, combined activation of VT by acid washing followed by calcination was not investigated in OMW treatment.

1.5.3 Magnetic Nanoparticles

Nanotechnology plays an important role in industry. Its applications may result in a cleaner and healthier environment. The usage of nanoparticles typically poses several advantages over conventional materials owing to their size effects, the ratio of their surface to volume, interaction and surface chemistry yielding in highly powerful adsorbents (Lakshmanan, 2013).

Application of magnetic nanoparticles in wastewater treatment allows one to design a process where nanoparticles not only remove contaminants from wastewater efficiently, but also can readily be separated from the medium via a simple magnetic process, that can be efficient, scalable and harmless material (Krug, 2008 and Hariani et al., 2013).

Maghemite nanoparticles (γ-Fe_2O_3) for instance were investigated as adsorbent for color, phenols and COD removal from OMW via batch and column processes by Nassar et al. It was found that the adsorption process was rapid and the equilibrium was achieved within 30 min. Multi layers adsorption was proved for magnetic nanoparticles after conducting kinetic studies (Nassar et al., 2014).

Magnetite nanoparticles (Fe_3O_4) are commonly used owing their unique properties i.e. two types of cations (Fe^{+3} and Fe^{+2}) are present in their crystal structure. Many procedures are described in literature for monodispersed magnetite nanoparticles synthesis including microemulsion, chemical coprecipitation, thermal decomposition, sol gel and hydrothermal synthesis. Out of all these, chemical coprecipitation method is considered as a convenient and facile approach to synthesize magnetite nanoparticles from aqueous solutions of ferric and ferrous salts through dropwise addition of a base at room temperature or at an elevated temperatures (Lakshmanan, 2013).

The mechanism of magnetite nanoparticles formation by chemical coprecipitation process can be written as follow (Dufour et al., 1997):

$$Fe^{3+} + 3OH^{-} \longrightarrow Fe(OH)_{3\,(s)} \quad (1)$$

$$Fe(OH)_{3\,(s)} \xrightarrow{\text{decomposition}} FeO(OH)_{\,(s)} + H_2O \quad (2)$$

$$Fe^{2+} + 2OH^{-} \longrightarrow Fe(OH)_{2\,(s)} \quad (3)$$

$$2FeO(OH)_{\,(s)} + Fe(OH)_{2\,(s)} \longrightarrow Fe_3O_{4\,(s)} + 2H_2O \quad (4)$$

The overall reaction:

$$Fe^{3+} + Fe^{2+} + 5OH^{-} + FeO(OH) \xrightarrow{\text{fast}} Fe_3O_4 + 3H_2O$$

in which FeO(OH) is ferrihydrite

In many cases, providing a stationary phase for the nanoparticles can make their application more feasible. There are many examples of these cases such as: core-shell-shell $Fe_3O_4/SiO_2/TiO_2$. These nanoparticles with silica and titania combination were investigated for photocatalytic degradation of organic compounds in OMW. They were prepared by coating a TiO_2 layer and SiO_2 layer on magnetic nanoparticles. The obtained results showed a high photocatalytic activity of synthesized nanoparticles for degradation of the OMW organic compounds (Ruzmanova et al., 2013).

In another study, ZnO-Magnetite nanocomposite was synthesized and investigated for photocatalytic degradation of phenolic compounds from OMW. The results showed that COD and TPC removal were found as 80% and 75% respectively (Sponza et al., 2018).

1.6 Aim of the Study

The main objective of this project is to develop cost effective and environmentally friendly approach to remove organic and phenolic compounds from OMW. The developed approach include pretreatment of OMW by coagulation/ flocculation/ sedimentation processes followed by filtration through different media. The media contain magnetite nanoparticles, GAC and VT in different ratios and through three different scenarios (mixing, layering and nanocomposites) and tested via batch and column processes.

Chapter Two: Materials and Methods

2.1 OMW Samples Collection and Preservation

OMW samples used in this project were collected during the harvesting time from a three phase olive mill located in Amman- Wadi Al-Sear (Bilal Olive Press). OMW was filtered and acidified with hydrochloric acid (37%, VWR, USA). pH meter (GonDO PL-700PV, Taiwan) was used to control the pH range to be from 2-3 to prevent degradation of phenolic compounds (Ruiz-Méndez et al., 2012). OMW was stored in polyethylene containers (20 L) at room temperature and kept in dark place to prevent photodegradation of phenols until used in this study.

2.2 Pretreatment of OMW by Coagulation/Flocculation/Sedimentation Processes

OMW samples were pretreated by coagulation/flocculation which carried out using jar test apparatus (VELP SCIENTIFIICA JLT6, Italy) equipped with stainless steel stirring impellers and six 1-L beakers (Figure 6). Coagulation is a rapid mixing stage that aims to destabilize colloidal or suspended particles present in OMW. Coagulation process was followed by a slow mixing stage known as flocculation process to increase aggregation between destabilized particles. Sedimentation process was the last stage, where the mixing was stopped and aggregated flocs were allowed to settle down. In this study 20% w/v solution of ferric chloride hexa hydrate ($FeCl_3.6H_2O$) (AR grade, FISCHER Chemicals, China) was used as coagulant and polymeric quaternary amine (SUPERFLOC C 577, KERMIRA, Finland) was utilized as a flocculent.

Optimization of variables such as slow and rapid mixing time and speed, coagulant and flocculent doses, pH and settling time was carried out based on the highest removal percentage of OMW constituents and each experiment was repeated triplicate. pH of the samples was adjusted before the addition of ferric chloride. TSS, COD, TPC and sludge volume were determined before and after coagulation/flocculation/sedimentation processes.

Six beakers, each filled with 500 mL OMW were used to optimize the parameters of coagulation/ flocculation/ sedimentation. In each optimization experiment, one parameter was varied while fixing other parameters. The optimum rapid mixing speed was obtained by running the experiment with varied speed of 80, 90, 100, 150, 200 and 250 rpm. The best rapid mixing time was found by conducting the experiment with different rapid time of 1, 2, 3, 4, 5 and 6 min. The optimum slow mixing speed was determined by running the experiment with varied speed of 10, 20, 30, 40, 50 and 60 rpm. Slow mixing time of 5, 10, 15, 20, 25, 30, 35, 40 and 45 min., pH of 1, 3, 5, 7, 9 and 11, ferric chloride dose of 0, 1000, 2000, 3000, 4000 and 5000 mg/L were tested to find the optimum values. While flocculent doses of 0.5, 0.75, 1, 1.25, 1.50, 1.75 and 2% ($V_{flocculent}$/ V_{OMW}) % and settling time of 10, 20, 30, 40, 50 and 60 min. were tested.

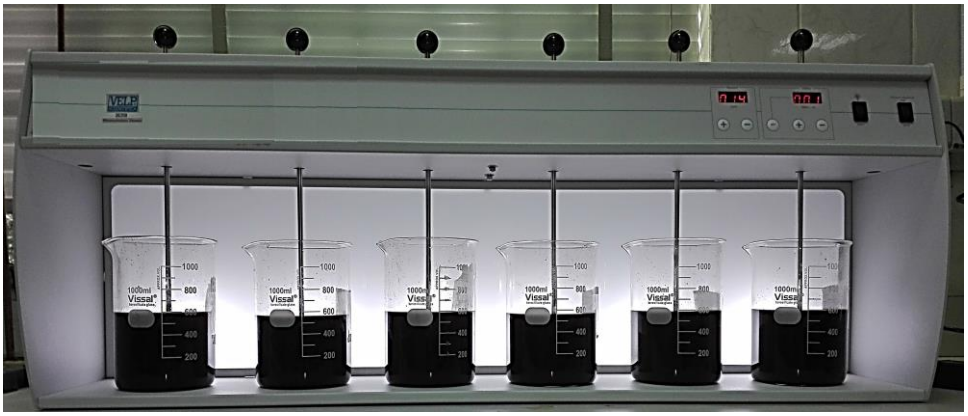

Figure 6: Jar test apparatus (VELP SCIENTIFIICA JLT6, Italy)

2.3 Media Preparation

2.3.1 Magnetite Nanoparticles Preparation

Magnetite nanoparticles were prepared by co-precipitation method according to Wei et al. procedure (Wei et al., 2012).

A 200 mL of 0.05 M aqueous solution of ferrous chloride tetrahydrate ($FeCl_2.4H_2O$) (AR grade, BBC Chemicals, EU), was mixed with 200 mL of 0.1 M ferric chloride hexahydrate solution for 10 minutes using shaking water bath (KÖTTERMAN 3047, Germany) maintained at 40°C and constant shaking speed of 150 rpm. Then 3 M Sodium hydroxide (NaOH) (AR grade, alpha chemika, India) solution was added to the above mixture using a peristaltic pump (masterflex, USA) at a rate of 0.9 mL/min for 30 min to a final pH of 10. The produced nanoparticles were cooled to room temperature and washed several times with deionized water and ethanol (99.8%, C & S chemicals, Georgia) until their pH equal to 7. Magnetite nanoparticles were separated using external magnetic field and dried in the oven (GEMMY, yco-No1, Taiwan) at 60°C. Deionized water was used as solvent for preparing the solutions. The step by step schematic procedure is described in Figure 7.

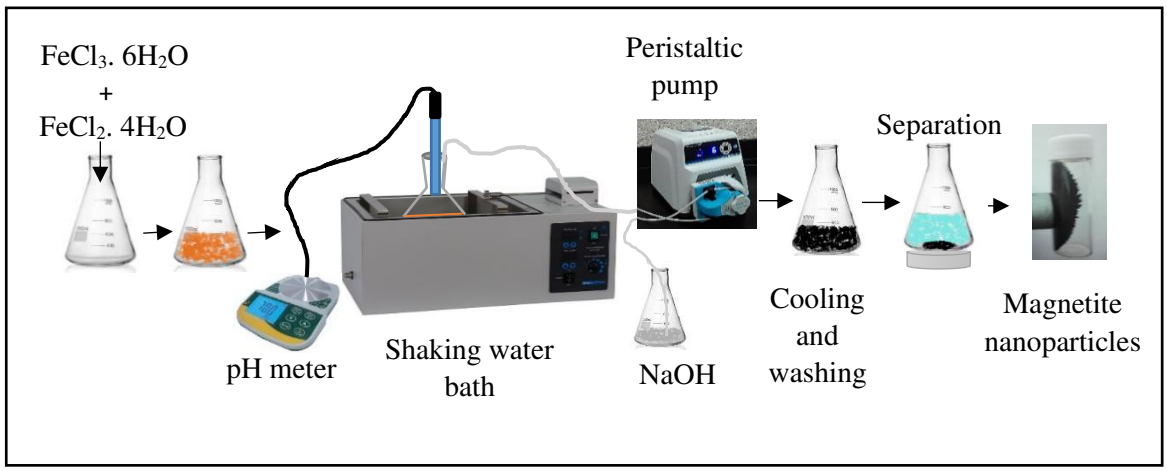

Figure 7: Schematic diagram for magnetite nanoparticles preperation by coprecipitation method

2.3.2 Volcanic Tuff (VT) Media Preparation

Volcanic tuff (VT) used in this study was collected from Tell Geis – Al Mafraq, a natural volcanic tuff deposit site, located in the northern area of Jordan. VT was grinded, sieved and categorized into two categories according to their particle size ranges:

- The small particle size range: less than 45 μm.
- The large particle size range: 125 μm- 150 μm.

VT media were prepared by activation using three different approaches (Figure 8):

1. Calcination alone.
2. Activation with acid impregnation followed by calcination according to (Susilawati et al., 2018) with minor changes.
3. Activation with base impregnation followed by calcination.

Calcination procedure was unified and conducted using muffle furnace (witeg, AC 460V, Germany) heated at 350^{o}C for 3h. Acid impregnation was performed using 2 M sulfuric acid (H_2SO_4) (95-97%, sigma- Aldrich, Germany) solution. Four VT samples were impregnated with sulfuric acid on 50^{o}C hot plate (AREX DIGITAL, VELP SCIENTIFICA, Italy) equipped with a magnetic stirrer maintained at 1500 rpm for different impregnation time of 2, 24, 48 and 72 hr. Then filtered and washed with deionized water several times to ensure removal of residual acid. However, base impregnation was performed using 2 M NaOH solution according to Djaeni et al. procedure (Djaeni et al., 2010). VT sample was impregnated with NaOH for 2 hr at 50^{o}C hot plate equipped with magnetic stirrer maintained at 1500 rpm. Then filtered and washed with deionized water several time to ensure removal of residual basicity. So seven samples of VT were utilized in this study; VT without activation (untreated VT), VT activated with calcination alone (VTC), VT activated with acid impregnation for 2 hr followed by calcination (VTA2C), VT activated with acid impregnation for 24 hr followed by calcination (VTA24C), VT activated with acid impregnation for 48 hr followed by calcination (VTA48C), VT activated with acid

impregnation for 72 hr followed by calcination (VTA72C) and VT activated with base impregnation for 2 hr followed by calcination (VTB2C). Figure 9 presents all VT samples used in this study.

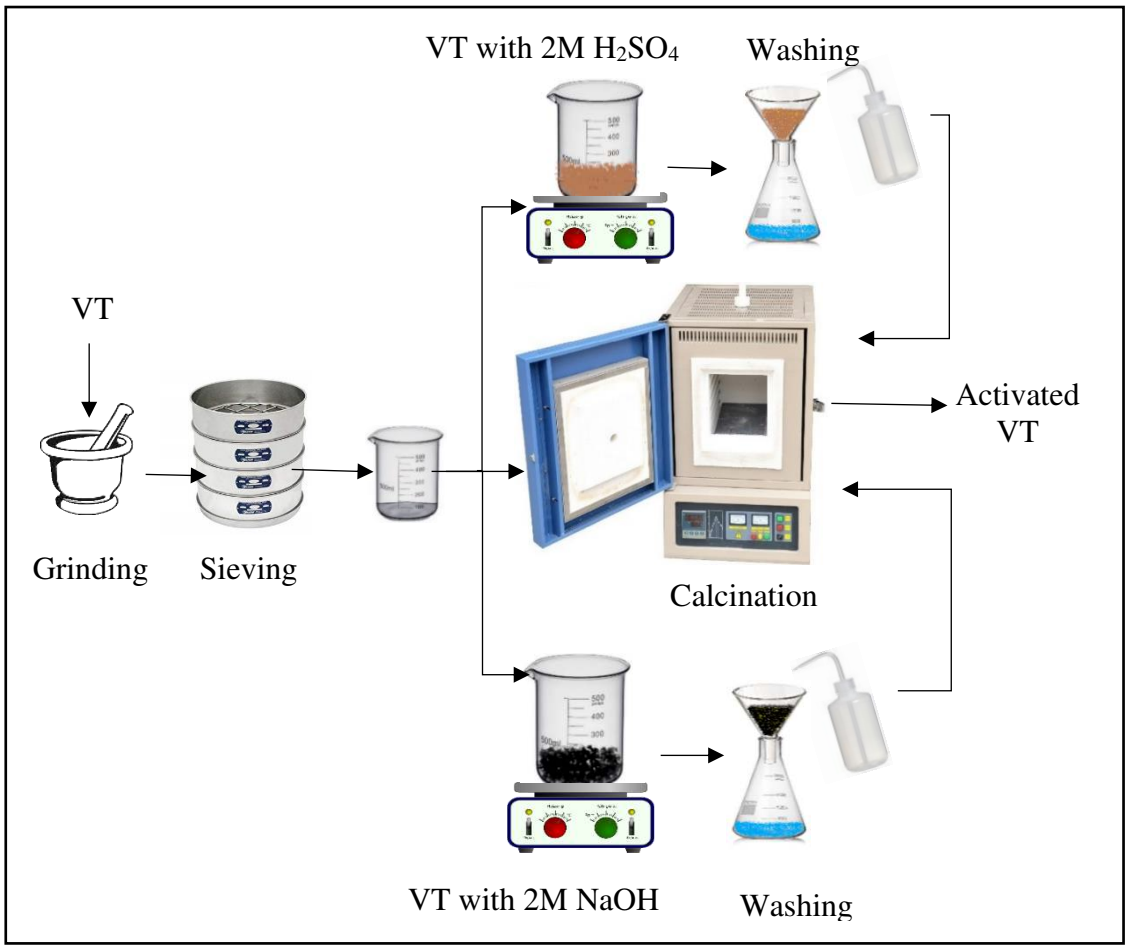

Figure 8: Schematic diagram for VT activation methods used in this study

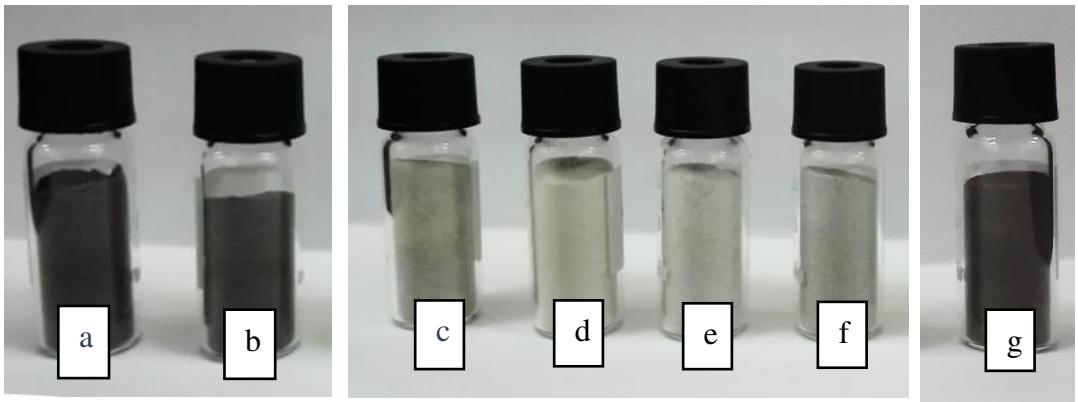

Figure 9: VT samples used in this study (a): untreated VT, (b) VTC, (c) VTA72C, (d) VTA48C, (e) VTA24C, (f) VTA2C, (g) VTB2C

2.3.3 Modification of VT with Polymeric Quaternary Amine

10 g of VTA24C were soaked in 0.1 mL of polymeric quaternary amine that was dissolved in 20 ml deionized water. Then stirred for 1 hr using magnetic stirrer at 1500 rpm. The sample was then dried at room temperature and kept on desiccator until used.

2.3.4 Preparation of VT /Magnetite Nanocomposites

0.5% by weight magnetite nanoparticles was suspended in 50 ml deionized water and added to 20 g of VTA24C. Then sonicated for 1 hr at 70ºC using probe sonicator (SONICS, VC505, USA, probe material: titanium alloy (Ti-6Al-4V), tip diameter: 13 mm, net power output: 500 watts, frequency: 20 kHz). After that the nanocomposite was filtered and dried in air as shown in Figure 10. Preparation steps of VT/magnetite nanocomposites is presented in Figure 11.

Figure 10: The prepared VT/magnetite nanocomposites

Figure 11: Schematic diagram for VT/ magnetite nanocomposite preparation

2.3.5 Granular Activated Carbon (GAC)

Granular activated carbon (GAC) (chemviron carbon, USA) was used as adsorbent and treated either by chemical reduction or chemical oxidation.

2.3.5.1 Reduction of GAC

GAC was reduced according to Shaarani et al. (Shaarani et al., 2011). 8g of GAC were soaked in 300 ml of 10% ammonia solution (25%, LabChem, USA) for 48 hr at room temperature. Then, filtered and dried in the oven at 105^{o}C for 24 hr and kept in the desiccator until used.

2.3.5.2 Oxidation of GAC

Oxidation of the GAC was performed according to Abu-Dalo et al. procedure (Abu-Dalo et al., 2013). 25 g of GAC was impregnated in 60 ml of 20% nitric acid (HNO_3) (69-71%, SDFCL, India) and kept on hot plate that was equipped with magnetic stirrer for 8 hr at 90-95^{o}C and stirring speed of 500 rpm. Subsequently, GAC was washed several times with deionized water until its final pH was 3, dried in the oven at 90^{o}C for 48 hr and kept in the desiccator until used.

2.4 Media Characterization

2.4.1 Point of Zero Charge (pH_{PZC})

Point of zero charge of magnetite nanoparticles, GAC and VT samples were determined using pH drift method described previously (Lazarević et al., 2007). A set of samples of 25 mL of sodium nitrate ($NaNO_3$) (0.1 M) (Hopkin & Williams, England) were used to measure pH_{PZC}. Their initial pH (pH_i) were adjusted from 2 to 12 using 0.1 M solutions of NaOH or HCl. Then, 0.05 g of the tested media i.e. magnetite nanoparticles, VT or GAC was added to each sample. The samples were left on the shaker for 24 hr, at room temperature to reach equilibrium. The final pH of each sample was determined after filtration. Each experiment was repeated triplicate and pH_{PZC} - the point where $pH_i = pH_f$ - was determined from pH_f vs. pH_i plot. Figure 12 describes the step by step procedure for pH_{PZC} determination.

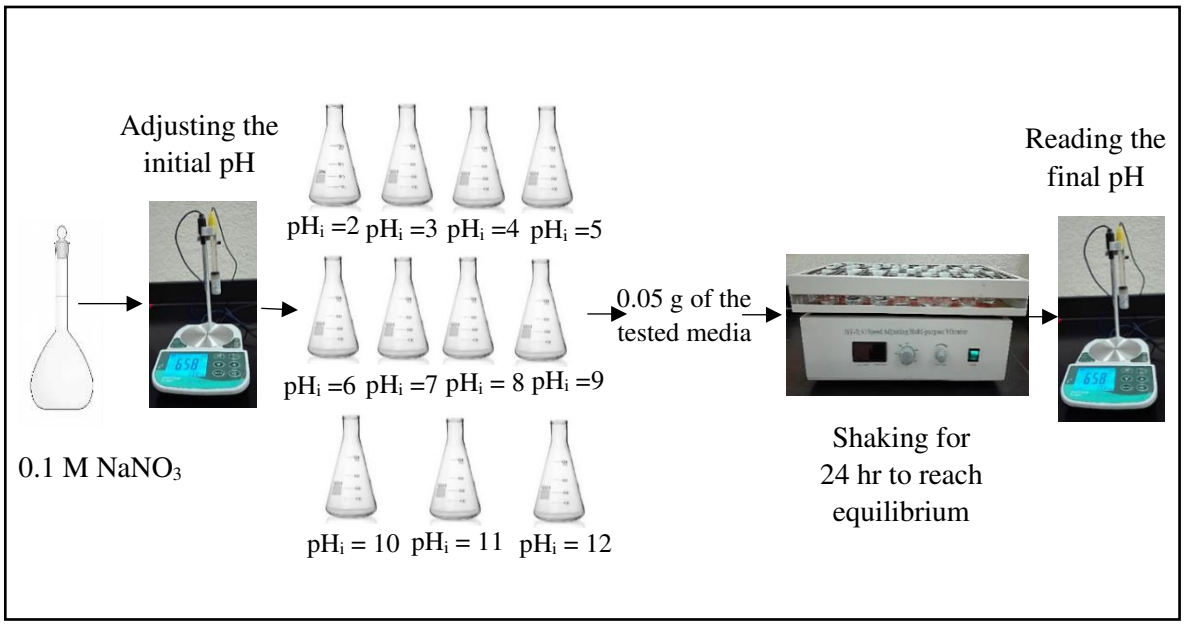

Figure 12: Schematic diagram for pH_{PZC} determination steps

2.4.2 Surface Area

Brunauer, Emmett and Teller (BET) technique (Quantachrome, NOVA 2200e, USA) located in the University of Jordan was used to determine the surface area, total pore volume and average pore size for VT samples. 0.5 g of each sample was weighted using analytical balance (Precisa 410AM-FR, Precisa, Switzerland) and then degassed for 3 hr at 300°C.

Each sample was then analyzed in the linear range; P/P_0 = (0.05- 0.35). BET equation was utilized to find the total external and internal surface area of multilayer adsorption system.

$$\frac{P}{Va\,(P0-P)} = \frac{1}{Vm\,C} + \frac{C-1}{Vm\,C} \times \frac{P}{P0} \quad (1)$$

where:

P: the equilibrium pressure of $N_{2\,(g)}$

P_0: the saturation pressure of $N_{2\,(g)}$

V_a: the volume of adsorbed $N_{2\,(g)}$

V_m: the monolayer capacity

C: BET constant

Plotting [P/ (V_a (P_0-P))] versus [P/P_0] resulted in a straight line at a relative P/P_0 pressure between 0.05- 0.35. The intercept of this line equal $1/(V_m\,C)$ and the slope equal $(C-1)/(V_m\,C)$.

The surface area can be calculated using:

$$S_{\,total} = \frac{Vm\,N\,S}{V} \quad (2)$$

Where:

$S_{\,total}$: the surface area in (m^2)

N: Avogadro's number

V: the molar volume of $N_{2\,(g)}$ which equal 34.7 cm^3/mol

S: the cross section of the adsorbing species (m^2)

The specific surface area was found by dividing the surface area obtained from BET equation by the mass of the sample.

The total pore volume was calculated from the amount of $N_{2\ (g)}$ adsorbed using the porosity equation:

$$V_{liq} = \frac{R\,T}{Pa\,V\,ads\,Vm} \qquad (3)$$

Where:

V_{liq}: volume of liquid nitrogen in pores

V_{ads}: volume of gaseous nitrogen adsorbed

P_a: ambient pressure

R: ideal gas constant

T: ambient temperature

The average pore size was estimated from pore volume (Brunauer et al., 1938) and (Gregg et al., 1967).

2.4.3 Transmission Electron Microscopy (TEM)

Transmission electron microscopy (TEM) which is a technique based on transmission of a beam of electrons through the sample to create an image. The sample is suspended on a grid then an image is created from the interaction of the electrons with the sample as the beam is transmitted through it. The image is then focused and magnified onto an imaging device (Williams et al., 1996). TEM (MORGAGNI 268- FEI company, Netherlands) located in the University of Jordan was used to study the morphology, shape and size distribution of the prepared magnetite nanoparticles.

2.4.4 X-Ray Diffraction Pattern

X-ray diffraction is a technique utilized to explore the atomic spacing and crystal structures. A cathode ray tube generated X-rays that are then filtered to yield monochromatic radiation, exposed to concentrate, then directed to the crystalline solid. When the incident rays conditions fulfil Bragg's Law ($n\lambda=2d\sin\theta$), they diffracted upon interaction with

crystalline solid. Bragg's law relates the wavelength (λ) of the radiation to the lattice spacing (d) and diffraction angle (θ) of a crystalline solid. Then the diffracted X-rays are detected. Upon scanning the crystalline solid over a range of 2θ angles, all promising diffraction directions of the lattice should be achieved. Transformation of the diffraction peaks to d-spacings permits recognition of the crystalline material since each material has a set of unique d-spacings. Usually, this is accomplished by comparison of d-spacings with standard reference arrangements (Warren, 1969). XRD (MAXIMA, Shimadzu, Japan) located in the University of Jordan was used to study the crystal structures of the prepared magnetite nanoparticles, VT samples and VT/magnetite nanocomposites.

2.4.5 Scanning Electron Microscopy (SEM)

A scanning electron microscope (SEM) is a technique used a beam of electrons to scan the surface and produce images of a sample. The interaction between the electrons and the atoms in the sample, generating many signals such as secondary electrons that can be detected to know the composition and topography of the sample (Smith and Oatley, 1955). SEM (FEI Company – Inspect F50 High Vacuum ~ 6e-4 Pa Eindhoven, Netherlands, located in the University of Jordan) was used to study the topography, morphology and composition of VT samples and VT/magnetite nanocomposites.

2.4.6 Zeta Potential

Zeta potential describes the electrokinetic potential in dispersions. Theoretically, zeta potential is the electric potential in the slipping plane of the double layer as shown in Figure 13. The zeta potential is an important indicator for the dispersions stability. The degree of electrostatic repulsion among neighboring charged particles in a dispersion is reflected on the magnitude of the zeta potential. As the electrical stability of the dispersion increased the magnitude of the zeta potential will be increased, hence the dispersion will resist aggregation of the particles as shown in Table 2 (Greenwood et al., 1999) and (Hanaor et

al., 2012). Zeta potential analyzer (Microtrac Zetatrac, USA) located in the University of Jordan was utilized in this study to estimate the stability of the prepared magnetite nanoparticles.

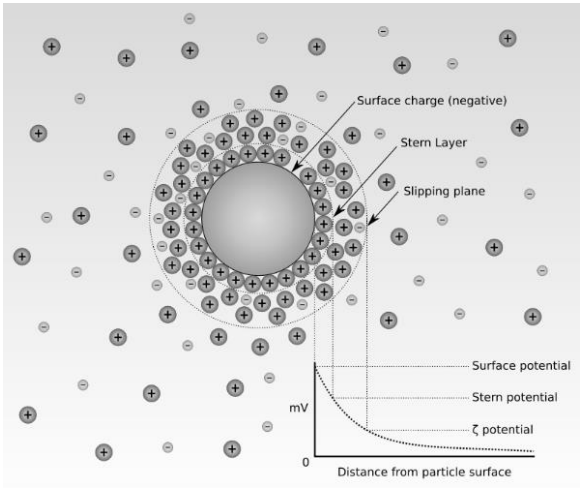

Figure 13: Potential difference as a function of distance from the charged particle in a dispersion

Table 2: The effect of colloidal stability on the magnitude of zeta potential

Zeta potential (mv)	**Stability behavior of the colloid**
from 0 to ±5,	Rapid coagulation or flocculation
from ±10 to ±30	Incipient instability
from ±30 to ±40	Moderate stability
from ±40 to ±60	Good stability
more than ±61	Excellent stability

2.4.7 Saturation Magnetization Test

Saturation magnetization is a property of ferrimagnetic and ferromagnetic materials. This state is achieved upon steadiness of the total magnetic flux density (B) though increasing in applied external magnetic field (H). In hysteresis curve (also called magnetization curve or BH curve) as (H) increases (B) approximately reaches a maximum value, which is the saturation magnetization of the substance (Steinmetz, 1917). In this

study magnetic measurements were carried out for powdered samples using vibrating sample magnetometer (VSM) (MicroMag 3900, Princeton Measurements Corporation) located in the Hashemite University, with a maximum applied field of 795 kA/m, high sensitivity (0.5 μemu at 1 s/point, high speed measurements (10 ms/point), and all magnetic measurements were performed at room temperature.

2.4.8 X-ray Fluorescence (XRF)

X-ray fluorescence (XRF) is a technique utilized for elemental analysis and chemical analysis using x-ray or gamma ray to excite fluorescence radiation from samples under investigation (Jenkins and De Vries, 1973). XRF (PHILPS, 7602 EA Almelo, Netherlands) technique located in Al Al-Bayt University was utilized in this study to examine the elements present in the media.

2.5 OMW Treatment

2.5.1 Batch Experiments

Batch experiments were conducted to investigate the potential of all prepared media on COD, and TPC removal from OMW and to determine the optimum conditions (adsorption equilibrium time, optimum pH, and magnetite nanoparticles dose) as described below. Each experiment was repeated triplicate and the coupling between magnetite nanoparticles and sorbent media was performed through two different scenarios: 1) by mixing magnetite nanoparticles with sorbent media and 2) by using nanocomposites of magnetite nanoparticles and sorbent media. OMW used in this investigation was pretreated with coagulation/ flocculation/ sedimentation processes before testing.

2.5.1.1 Contact Time

OMW with pH of 5.3 was added to 1% by weight magnetite nanoparticles that were mixed with 0.5 g sorbent materials. This corresponding to 5% by weight of the media to

OMW. The samples were then kept in a shaker (MOVIL-TUB, SELECTRA, Spain) for 2 hr, 24 hr, 48 hr, 72 hr and 96 hr. After the passing of the required contact time the samples were centrifuged using benchtop centrifuge (Labofuge 200, ThemoFisher Scientific, USA) maintained at 5300 rpm for 30 min to insure complete separation of the media. The supernatants were then withdrawn and subjected to COD or total phenol tests as presented in Figure 14.

2.5.1.2 Magnetite Nanoparticles Dose

5% by weight of the media was added to OMW and the experiments were conducted at pH of 5.3 with the best contact time found from the previous experiment. Different magnetite nanoparticles doses of 0, 0.5, 1, 2, 5 and 10% by weight were coupled with VT to find the optimum dose.

2.5.1.3 pH

5% by weight of the media was added to OMW with different influent pH of 2, 4, 6, 8, 10 and 12. The experiments were conducted at the optimum contact time and VT was coupled with the optimum magnetite nanoparticles dose.

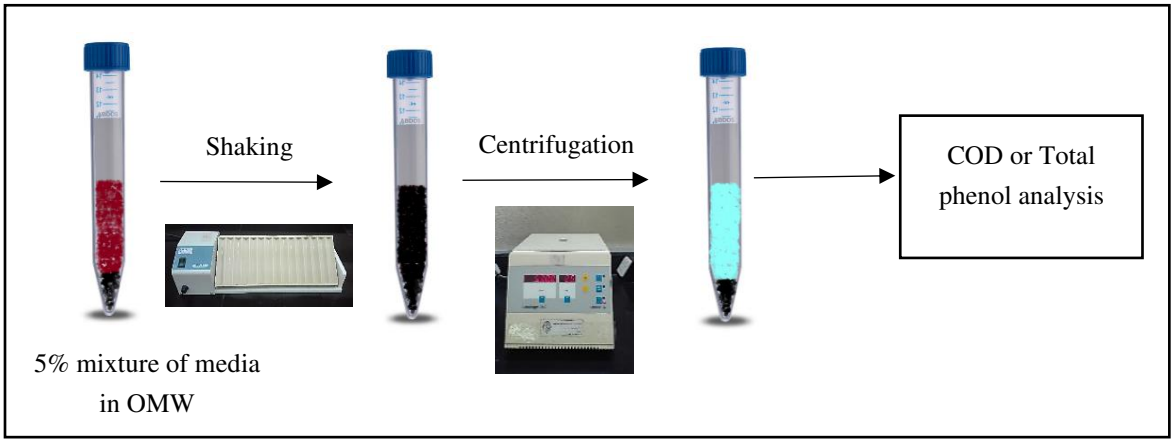

Figure 14: Schematic diagram for batch experiments

2.5.2 Column Experiments

The continuous adsorption examinations were performed in a translucent polypropylene column (KIMBLE CHASE, USA) (length 20 cm, inner diameter 1 cm). The column was filled with 6 g of the media followed by a layer of glass wool. The media were composed of VT, AC and magnetite nanoparticles that coupled through three different scenarios. The first scenario was based on mixing VT with magnetite nanoparticles, the second scenario was based on using separate layers of VT, GAC and magnetite nanoparticles. While the third scenario was based on using nanocomposites of VT and magnetite nanoparticles. Pretreated OMW was pumped into the column in up flow mode of 0.9 ml/ min, using a peristaltic pump and fraction collector (Eldex, USA) was used to collect the treated samples. The pH of OMW and the magnetite nanoparticles dose were adjusted to the optimum values obtained from batch preliminary tests and each experiment was repeated triplicate. The setup of peristaltic pump, column and fraction collector is presented in Figure 15. The summary of OMW treatment with successive coagulation, flocculation, sedimentation and adsorption processes performed in this study is shown in Figure 16.

Figure 15: Column (KIMBLE CHASE, USA)

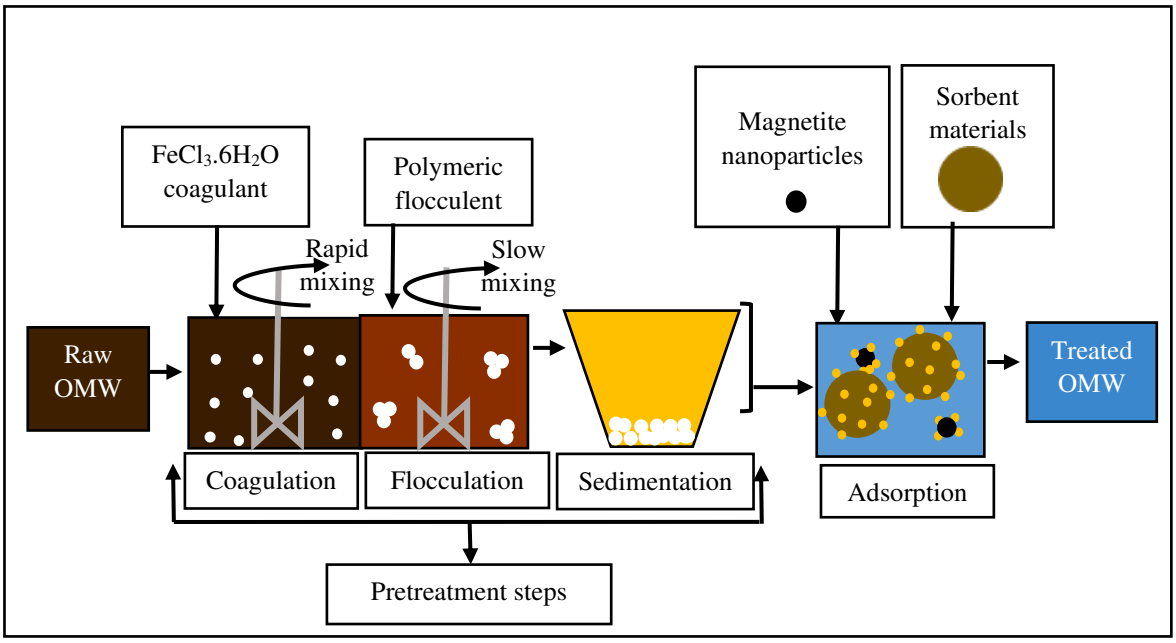

Figure 16: Schematic diagram represents all treatment steps performed on raw OMW

2.6 OMW Treatment Evaluation

2.6.1 Determination of Total Phenols

2.6.1.1 Phenolic Compounds Extraction

Phenolic compounds from treated and untreated OMW were extracted according to Leouifoudi et al. procedure (Leouifoudi et al., 2015). The pH of the samples was adjusted to 2 to assure the best recovery of phenols (Niaounakis et al., 2006). OMW sample was then defatted with hexane (95%, ACS, USA) (1:1 v/v). After shaking with hexane for 15 min, wastewater was centrifuged at 4500 rpm for 15 min. Clarified and defatted phenolic compounds in olive mill wastewaters were then extracted twice by liquid-liquid extraction using ethyl acetate (99.5%, FICHER CHEMICAL, India) (1:1 v/v), then centrifuged at 4500 rpm for 10 min, after shaking for 10 min. Ethyl acetate extracts were concentrated to dryness using rotary evaporator (RE 300, MESLO, Cyprus) at 40°C. The dried residues were then dissolved in 10 mL methanol (HPLC grade, ACS, USA) and used for subsequent analysis.

2.6.1.2 Total Phenolic Content Determination

Folin ciocalteau colorimetric method (also called the Gallic acid equivalence method GAE) was used for total phenolic compounds determination in this study. Generally, Gallic acid (3,4,5-trihydroxybenzoic acid) presented in Figure 17, was used as standard reference compound and results were stated as (mg/L) GAE. Folin ciocalteau (FC) reagent contains phosphomolybdic/phosphotungstic mixed acids with the following formulas: $3H_2O.P_2O_5.13WO_3.5MoO_3.10H_2O$ and $3H_2O.P_2O_5.14WO_3.4MoO_3.10H_2O$ (Person, 1979).

In alkaline medium, phenolic compounds are not protonated, so oxidation reduction reaction take place, where electrons transfer from phenolic compounds to reduce phosphomolybdic/phosphotungstic mixed acids to blue complexes to facilitate it's detected by spectrophotometer (Singleton et al., 1999).

According to John *et al* procedure (John et al., 2014), 1 mL of Gallic acid (99%, XILONG, China) standard solutions (100, 200, 300, 400, 500 mg/L), OMW samples or blank was added to 9 mL of deionized water in 25 mL volumetric flask. Blank solution was prepared from deionized water. 1 mL of folin (Merck KGaA, Germany) was added to each sample. After shaking for 5 minutes, 10 mL of 7% Sodium carbonate (Na_2CO_3) (analytical reagent grade, FISCHER Chemicals, china) was added to the above mixture and then completed to the mark with deionized water. The mixtures were kept in dark for 90 minutes to prevent light decomposition of FC reagent hindering its reaction with phenols. The absorbance was measured against the blank at 550 nm using spectrophotometer (SpectroDirect-Lovibond single-beam, UK) and experiment was repeated triplicate.

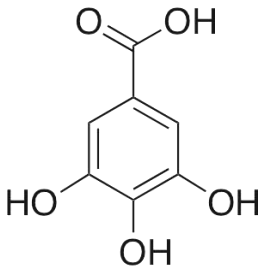

Figure 17: Structural formula of Gallic acid

2.6.2 Determination of COD

Chemical oxygen demand (COD) was measured according to the standard methods of the examination of water and wastewater and each measurement was repeated triplicate. 2.5 mL of diluted samples were added to a commercially available COD kits (lovibond vario, UK), digested for 2 hours at 148^{o}C using COD digester (MACHEREY-NAGEL, NANOCOLOR VARIO COD reactor, Germany) and cooled slowly to room temperature to avoid precipitate formation. COD was then measured using COD photometer (MD 100, Lovibond, UK) as described in Figure 18.

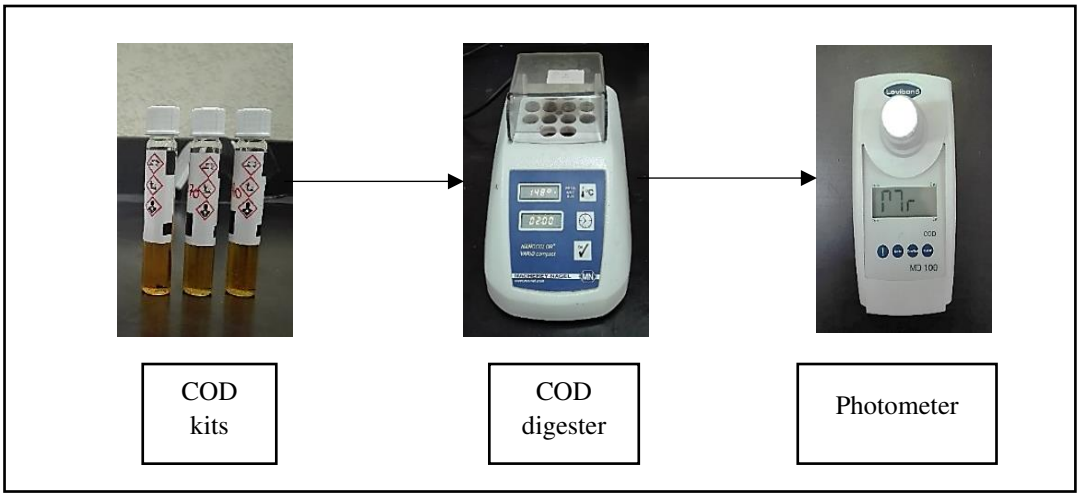

Figure 18: Schematic diagram for determination of COD

2.6.3 Determination of TSS

Total suspended solid was determined according to the standard methods of the examination of water and wastewater and each experiment was repeated triplicate. 5 ml portions of well mixed wastewater samples were filtered through a pre-weighted filter paper

by suction filtration. Filter paper was then dried to a constant weight at 100°C, cooled in desiccator and weighted. The cycle of drying, desiccating, weighing was repeated until a constant weight was achieved.

2.6.4 Determination of Residual Iron

Investigation of the residual iron by inductively coupled plasma technique (ICP), demands complete dissolution (digestion) of the element into a solution. In this study, acid digestion was conducted according to the standard methods of the examination of water and wastewater. 10 ml of pretreated OMW samples (the first sample was pretreated by adding a flocculent while the second sample was pretreated without adding a flocculent) were transferred to clean beakers. In the fume hood, 5 ml of concentrated nitric acid (HNO_3) (69-71%, SDFCL, India) was added to each pretreated sample and covered with watch glass. On a hot plate, the samples were evaporated to about 3 ml. After cooling, 10 ml of nitric acid and 10 ml of perchloric acid ($HClO_4$) (analytical grade 70-72%, Xilong, china) were added and evaporated gently. Another 10 ml of nitric acid was added until the appearance of clear solution. The solutions were then cooled and diluted to 50 ml with deionized water then boiled to expel any chlorine or oxides of nitrogen. After that the solutions were filtered, transferred to 100 ml volumetric flasks and completed to the mark. Mixed thoroughly and used for determination of ferric ion concentration by inductively coupled plasma technique (QUANTIMA, GBC, Australia) located in the University of Jordan.

Chapter Three: Results and Discussion

3.1 Characterization of OMW

The OMW used in this study was analyzed before any treatment for pH, TSS, TPC and COD, the literature values and experiments values are shown in Table 3. Calibration curve of Gallic acid was used to estimate TPC and is presented in Appendix A. It is worth noting that experimental results are in good agreement with values reported in literature.

Table 3: Some physical and chemical characteristics of OMW

Parameter	Unit	Experimental Values (this study)	Literature values	References
pH initial	_	5.0-5.5	5.04	Nassar et al., 2014
			5.1-5.5	Papaphilippou et al., 2013
			5.4-6.3	Azzam, 2018
TSS	g/L	46 - 68	21	Azzam, 2018
			17.6 - 56.7	Papaphilippou et al., 2013
			51	Nassar et al., 2014
TPC	mg/L	170 - 206	250-350	Azzam, 2018
			360	Azzam et al., 2015
			179	Hodaifa et al., 2015
COD	g/L	125 -150	153	Nassar et al., 2014
			118.8	Rusan et al., 2015
			140	Azzam et a., 2010

3.2 Pretreatment and Optimization of Coagulation / Flocculation / Sedimentation Processes

3.2.1 The Effect of Rapid Mixing Time and Speed

Rapid mixing stage offers quick and uniform distribution of chemical coagulant that enhances the destabilization of colloidal particles present in OMW (Pongchalermporn, 2002). Throughout this stage 2000 mg/L ferric chloride hexahydrate was added to intensively mixed wastewater where pH was adjusted to 7.0. The effect of rapid mixing time and speed were tested between 80 to 250 rpm and for a period between 1 to 6 min using Jar test apparatus.

The results are shown in Figure 19, indicating that the best rapid mixing time was 5 min with 95%, 42% and 26% TSS, COD and TPC removal, respectively with sludge volume of 76 ml (Table 4). When the best rapid mixing speed was 200 rpm with 94%, 39% and 36% TSS, COD and TPC removal respectively as shown in Figure 20, the sludge volume was 123 ml (Table 4). Tasdemir et al. in 2016 reported the same results of 5 min and 200 rpm as optimum mixing time and speed for the rapid mixing stage (Tasdemir et al., 2016).

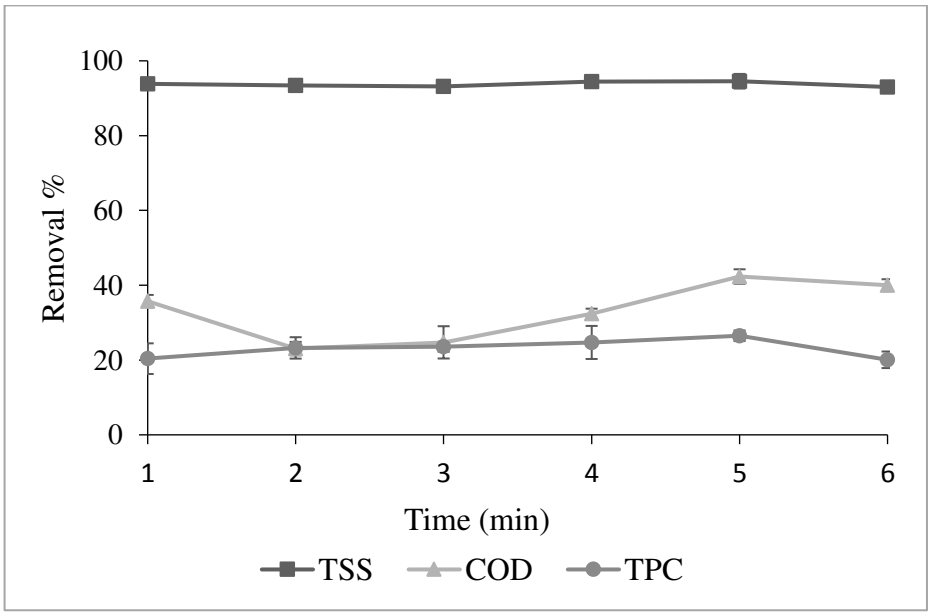

Figure 19: Percentage removal of TSS, COD and TPC at optimum rapid mixing time with rapid mixing speed of 150 rpm, ferric chloride dose of 2000 mg/L, pH 7.0, slow mixing time of 20 min at 200 rpm and settling time of 30 min

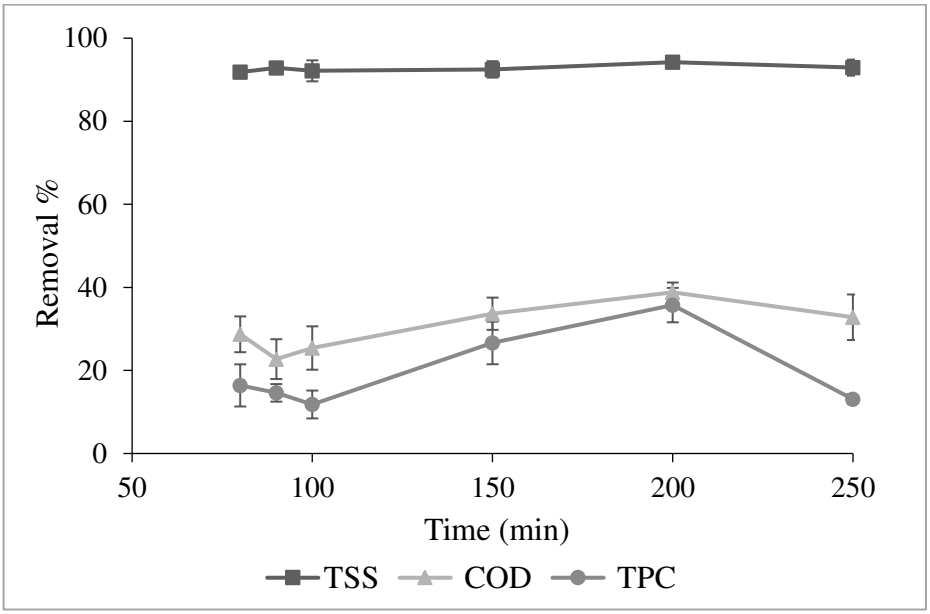

Figure 20: Percentage removal in TSS, COD and TPC at optimum rapid mixing speed with rapid mixing time of 5 min, ferric chloride dose of 2000 mg/L, pH 7.0, slow mixing time of 20 min at 200 rpm and settling time of 30 min

3.2.2 The Effect of Slow Mixing Time and Speed

Slow mixing is responsible for aggregation of destabilized particles to form a settable mass (Pongchalermporn, 2002). During this stage slow mixing speed was varied from 10 to 60 rpm and a duration of 5 to 45 min. 2000 mg/L of ferric chloride was added to 500 ml of OMW with adjusted pH of 7.0. The rapid mixing speed and time used in this stage were 200 rpm and 5 min respectively. Figure 21 represents the effect of slow mixing time. The optimum time was found to be 20 min with 95%, 43% and 17% TSS, COD and TPC removal percent respectively and 78 ml sludge volume (Table 4). While Figure 22 shows the optimum slow mixing speed of 30 rpm with 98%, 52% and 36% TSS, COD and TPC removal percent respectively and 92 ml sludge volume (Table 4). Our results are in agreement with Rui et al. in 2012 for wastewater treatment optimization (Rui et al., 2012).

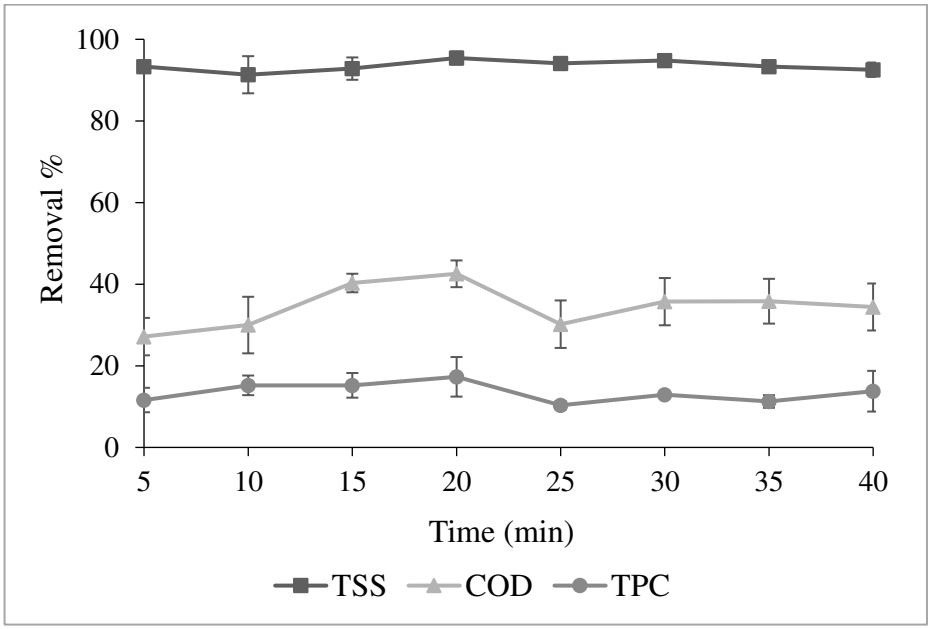

Figure 21: Percentage removal in TSS, COD and TPC at optimum slow mixing time with slow mixing speed of 20 rpm, ferric chloride dose of 2000 mg/L, pH 7.0, rapid mixing time of 5 min at 200 rpm and settling time of 30 min

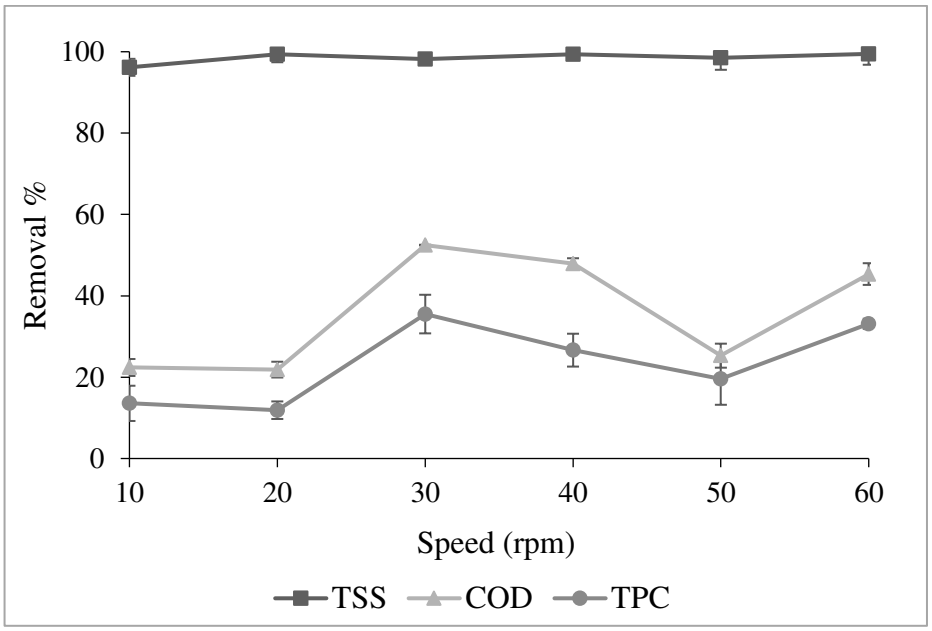

Figure 22: Percentage removal in TSS, COD and TPC at optimum slow mixing speed with slow mixing time of 20 min, ferric chloride dose of 2000 mg/L, pH 9.0, rapid mixing time of 5 min at 200 rpm and settling time of 30 min

3.2.3 The Effect of pH

The pH of OMW was adjusted from 1 to 11 using 1 M NaOH or 1 M HCl solutions. The optimum pretreatment pH was tested using jar test apparatus at the optimum coagulation/ flocculation/ sedimentation test conditions (rapid mixing speed of 200 rpm for 5 min, slow mixing speed of 20 rpm for 20 min, ferric chloride dose of 2000 mg/L and settling time of 30 min). As shown in Figure 23, the best pH value was found to be 7.0 with 98%, 31% and 36% TSS, COD and TPC removal percentage respectively and 90 ml sludge volume (Table 4). The same result for pH was reported by Rui et al. for treatment of Leachate wastewater with ferric chloride combined with micro zeolite (Rui et al., 2012). This can be explained based on the speciation diagram of the hydrated ferric ions (Figure 24). The predominant hydrated species of ferric ions at 2000 mg/L dosage and pH of 7.0 is $Fe(OH)_{3(s)}$ and $Fe(OH)_2^+$, thus the expected coagulation mechanism is a combination of sweep flocculation, adsorption and charge neutralization. At high concentration of $FeCl_3$, ferric hydroxide $Fe(OH)_{3(s)}$ precipitate will be formed and enmesh the colloidal particles by electrostatic attraction during or after its formation thus the colloidal particles will be removed by sweep flocculation. Moreover, at pH 7.0 $Fe(OH)_3$ will be positively charged i.e. $Fe(OH)_2^+$ since its pH_{PZC} is equal to 8.5 (Ghernaout et al., 2012). Consequently, it can be adsorbed on the surfaces of negatively charged colloidal particles thus neutralize their charge, decrease their electrostatic repulsion and increase the removal of COD and TPC (Ghernaout et al., 2012). At pH values lower than 7.0, the expected mechanism is only adsorption and charge neutralization with no evidence for the role of sweep flocculation mechanism. The positively charged species i.e. $Fe(OH)_2^+$ and $Fe(OH)^{2+}$ get adsorbed on the colloidal or suspended particles, neutralize their charges and enhance their agglomeration (Ghernaout et al., 2012). On the other hand, at pH values higher than 7.0, the dissociated ferric ion hydrolyze to produce negatively charged ferric hydroxide that can poorly destabilize the negatively charged colloidal system by charge neutralization or adsorption

mechanisms so decrease in the removal efficiencies of COD and TPC was observed. Thus, the expected mechanism is electrical double layer compression in which destabilization of colloid is achieved via increasing in the ionic strength of solution. The compression of electrical double layer allows colloidal particles to predominate the attractive van der Waal forces over electrostatic repulsive forces to achieve flocculation (Ghernaout et al., 2012).

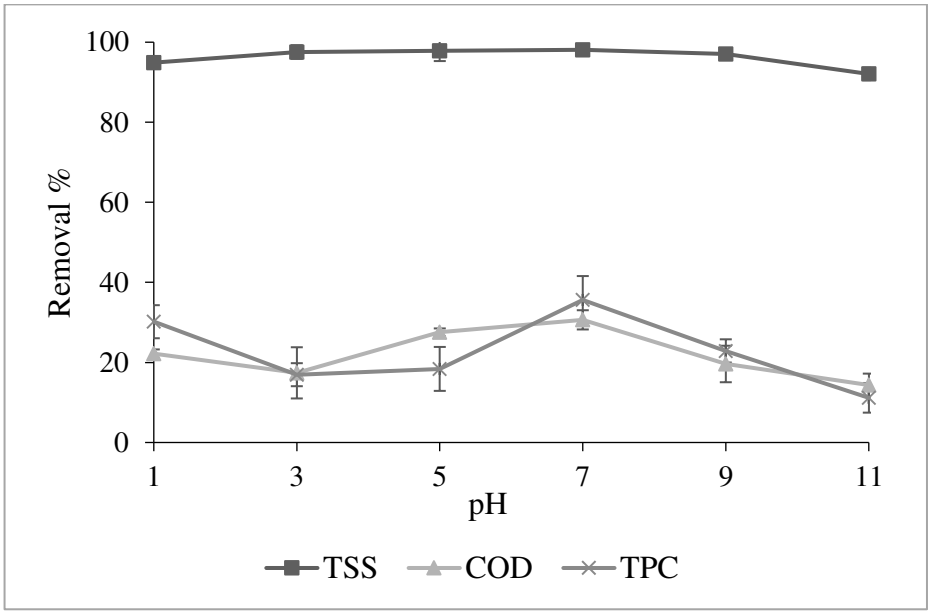

Figure 23: Percentage removal in TSS, COD and TPC at optimum pH with slow mixing speed of 20 rpm, slow mixing time of 20 min, ferric chloride dose of 2000 mg/L, rapid mixing time of 5 min at 200 rpm and settling time of 30 min

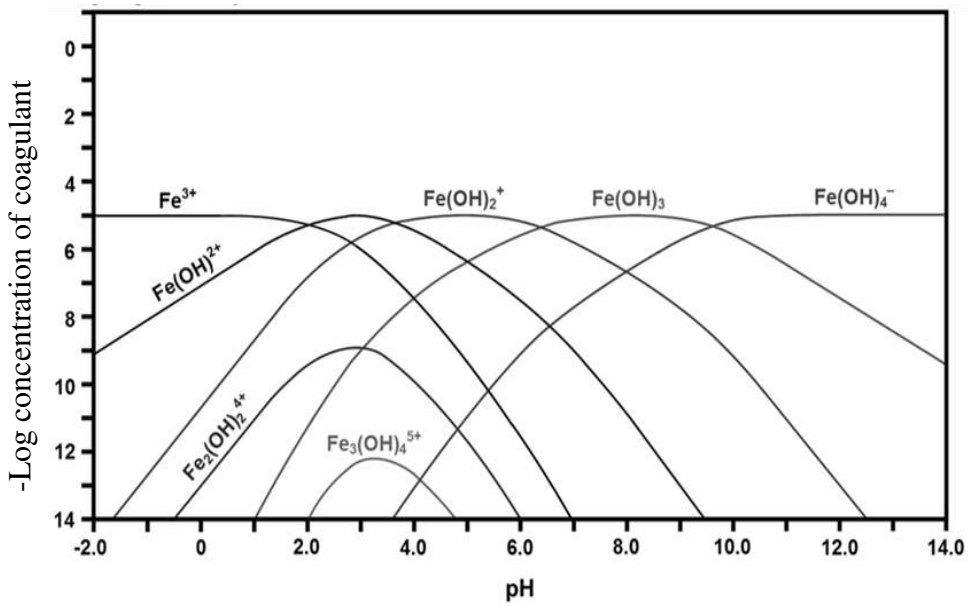

Figure 24: Speciation diagram for the hydrated ferric ions (Channei et al., 2017)

3.2.4 Coagulant Dosages

Positively charged coagulant was used to neutralize the negatively charged colloidal or suspended particles present in OMW to destabilize the colloid or suspension by reducing the repulsive forces between the negatively charged particles followed by flocculation or aggregation of the destabilized particles to form flocs that successively settled down and separated (Lee et al., 2014).

Different ferric chloride coagulant concentrations of 0, 1000, 2000, 3000, 4000 and 5000 mg/L were added at rapid mixing speed of 200 rpm for 5 min followed by slow mixing speed of 20 rpm for 20 min. After 30 min settling time the TSS, COD and TPC removal percentages were found to be 97%, 36% and 28% respectively obtained for the best coagulant dose of 3000 mg/L as shown in Figure 25. The sludge volume was 110 ml as shown in Table 4. This results agree with the results found by Rui *et al* for treatment of Leachate wastewater with ferric chloride combined with micro zeolite (Rui et al., 2012), Yazdanbakhsh et al. for OMW treatment with ferric chloride coagulant (Yazdanbakhsh et al., 2015) and Ozan Eskikaya et al. for post treatment of OMW with ferrous sulphate (Ozan Eskikaya et al., 2017).

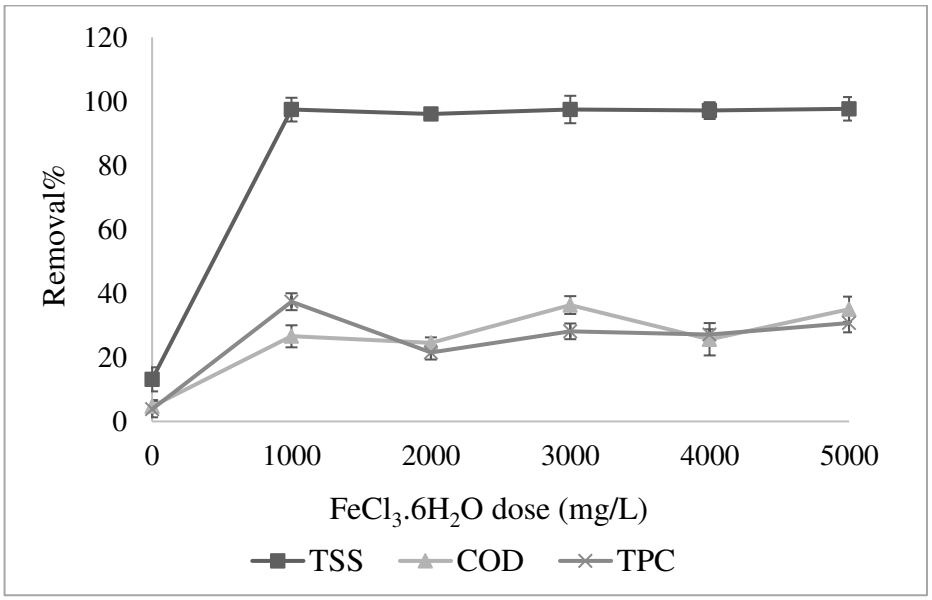

Figure 25: Percentage removal in TSS, COD and TPC for the optimum coagulant dose, slow mixing speed of 20 rpm for 20 min, pH 9.0, rapid mixing time of 5 min at 200 rpm and settling time of 30 min

3.2.5 Settling Time

Settling time was varied from 10 to 60 min and the optimum value was found to be 50 min where the TSS, COD and TPC removals were 99%, 36% and 28% respectively as presented in Figure 26 with sludge volume of 62 ml as presented in Table 4.

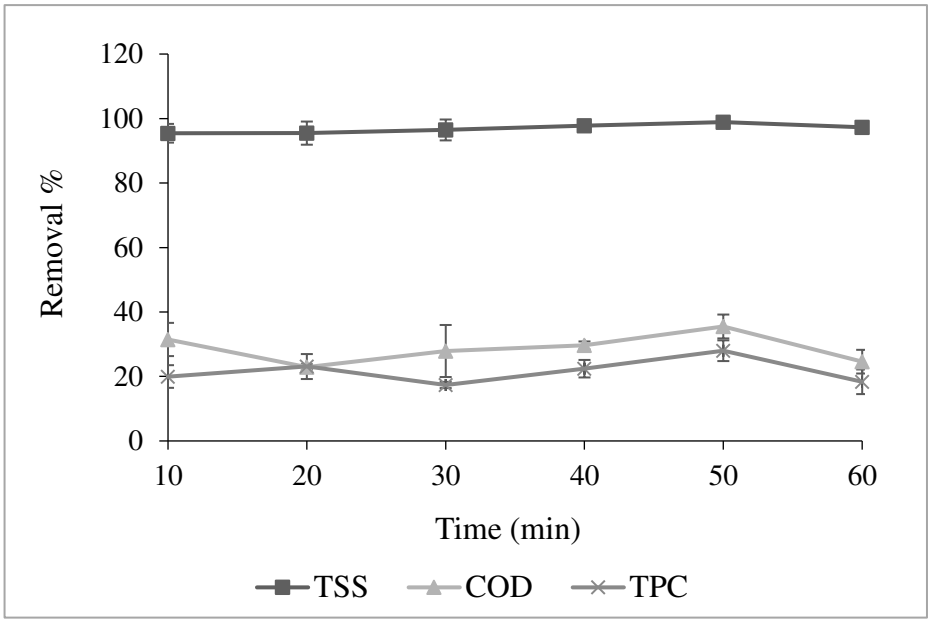

Figure 26: Percentage removal in TSS, COD and TPC at optimum settling time, slow mixing speed of 30 rpm for 20 min0.., pH 7.0, coagulant dose of 4000 mg/L rapid mixing time of 5 min at 200 rpm

3.2.6 Flocculent Dosages

Flocculent polymer was added to enhance and increase the settling rate of flocs. Numerous studies were conducted by combining polymeric flocculent and chemical coagulant in OMW treatment (Pelendridou et al., 2014 and Hodaifa et al., 2015).

The best flocculent dose was determined by adding 0.5%, 1%, 1.25%, 1.50%, 1.75% and 2% by volume of polymeric flocculent doses with 3000 mg/L coagulant dose, rapid mixing time and speed of 5 min and 200 rpm respectively, slow mixing time and speed of 20 min and 30 rpm respectively, pH of 7.0 and 50 min settling time. The best polymeric flocculent dose was found to be 1% by volume as shown in Figure 27 with TSS, COD and TPC of 99%, 48% and 44% respectively and sludge volume of 23 ml (Table 4). The high

removal efficiencies, sharp reduction in the sludge volume and vast strength of the flocs can be attributed to the predominant mechanism of combined adsorption and interparticle bridging (Ghernaout et al., 2012). The destabilization of colloidal system occurs by binding the colloidal or suspended particles with the polymer on its reactive groups. Many particles bring together or bridged by the polymer, which increases the mass of the colloidal particles and enhances their sedimentation. A reduction in the removal efficiencies was noticed at lower polymer dose due to inefficient bridging of all colloidal particles present in OMW and at higher dosage of polymer due to re-stabilization of the colloid that can occur by using high polymeric flocculent doses. Figure 28 shows the efffect of polymeric flocculant dose on the intensity of the supernatent color after coagulation/ floculation/ sedimentation processes.

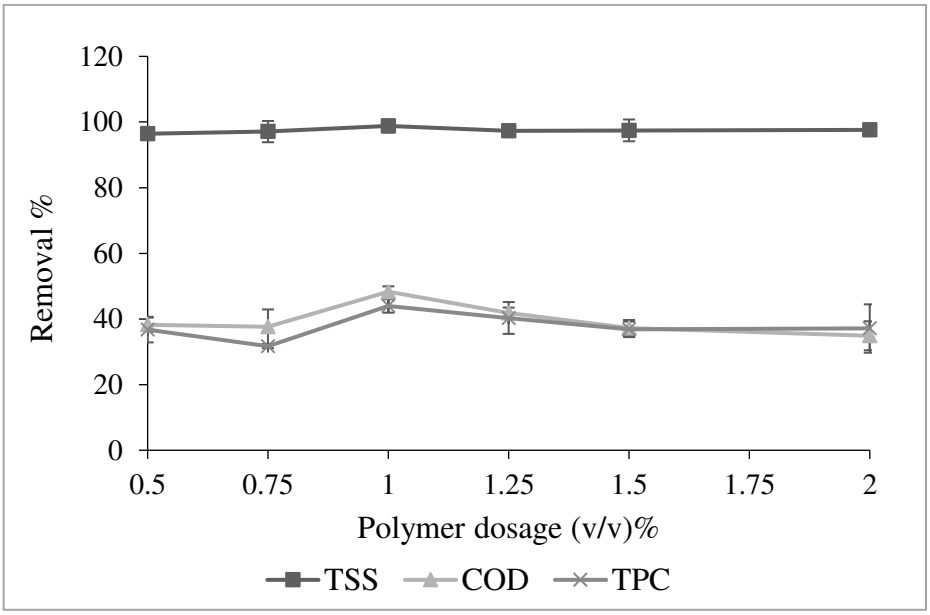

Figure 27: Percentage removal in TSS, COD and TPC at optimum polymer dose, slow mixing time of 20 min at 30 rpm, pH 7.0, coagulant dose of 3000 mg/L rapid mixing time of 5 min at 200 rpm, and settling time of 50 min

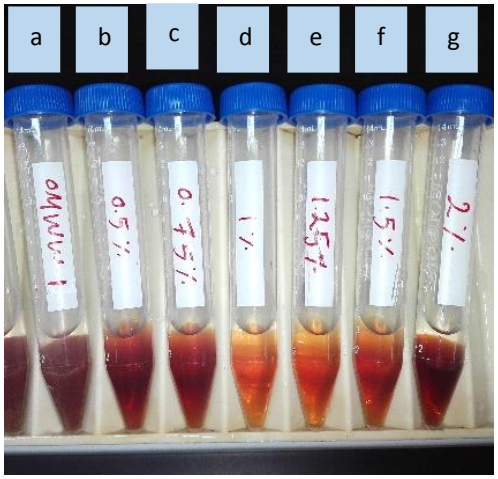

Figure 28: The color effect of different flocculent doses with 1% (v/v) as best dose, (a) untreated OMW, (b) 0.5% (v/v), (c) 0.75% (v/v), (d) 1% (v/v), (e) 1.25% (v/v), (f) 1.5% (v/v), (g) 2% (v/v)

Table 4: Sludge volume for all parameter tested in coagulation/ flocculation/ sedimentation processes

Parameter		Sludge volume (mL)
Rapid mixing speed (rpm)	80	97 ± 7
	90	81± 7
	100	77± 3
	150	88 ± 4
	200	123 ± 7
	250	85± 5
Rapid mixing time (min)	1	63 ± 7
	2	55 ± 6
	3	60 ± 2
	4	57 ± 9
	5	76 ± 5
	6	61 ± 4
Slow mixing speed (rpm)	10	85 ± 6
	20	82 ± 9
	30	92 ± 9
	40	78 ± 9
	50	62 ± 9
	60	52 ± 9

Parameter		Sludge volume (mL)
Slow mixing time (min)	5	55 ± 6
	10	75 ± 6
	15	73 ± 9
	20	78 ± 3
	25	68 ±9
	30	72 ±9
	35	67 ± 9
	40	70 ± 6
pH	1	82 ± 9
	3	92 ± 9
	5	95 ± 6
	7	97 ± 7
	9	72 ± 9
	11	48 ± 9
Coagulant dose (mg/L)	0	9 ± 2
	1000	68 ± 9
	2000	85 ± 6
	3000	110 ± 11
	4000	65 ± 6
	5000	75 ± 10
Flocculent dose (v/v)%	0.5	10 ± 3
	0.75	18 ± 3
	1	23 ± 3
	1.25	17 ±3
	1.5	14 ± 4
	2	16 ± 5
Settling time (min)	10	102 ± 9
	20	87 ± 9
	30	65 ± 6
	40	63 ± 7
	50	62 ± 12
	60	60 ± 11

3.2.7 Determination of Residual Coagulant

The aim of determining the residual iron in the supernatant of treated OMW is to ascertain the correctness of the chosen coagulant dose (Aguilar et al., 2005). The results showed that the residual iron concentrations that remains in the supernatant are 155.4 mg/ L and 408.8 mg/ L for combined chemical coagulant with polymeric flocculent and for using coagulant alone, respectively. The results indicated that more than 85% of the added coagulant was involved in the neutralization of the negatively charged suspended or colloidal particles thus confirm the sweep flocculation mechanism. Moreover, adding polymeric flocculent increases the efficiency of coagulation/ flocculation/ sedimentation processes.

3.2.8 Summary

Coagulation/ flocculation/ sedimentation processes were optimized using jar test apparatus and the best conditions were determined and presented in Table 5.

Table 5: The optimum parameters of coagulation/ flocculation/ sedimentation processes

Parameter	Optimum value
Rapid mixing time	5 min
Rapid mixing speed	200 rpm
Slow mixing time	20 min
Slow mixing speed	30 rpm
pH	7.0
Coagulant dose	3000 mg/L
Flocculent dose	1% by weight
Settling time	50 min

At the optimum parameters the TSS, COD and TPC removal percentages were 99%, 48% and 44% respectively, with sludge volume of 23 ml. Figure 29 shows the difference in color between raw and pretreated OMW. The pH after coagulation/ flocculation/ sedimentation processes conducted at the optimum conditions was 5.3, this is due to formation of ferric hydroxide precipitate that decrease the concentration of [OH^-] in the solution thus decrease its pH.

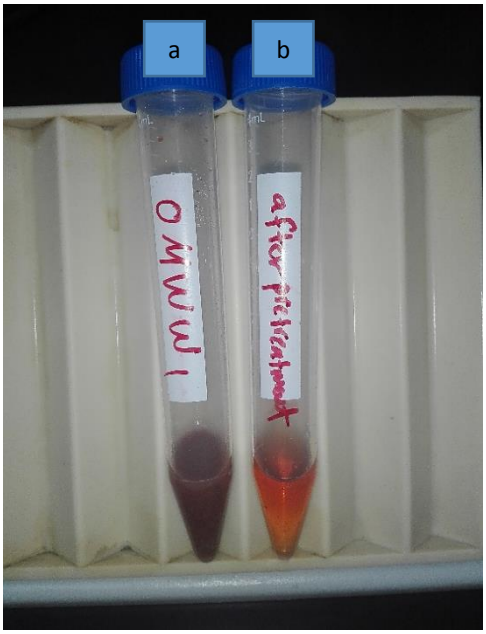

Figure 29: The effect of OMW pretreatment on the color, (a) untreated OMW, (b) OMW after pretreatment

3.3 Materials Characterization

3.3.1 Characterization of Volcanic Tuff (VT) before and After Activation

Activated and non-activated Volcanic Tuff were characterized using pH_{PZC}, BET, SEM, XRD and XRF based on these results the best activation conditions in removing COD and TPC from OMW were used.

3.3.1.1 Point of Zero Charge (pH_{pzc})

Point of zero charge (pH_{pzc}) is defined as the pH at which the net electrical charge density on adsorbent surface is zero. Above this value, the surface is negatively charged,

and below this value it is positively charged. To understand the adsorption behavior of different VT samples, the pH_{pzc} was measured using pH drift method. As presented in Figure 30 the pH_{pzc} for untreated VT was 8.8, which is compatible with the result attained by Claudia et al. (Claudia et al., 2015). The pH_{PZC} were 9.2, 7.0, 3.4, 3.4 and 3.7 for VTC, VTA2C, VTA24C, VTA48C and VTA72C respectively. The results indicate that calcination process did not affect the charge of the surface, may be because calcination process didn't lead to substitution of the surface metals as indicated by XRF. On the other hand, treatment with sulfuric acid followed by calcination led to decreases the pH_{PZC} values and the reduction increases as acid impregnation period increases. However, no significant changes in the pHpzc was noticed after 24 hr of impregnation period.

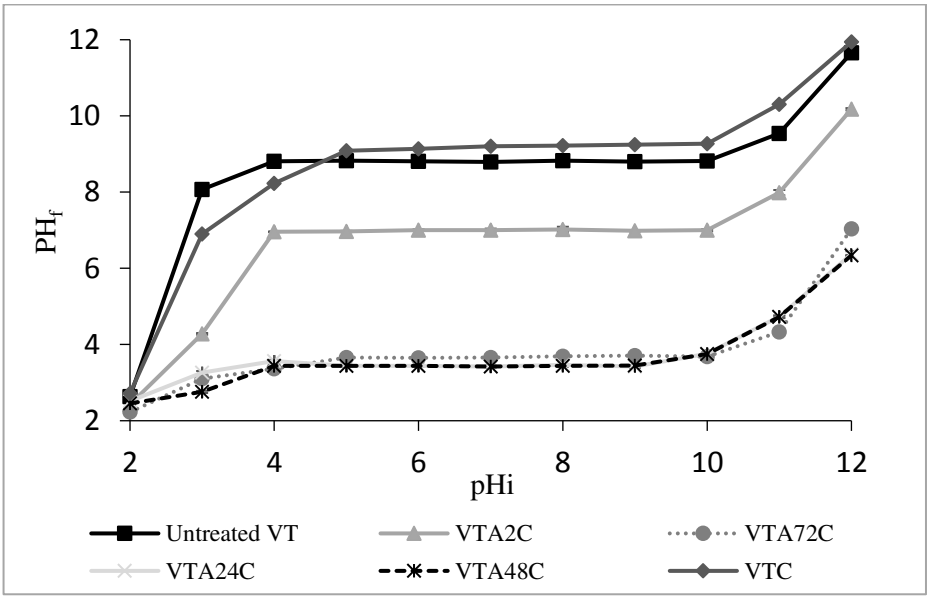

Figure 30: Point of zero charge for all VT samples

3.3.1.2 Surface Area

BET method was used to determine the surface area, total pore volume and pore size for activated and non-activated VT samples, at two different particle size ranges of 125-150 µm and <45 µm. As shown in Table 6, surface area values are inversely related with particles size. Untreated VT has very low surface area of 1.4 m^2/g and 1.5 m^2/g for 125-150 µm and <45 µm particle size ranges, respectively. These values are comparable to

values reported by Reddy & Claassen (Reddy & Claassen, 1994) in which they tested the surface area for zeolite and some standard minerals such as labradorite and augite with particle size less than 212 μm. Activation of the samples increased their surface area. However, the mesoporosity nature (having pore size between 2-50 nm) of the samples was almost attained (Zdravkov et al., 2007).

Table 6: Surface area, total pore volume and pore size for all VT samples with two particle size ranges

Sample	Particle size (μm)	Surface area (m^2/g)	Total pore volume (cc/g)	Pore size (nm)
Untreated VT	125-150	1.4	4.4×10^{-3}	12.4
VTC	125-150	1.8	3.7×10^{-3}	8.2
VTA2C	125-150	23.6	15.0×10^{-3}	2.6
VTA24C	125-150	18.6	16.7×10^{-3}	3.5
VTA48C	125-150	16.8	15.1×10^{-3}	4.5
VTA72C	125-150	5.5	7.0×10^{-3}	5.1
Untreated VT	<45	1.5	5.1×10^{-3}	13.9
VTC	<45	.23	$.75 \times 10^{-3}$	13.3
VTA2C	<45	87.0	62.0×10^{-3}	2.9
VTA24C	<45	60. 3	58.0×10^{-3}	3.8
VTA48C	<45	52.9	46.0×10^{-3}	1.7
VTA72C	<45	29.0	29.0×10^{-3}	4.0

3.3.1.3 Scanning Electron Microscopy (SEM)

Scanning Electron Microscope (SEM) images of all VT samples are presented in Figure 31. SEM image for untreated VT exhibits low crystallinity and irregularity in the particles shape (Figure 31-a). The crystallinity was slightly enhanced by thermal activation (calcination) but the shape still irregular (Figure 31-b). SEM image for VT that was

activated by acid impregnation for 2 hr followed by calcination also displays irregularity in the particles shape however, the homogeneity in the size and crystallinity was slightly enhanced (Figure 31-c). On the other hand, SEM images for VT samples that were activated with acid impregnation for 24, 48 and 72 hr followed by calcination offered higher crystallinity (Figure 31-d to f).

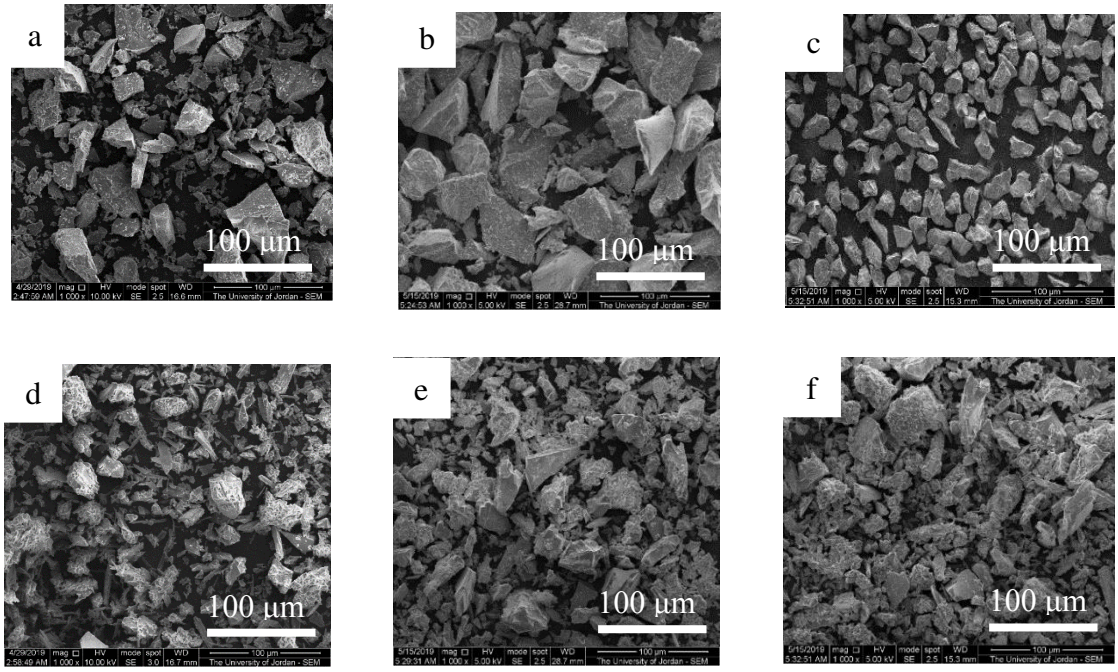

Figure 31: SEM images for (a) untreated VT, (b) VTC, (c) VTA2C, (d) VTA24C, (e) VT48C, (f) VTA72C

3.3.1.4 X-Ray Diffraction Pattern (XRD)

As shown in Figure 32, the XRD patterns for VT before and after activation reveal that all VT samples are rich in Clinopyroxene (Augite) with a formula (Ca, Mg, Fe)(Mg, Fe)Si_2O_6 and Plagioclase (Labradorite) with a formula of (Ca, Na)(Al, Si)$_4O_8$, that considered as non zeolitic minerals (Searle, 1961). However, the spectrum of VTA72C indicates that new phase of gypsum ($CaSO_4.2H_2O$) was occurred through activation by the reaction between Ca^{2+} from VT and SO_4^{2-} from sulfuric acid used for activation. The absence of gypsum peaks in VTA2C, VTA24C and VTA48C spectra may indicates that gypsum needs impregnation of VT in sulfuric acid for 72 hr to crystalline. In addition to

that, Untreated VT exhibits low crystallinity while activated samples had higher crystallinity since their main peaks showed an increase in their intensities.

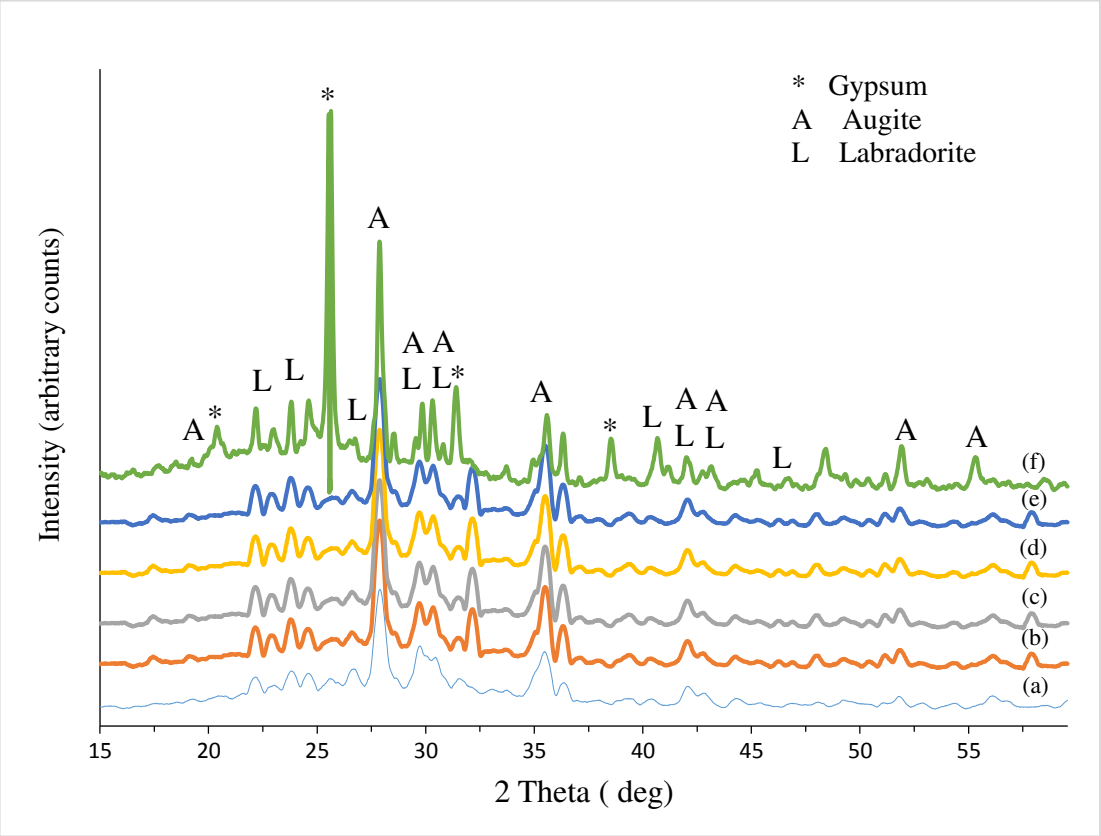

Figure 32: XRD patterns of all volcanic tuff samples (a) untreated VT, (b) VTC, (c) VTA2C, (d) VTA24C, (e) VTA48C, (f) VTA72C

3.3.1.5 X-ray Fluorescence (XRF)

The chemical composition of all VT samples obtained by X-ray fluorescence (XRF) technique are shown in Table 7. It is clear that calcination process did not have a significant effect on the chemical composition of VT as Si/Al ratio remained unchanged, in contrast to combined acid impregnation and calcination that led to dealumination of VT as Si/Al ratio increased twice than in the untreated or calcinated samples. The effect of acid impregnation on decreasing the aluminum content in VT increases with increasing the acid impregnation period. Which mean that VT samples activated with acid impregnation followed by calcination are more thermally stable and attained more hydrophobic properties (Dumitriu et al., 2009). The VT content of other metal present as ions and oxides such as Fe, Mn, Na,

K…etc. was decreased after acid treatment due to chemical replacement by H^+ cations from sulfuric acid solution (Dumitriu et al., 2009).

Table 7: Chemical composition of the VT samples (%, oxide)

Component	VT sample					
	Untreated VT	**VTC**	**VTA2C**	**VTA24C**	**VTA48C**	**VTA72C**
Fe_2O_3	11.900	12.413	5.659	5.777	4.529	4.290
MnO	0.148	0.153	0.076	0.079	0.061	0.061
TiO_2	2.597	2.425	2.119	1.895	2.697	1.581
P_2O_5	0.363	0.305	0.281	0.282	0.533	0.196
SiO_2	38.961	37.689	56.789	57.058	59.751	50.075
Al_2O_3	13.434	13.211	9.949	9.590	9.203	8.327
MgO	4.085	5.088	1.494	1.980	1.502	1.573
Na_2O	3.117	3.030	1.606	1.512	1.435	1.338
CaO	8.355	8.056	11.641	7.359	9.596	10.931
K_2O	1.320	1.232	0.488	0.513	0.522	0.442
Si/Al ratio	2.900	2.853	5.708	5.950	6.493	6.014

3.3.2 Characterization of Granular Activated Carbon (GAC)

MRX-M Granular Activated Carbon (GAC) was characterized by pH_{PZC} and BET to understand the adsorption behavior of the GAC samples i.e. untreated GAC, GAC modified by base impregnation (reduced) and GAC modified by acid impregnation (oxidized). Table 8 presents the pHpzc, surface area, total pore volume and average pore size for reduced MRX-M samples. The values were compared with parameters for untreated and oxidized MRX-M that were measured in previous studies by Abu Dalo et al., 2013 and Kannan, 2017. The obtained pH_{PZC} for reduced MRX-M using pH drift method, was 9.8, compared to 7.2 and 3.1 for untreated and oxidized MRX-M, respectively. Which indicated that the chemical reduction was done appropriately. The surface area for untreated, reduced and oxidized

GAC was 904, 924 and 827, respectively. It is obvious that reduction of GAC increases the surface area may be due to breaking and widening the pores thus increases in the surface area and pore volume (Li et al., 2011) in contrast to oxidation process led to decrease in the surface area maybe due to adsorption of the nitric acid in the pores thus blocking the pores and decrease the surface area and pore volume (Chen et al., 2003).

Table 8: pH_{pzc}, surface area, total pore volume and average pore size for untreated, reduced and oxidized GAC samples

Sample	pH_{PZC}	Reference for pH_{PZC}	Surface area (m^2/g)	Total pore volume (cc/g)	Average pore size (nm)	Reference for BET analysis
Untreated GAC	7.2	Abu Dalo et al., 2013	904	472×10^{-3}	2.1	Kannan, 2017
Reduced GAC	9.8	This study	924	482×10^{-3}	2.1	Kannan, 2017
Oxdized GAC	3.1	Abu Dalo et al., 2013	827	420×10^{-3}	2.0	Kannan, 2017

3.3.3 Characterization of Magnetite (Fe_3O_4) Nanoparticles

Magnetite nanoparticles were prepared using chemical coprecipitation method. They were used in nanocomposite media preparation. To ensure that the nanoparticles were successfully prepared, size, size distribution, stability, purity, magnetization and pH_{PZC} were characterized.

3.3.3.1 Transmission Electron Microscopy (TEM)

TEM images were utilized to study the morphology, shape and size distribution of the prepared magnetite nanoparticles. Figure 33 verified that magnetite particles is in the nanoscale with an average particle size of 23 nm (estimated using ImageJ software), had spherical shape and small size distribution.

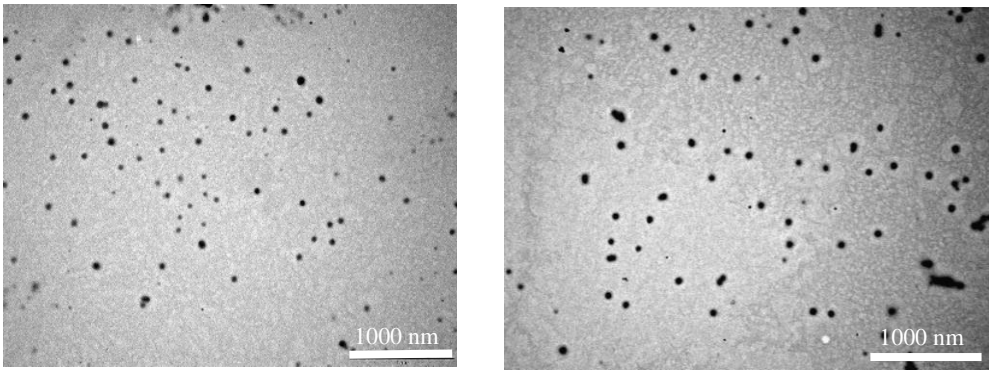

Figure 33*:* TEM images of prepared magnetite nanoparticles

3.3.3.2 Magnetization Measurement

M-H hysteresis curve of magnetite (Fe_3O_4) nanoparticles is presented in Figure 34. Symmetric hysteresis indicates ferrimagnetic behavior with saturation magnetization of 61 emμ/g comparable with the result reported by León-Félix et al. (León-Félix et al., 2013).

Ferrimagnetic (Fe_3O_4) is known to be magnetic in an applied magnetic field (up to 2000 Oe in this study) and its crystals magnetic moments of Fe (II) and Fe (III) ions are unequal in magnitude and aligned in anti-parallel direction. Since the magnetic moments are of different magnitudes in opposite directions, a net magnetic field is still present. Thus Fe_3O_4 shows ferrimagnetic behavior at room temperature.

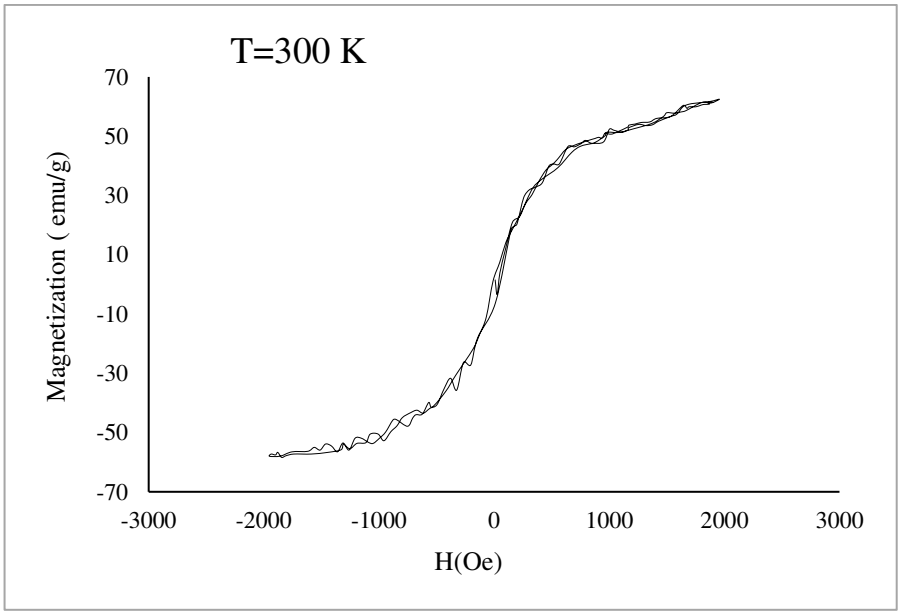

Figure 34: M-H hysteresis curve at room temperature for magnetite nanoparticles

3.3.3.3 X- ray Diffraction Pattern (XRD)

The purity of the prepared magnetite (Fe_3O_4) nanoparticles was confirmed by XRD pattern. As shown in Figure 35, the obtained peaks can be indexed at the 2 theta values of 18.2°, 30.1°, 35.5°, 43°, 53.5°and 57.1° corresponding to Miller indices of (111), (220), (311), (400), (422) and (511) respectively. This indicates the formation of crystalline magnetite with a cubic inverse spinel structure that matches well with characteristic pattern of cubic JCPDS reference code 00-001-1111 of black magnetite. Moreover, no extra peaks related to any impurities were observed in the pattern which indicates highly pure magnetic nanoparticles.

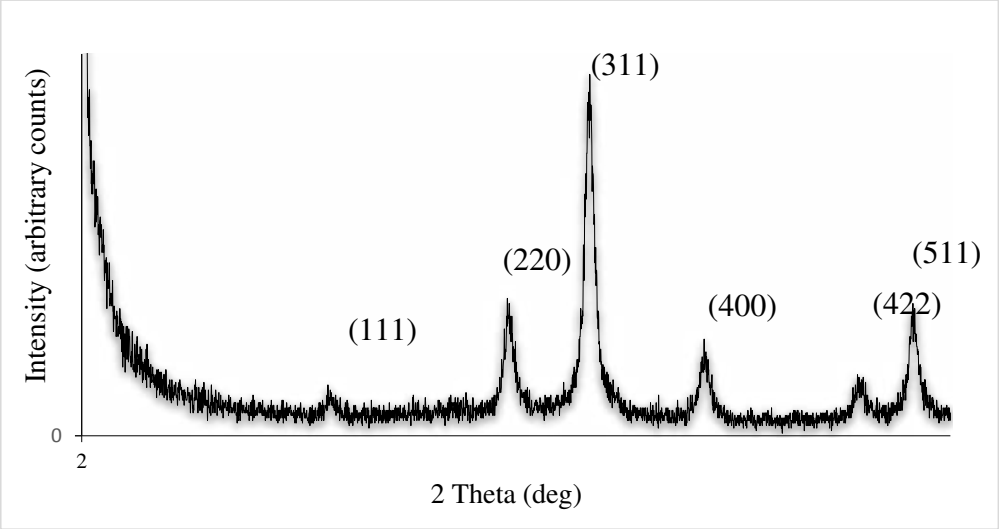

Figure 35: XRD pattern of prepared magnetite Fe_3O_4 nanoparticles

3.3.3.4 Point of Zero Charge for Magnetite (Fe_3O_4) Nanoparticles

pH_{PZC} for magnetite nanoparticles is shown in Figure 36. It was found that pH_{PZC} equals to 6.8 which means that at this pH the magnetite nanoparticle surface has FeOH neutral active site. It also indicates that the surface is negatively charged above this pH with an active surface group of FeO^- and positively charged below this pH with an active surface group of $FeOH^+$ (Ahribesh, 2016). Our finding was identical to result found for magnetite and magnetite nanoparticles pHpzc by Yean et al. (Yean et al., 2005).

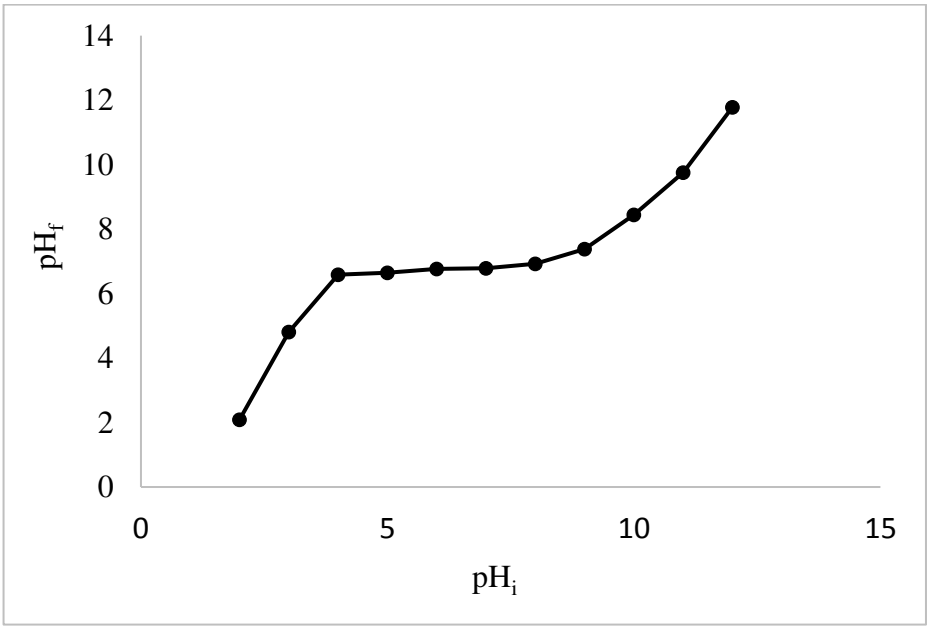

Figure 36: Point of zero charge for magnetite nanoparticles

3.3.3.5 Dynamic Light Scattering (DLS) and Zeta Potential

Hydrodynamic radius (R_H) of the hydrated Fe_3O_4 nanoparticles was found to be 253.6 nm. Comparing with TEM (23 nm), we can conclude that substantial amount of solvent binds to a surface of Fe_3O_4 nanoparticles. Zeta potential was equal -45 mV which indicates that the nanoparticles are highly stable according to Table 9 (Greenwood et al., 1999).

Table 9: The effect of colloidal stability on the magnitude of zeta potential

Zeta potential (mv)	**Stability behavior of the colloid**
from 0 to ±5,	Rapid coagulation or flocculation
from ±10 to ±30	Incipient instability
from ±30 to ±40	Moderate stability
from ±40 to ±60	Good stability
more than ±61	Excellent stability

3.3.4 Characterization of VT/Magnetite Nanocomposites

Nanocomposites were prepared using VTA24C coupled with 0.5% magnetite nanoparticles, sonicated for 1 hr at 70°C and dried in the air. Then characterized as follow:

3.3.4.1 Scanning Electron Microscope (SEM)

Figure 37 presents the SEM image of the prepared VTA24C/magnetite nanocomposites. It is obvious that magnetite nanoparticles are homogenously dispersed in the sample.

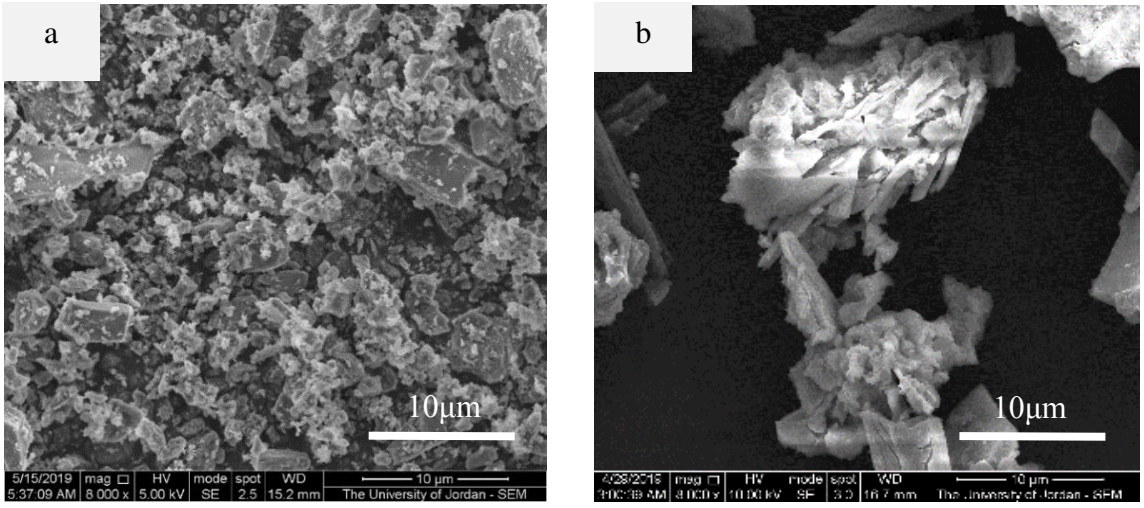

Figure 37: SEM images for (a) VTA24C/magnetite nanocomposites, (b) VTA24C

3.3.4.2 X-Ray Diffraction Pattern (XRD)

Figure 38 presents the XRD spectra for VTA24C/magnetite nanocomposites. It is obvious that the spectra of the nanocomposites matches well with the VTA24C and magnetite nanoparticles spectra. However, additional peaks appeared in the nanocomposites spectra at 2 theta = 11.5°, 20.5° and 28.9° which referred to $CaSO_4.2H_2O$ (gypsum) that formed from the interaction between Labradorite (Ca, Na)(Al, Si)$_4O_8$ or Augite (Ca, Mg, Fe)(Mg, Fe)Si_2O_6 minerals of the VT and H_2SO_4 used in VT activation. The proposed reason for the absence of this peak in the VTA24C spectra is the lack of crystallinity of the gypsum which was enhanced later by sonication process. The same secondary reaction of gypsum formation occurred through activation of volcanic ash with sulfuric acid by Djobo

in 2018 (Djobo, 2018). The formation of white gypsum explained the light colour of VT samples activated with successive acid impregnation and calcination.

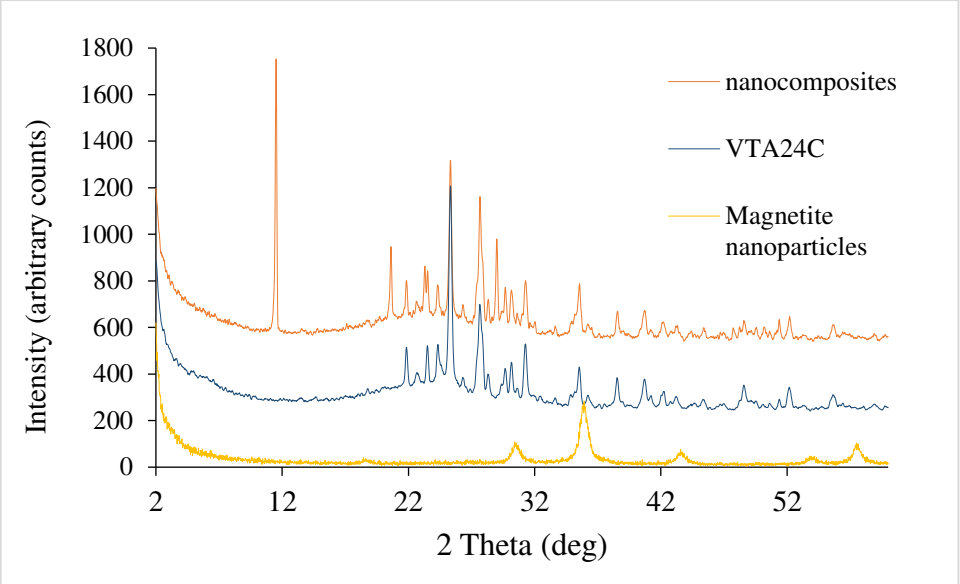

Figure 38: XRD pattern for VTA24C/magnetite nanocomposites in comparison with XRD patterns for VTA24C and magnetite nanoparticles

3.3.4.3 Surface Area

Table 10 shows the surface area, total pore volume and pore size for VTA24C/ magnetite nanocomposites and VTA24C. It is obvious that the presence of nano scaled particles with VT causes increase in the surface area, mesopores volume and diameter compared to VT alone.

Table 10: Surface area, Total pore volume and Pore size obtained from BET analysis for VT/magnetite nanocomposites

Sample	Particle size(µm)	Surface area (m^2/g)	Total pore volume (cc/g)	Pore size (nm)
VTA24C/magnetite nanocomposites	45-125	104.2	130×10^{-3}	4.9
VTA24C	<45	60. 3	58×10^{-3}	3.8

3.3.4.4 XRF

The chemical composition of VTA24C/magnetite nanocomposites in comparison to VTA24C obtained by X-ray fluorescence (XRF) technique are shown in Table 11. It is clear that the VTA24C/magnetite nanocomposites has lower Si/Al ratio than VTA24C. Which mean that VTA24C are more thermally stable and attained more hydrophobic properties (Dumitriu et al., 2009).

Table 11: Chemical composition of the VTA24C/magnetite nanocomposites and VTA24C samples (%, oxide)

Component	Sample	
	VTA24C/magnetite nanocomposites	**VTA24C**
Fe_2O_3	7.910	5.777
MnO	0.100	0.079
TiO_2	2.228	1.895
P_2O_5	0.226	0.282
SiO_2	65.566	57.058
Al_2O_3	12.008	9.590
MgO	2.065	1.980
Na_2O	1.730	1.512
CaO	6.891	7.359
K_2O	0.691	0.513
Si/Al ratio	5.434	5.950

3.4 Adsorption Evaluation via Batch Experiments

The removal of COD and TPC from OMW using untreated volcanic tuff (VT), activated VT by calcination (VTC), activated VT by acid impregnation followed by calcination (VTA2C, VTA24C, VTA48C and VTA72C), VT activated by base impregnation followed by calcination (VTB2C) and granular activated carbon (GAC) were tested through batch approach, each sample was coupled with magnetite nanoparticles to enhance its adsorption capability and each test was repeated triplicate.

3.4.1 The Effect of Different VT Activation Approaches on COD Removal from OMW

VT was subjected to different activation process and the effectiveness of VT activation approaches was investigated through testing COD removal efficiency. Screening tests were performed on three VT samples of 125-150 μm particle size to select the best media in treating pretreated OMW (pH 5.3 (the pH obtained after pretreatment without additional adjustment) and for 48 hr on shaker). 5% by weight of VT samples were activated by different activation paths i) calcination alone denoted VTC, ii) acid impregnation for 2 hr followed by calcination denoted VTA2C, iii) base impregnation for 2 hr followed by calcination denoted VTB2C. Each media was mixed with 0.5% by weight magnetite nanoparticles that believed to be a powerful adsorbent owing to their size effects. Base treated media (VTB2C) revealed low COD removal efficiency from OMW with 43% removal percentage (Figure 39) and this low efficiency is in a good agreement with the result attained by Ates and Akgül (Ates and Akgül, 2016) for zeolitic VT. The proposed explanation for that was the deformation of the structure and severe dealumination and desilication upon using high concentration of NaOH. This was confirmed by EDX analyses, in which a decrease in the VT surface area decreases the media capability for adsorption.

Calcinated (VTC) and acid treated (VTA2C) volcanic tuff had higher COD removal efficiencies in which their removal percentages were 48% and 51% respectively. Based on

the screening tests and due to the low removal efficiency of base treated VT, calcinated and acid impregnated VT were only selected for further testing. To enhance the activation process, the impregnation time was increased to 24, 48 and 72 hr then VTC, VTA2C, VTA24C, VTA48C and VTA72C were investigated.

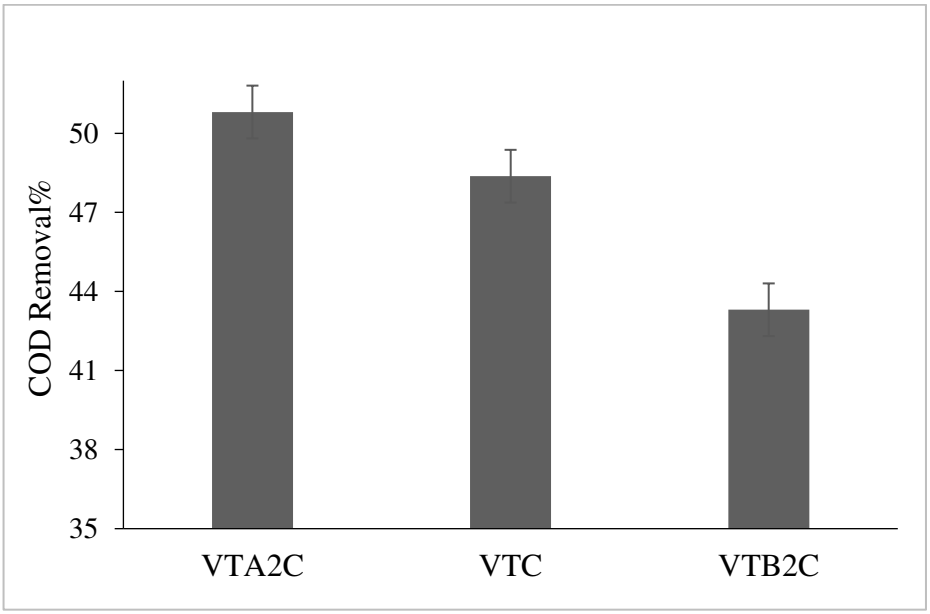

Figure 39: COD removal percentage for VTA2C, VTC and VTB2C with particle size range of 125-150 µm, magnetite dose of 0.5% by weight, pretreated OMW pH of 5.3 and contact time of 48 hr

3.4.2 Optimization of the Contact Time

To find the optimum contact time for VT activated by calcination alone and combined acid impregnation and calcination, 5% by weight of each media (VT + 1% by weight magnetite nanoparticles) was used to remove COD from pretreated OMW at pH of 5.3 with diffferent contact time (6 hr, 24 hr, 48 hr, 72 hr and 96 hr). As shown in Figure 40, untreated and calcinated VT samples requiered 48 hr to reach the equilibrim, while the contact time needed for the four samples that were activated by combined acid impregnation and calcination was 24 hr. This can be attributed to the higher surface areas of the VT samples activated by successive acid impregnation and calcination compared to those of untreated and calcinated samples.

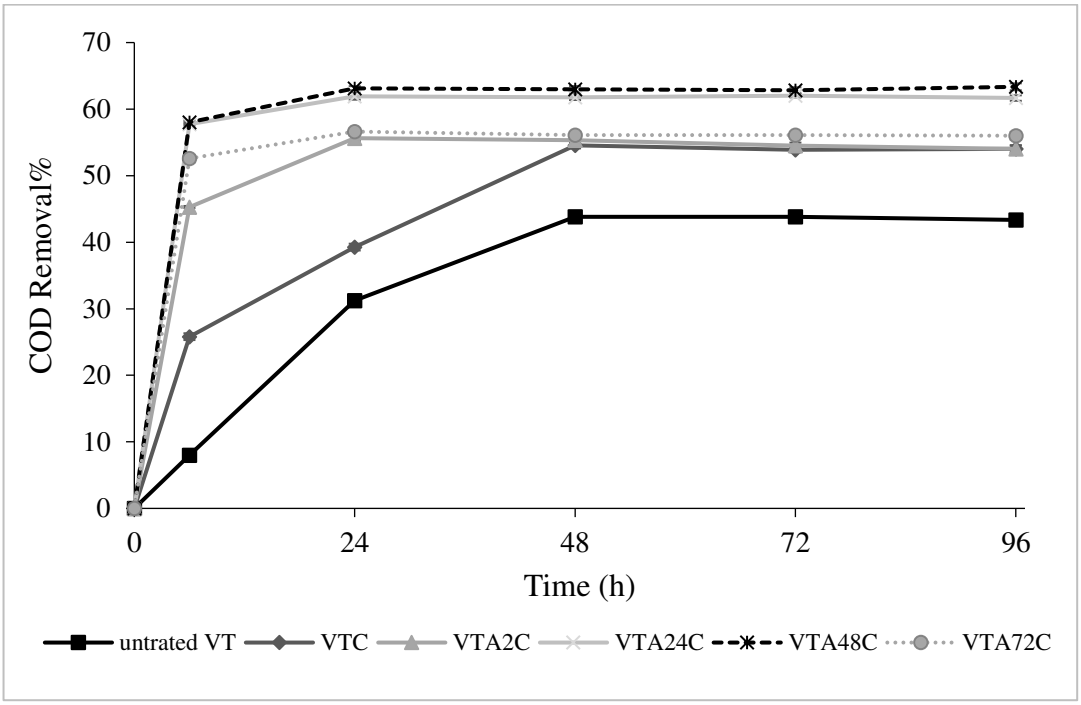

Figure 40: Contact time effect on adsorption removal of all VT samples at pH 5.3 and magnetite dose 1%

3.4.3 Optimization of the Magnetite Nanoparticles Dosage

The pretreated OMW samples at pH of 5.3 were exposed to different doses of magnetite nanoparticles (0%, 0.5%, 1%, 2%, 5% and 10% by weight) coupled with different VT. 5% by weight of the media (VT + magnetite nanoparticles) was added to each tested OMW sample. As shown in Figure 41, its obvious that 0.5% by weight was the obtimum dose of magnetite nanoparticles for all activated VT samples either by calcination alone or by combined acid impregnation and calcination while the 0% dose was the optimum for untreated VT sample. This may be due to the competion between magnetite nanaoparticles and organic compounds for surface adsorption at untreated VT thus blocked its pores and part of the external surface area. COD analysis also revealed that the adsorption capacities were approximitaly constant for magnetite nanoparticles doses higher than the optimum.

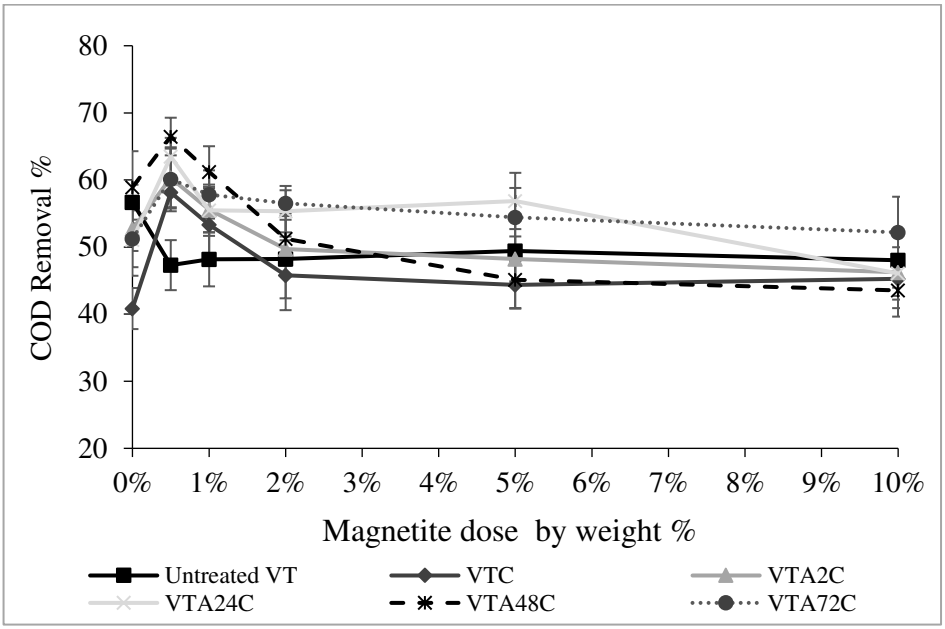

Figure 41: The effect of magnetite nanoparticles dosage on the adsorption removal of VT after 48 hr contact time at pH 5.3

3.4.4 Optimization of pH

Experiments were conducted with different OMW pH values of 2, 4, 6, 8, 10 and 12 to find the optimum pH for each adsorbent. 0.5% magnetite nanoparticles was coupled with each VT sample and used for removing COD at contact time of 48 hr. Experimental results revealed three types of adsorption behaviors according to VT activation approaches. To explain the effect of pH on COD removal; three categories of trends were chosen. The first category (Figure 42-a) comprises untreated VT whose maximum adsorption occurred at pH of 2 with COD removal percentage of 68%. This enhancement in the adsorption can be attributed to the formation of H-bonding between protonated organic and phenolic acids presented in OMW and hydrophilic sites of VT i.e. silanol or aluminol groups offered by VT surface at low pH values (Yousef & El-Eswed, 2009). While in the pH range of 4-12 the adsorption was pH independent. This behavior is expected to occur due to pH independent hydrophobic interaction of VT's hydrophobic sites and organic acids (Yousef & El-Eswed, 2009).

The second category (Figure 42-b) for VT samples activated by successive acid impregnation and calcination namely VTA2C, VTA24C, VTA48C and VTA72C whose optimum pH value was 8 with removal percentages of 69, 70, 70 and 66 respectively. In the pH range of 2-6 and 10-12 the adsorption behavior for the four samples was pH independent with hydrophobic interaction between VT and organic acids as proposed source for this behavior. At pH 8, a huge increase in the removal percentage. This behavior may be due to hydrophilic complexation reaction between organic anions and VT metals i.e. Si, Al, Fe, Ca, Na, etc. that may involve charge transfer from organic anions (carboxylic and/or phenolic groups) to the empty d-orbitals of metals present on the surface of VT. This type of interactions predominated as the pH increases due to enhancement of the electron density. However at pH > 8, the adsorption was decreased. The reduction was attributed to the replacement of surface metal ions, by H^+ thus the number of available metal ions for complexation decreased and becomes not sufficient for high concentrations of organic ions (Yousef and El-Eswed 2009).

The third category (Figure 42-c) was for VTC at optimum pH of 10 with 63% removal percentage. In the pH range of 2-8 the adsorption was pH independent due to hydrophobic interaction that doesn't depend on the pH while above pH 8, the COD removal was increased due to hydrophilic complexation reaction between organic anions and VT metals (Yousef and El-Eswed, 2009).

It seems that the removal of COD from OMW doesn't depend on electrostatic interaction between opposite charges thus insignificant effect for pHpzc values was observed on the adsorption.

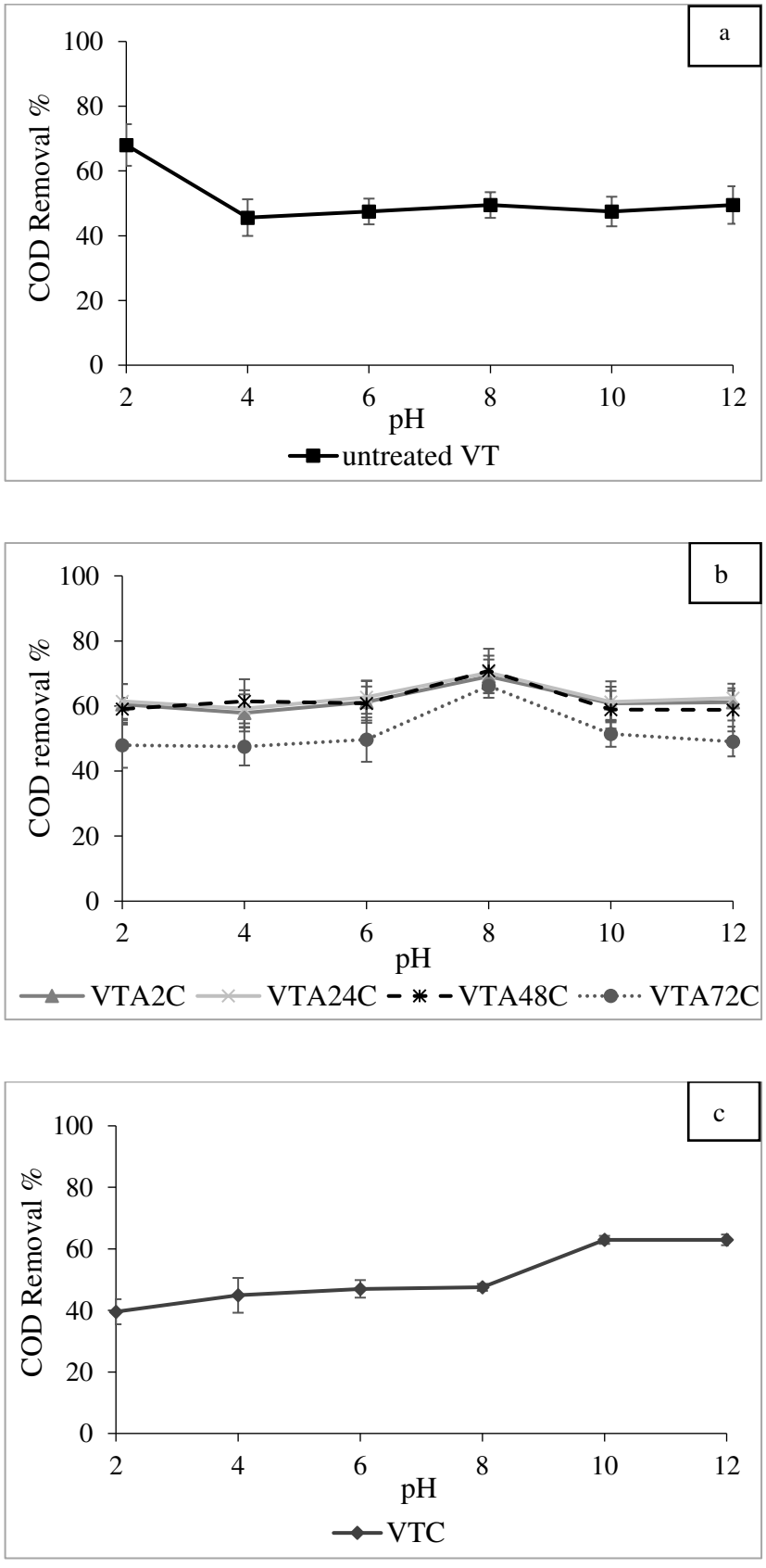

Figure 42: pH effect on the COD removal from pretreated OMW by (a) untreated VT, (b) VTA2C, VTA24C, VTA48C and VTA72C, (c) VTC

3.4.5 The Effect of Acid Impregnation Period of the VT Media on COD Removal from OMW

To increase the ability of the VT activated by combined acid impregnation and calcination, the acid impregnation period was increased to 24, 48 and 72 hr then four samples of activated VT denoted VTA2C, VTA24C, VTA48C and VTA72C were tested. All of them had the same particle size of 125-150 μm. 5% media (VT + 0.5% by weight magnetite nanoparticles) was added to pretreated OMW at pH of 5.3 and contact time of 24 hr. Figure 43 indicated that COD removal efficiencies were 52%, 61%, 63% and 49% COD removal for VTA2C, VTA24C, VTA48C and VTA72C, respectively. It's obvious that increasing the acid impregnation period from 2 hr to 24 hr enhances the ability of the VT to remove COD from OMW. This enhancement in adsorption can be attributed to the dealumination effect through activation of the VT where Si/Al ratios were 5.708 and 5.950 for VTA2C and VTA24C, respectively indicated that the hydrophobicity of the VTA24C was higher than that of VTA2C (Damjanovic et al., 2010). Additional increase in the impregnation period from 24 hr to 48 hr increased the removal efficiency slightly due to the slight increase in the Si/Al ratio from 5.950 to 6.493. The removal efficiency was decreased upon increasing the impregnation period to 72 hr due to lower surface area and Si/Al ratio of 5.5 m^2/g and 6.014, respectively. It seems that the hydrophobicity of the media is the main factor that affect the adsorption behavior followed by the surface area of the media as a minor factor.

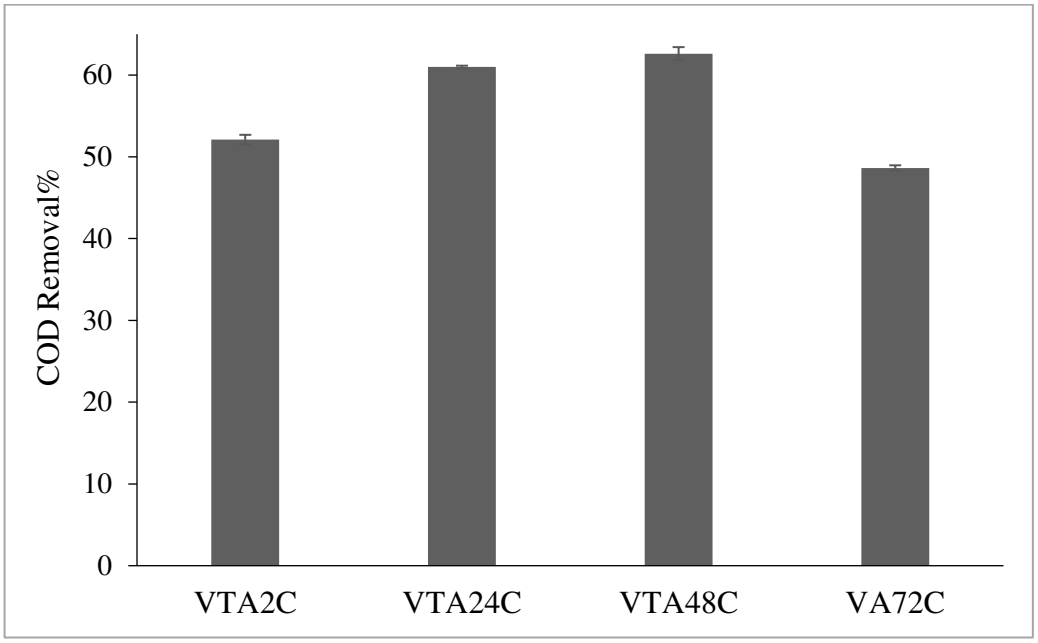

Figure 43: The effect of acid impregnation time in VT activation step on the COD removal percentage, using pretreated OMW at pH 5.3, magnetite dose 0.5% by weight and 24 hr contact time

3.4.6 The Effect of Quaternary Amine Cationic Polymer on the COD Removal

VTA24C was modified by impregnation with the quaternary amine cationic polymer (the flocculent used in the pretreatment process) denoted VTA24C-polymer and used along with VTA24C without additional modifications test. They were coupled with 0.5% magnetite nanoparticles and tested in removing COD from OMW at pH 8 and for 24 hr. The results in Table 12 show that COD removal percentages are 43% and 34% for VTA24C-polymer and VTA24C, respectively. At pH 8 it is expected that the surface of VTA24C-polymer is positively charged due to basicity of the cationic quaternary amine polymer. Then this enhancement in the COD removal at pH 8 can be attributed to electrostatic attraction between organic anions and positively charged surface (Anirudhan et al., 2008) in addition to the hydrophilic complexation reaction between organic anions and metals on the surface of VT.

On the other hand, OMW pretreated using coagulant alone (without polymeric flocculent) had adjusted to pH 8 and added to VTA24C-polymer that coupled with 0.5%

magnetite nanoparticles. The obtained result was reported in Table 12 with COD removal of 50%. Moreover, polymer was added as flocculent to OMW then after pretreatment, pH was adjusted to 8 and then subjected to VTA24C that was coupled with 0.5% magnetite nanoparticles for 24 hr. The COD removal efficiency was found to be 71%. The role of the polymer in both cases is different; in the first case (coupling the VT with the polymer), the polymer may enhance the surface properties of the VT (Anirudhan et al., 2008) thus increase the removal percentages. However, the pretreated OMW contains higher amounts of suspended solids that may compete with organic acids in the adsorption process. Moreover, OMW pretreated with coagulant alone contains higher amount of COD.

While in the second case (addition of the polymer to OMW), the polymer operated as a flocculent that enhance the removal of suspended solids that may decrease the efficiency of the adsorption process in addition to partial removal of organic compounds present in the OMW (Shammas et al., 2005).

Table 12: The effect of quaternary amine cationic polymer on the COD removal using VTA24C-polymer and VTA24C with particle size <45μm

Sample	Particle size	OMW	COD Removal %
VTA24C-polymer	<45μm	Without pretreatment	43±0.74
VTA24C-polymer	<45μm	Pretreated without polymer	50±1.10
VTA24C	<45μm	Pretreated with polymer	71±0.60
VTA24C	<45μm	Without pretreatment	34±1.70

3.4.7 The Effect of using VT/Magnetite Nanocomposites on COD Removal

VTA24C/magnetite nanocomposites and VTA24C that was mixed with magnetite nanoparticles were added to pretreated water whose pH was adjusted to 8 for 24 hr. The same ratio of magnetite nanoparticles of 0.5% by weight was used in both cases. As shown

in Figure 44, COD removal percentage of 74% was obtained for VTA24C mixed with magnetite nanoparticles. On the other hand, 57% removal was obtained for nanocomposites scenario. Although the surface area of the VTA24C/ magnetite nanocomposites is very high, the expected reason for this result is the adsorption of the magnetite nanoparticles to the surface of the VT in the nanocomposite scenario thus reducing the available surface site for COD adsorption in addition to decrease in the hydrophobicity with Si/Al ratio of 5.434 comparing with 5.950 for VTA24C. In the mixing scenario, magnetite nanoparticles and VT adsorbed COD independently without any effect on their performance.

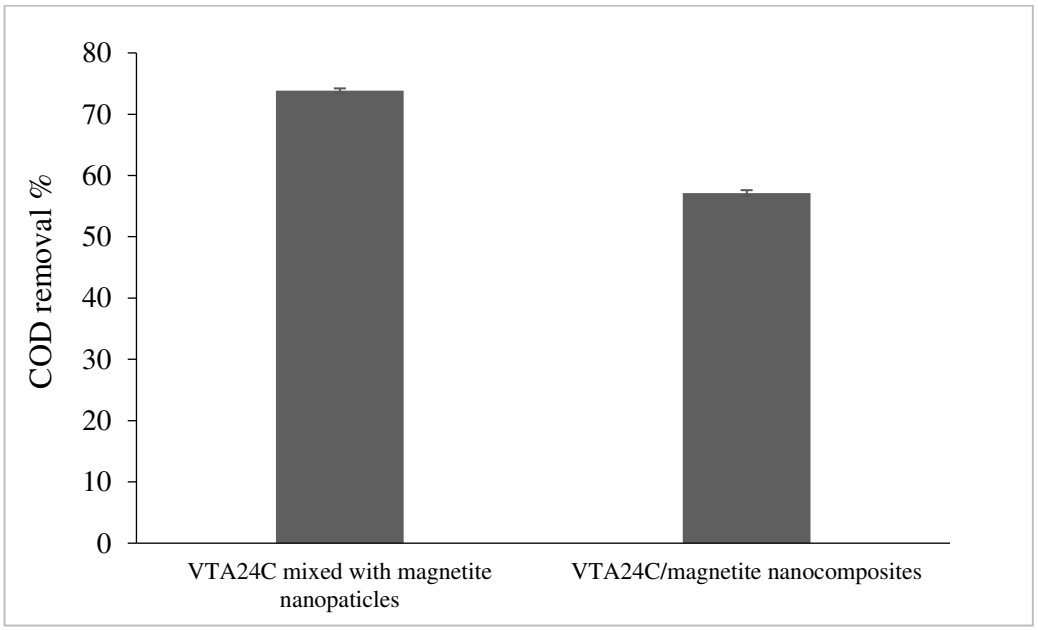

Figure 44: The effect of magnetite nanoparticles and VTA24C coupling procedures on COD removal

3.4.8 TPC and COD Removal on the Optimum Conditions for all VT Samples

To investigate the highest removal efficiencies of each adsorbent, tests were conducted at the optimum conditions of each adsorbent summarized in Table 13. Figure 45 shows that the COD and TPC removal percentages for all VT samples at the optimum conditions. The maximum TPC removal efficiency was 73% for VTC, this behavior may be due to high complexation reaction between phenolate anions at pH 10 and sufficient amount of metals on the surface of VTC as confirmed by XRF. While the minimum TPC removal efficiency was

47% for untreated VT. VT samples activated by successive acid impregnation and calcination had comparable TPC removal percentage of 60%, 61%, 61% and 59% for VTA2C, VTA24C, VTA48C and VTA72C, respectively. While the COD removal efficiencies for VTA24C and VTA48C was 75% and 76% respectively due to high hydrophobicity of these samples.

Table 13: The optimum adsorption conditions for all tested VT samples

Sample	Contact time (h)	Pretreated OMW pH	Magnetite dose (% by weight)	Particle size (µm)
Untreated VT	48	2	0	<45
VTC	48	10	0.5	<45
VTA2C	24	8	0.5	<45
VTA24C	24	8	0.5	<45
VTA48C	24	8	0.5	<45
VTA72C	24	8	0.5	<45

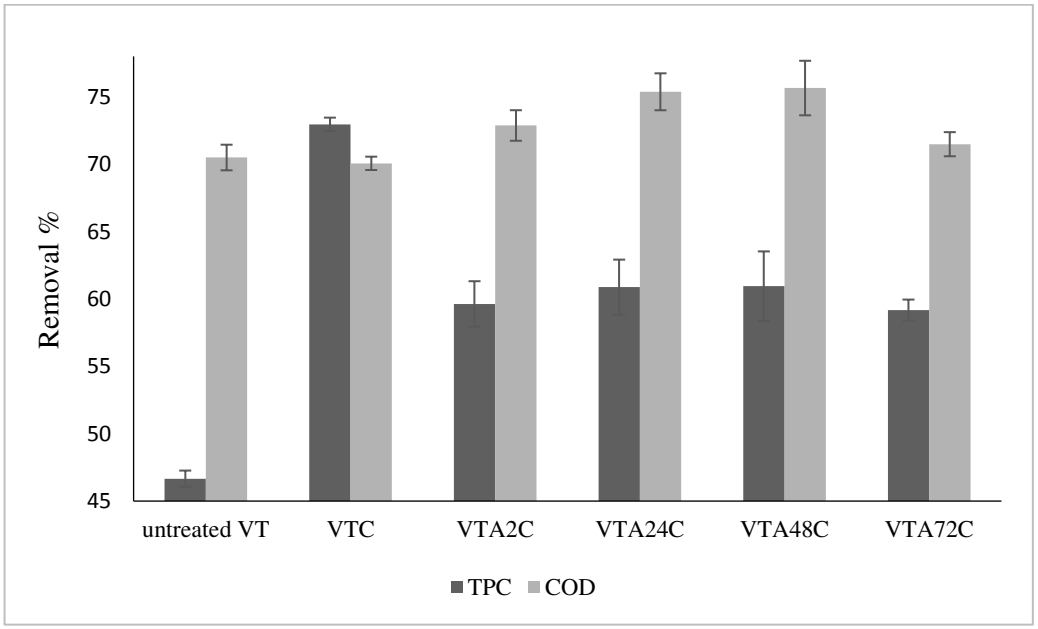

Figure 45: COD and TPC removal for all VT samples at the optimum conditions

3.4.9 The Effect of Activated GAC on TPC Removal Efficiency

Preliminary tests were conducted to investigate the removal efficiency of GAC MRX-M. It was activated through two different approaches i.e. acid impregnation and base impregnation procedures and used as adsorbent for TPC. 5% by weight of untreated, reduced and oxidized GAC samples with a particle size of 125-150 μm were investigated through preliminary batch test for TPC removal from pretreated OMW whose pH was 5.3 and for 24 hr contact time. The results presented in Figure 46 indicated that reduction of GAC is the best approach for treating TPC from OMW with removal efficiencies of 82% compared to 79% and 75% for untreated and oxidized GAC respectively. This result is expected since the surface area of reduced GAC was 924 compared to untreated and oxidized GAC (904 and 827) respectively. For that, the reduced GAC was chosen for subsequent investigations.

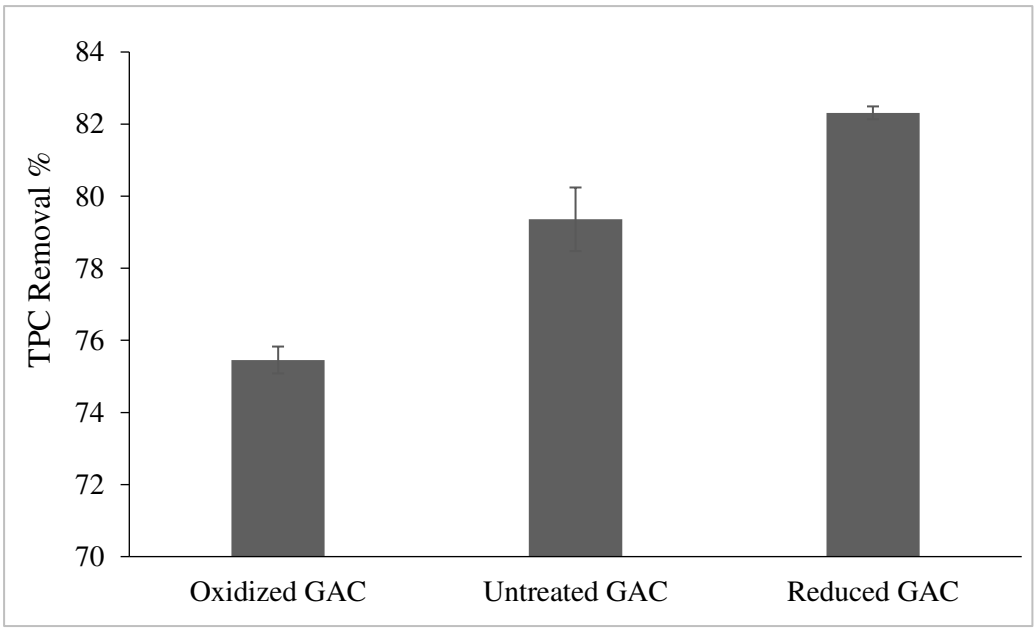

Figure 46: TPC removal efficiency for untreated, reduced and oxidized GAC at pH equal to 5.3 and contact time of 24 hr

3.4.10 The Effect of Coupling Magnetite Nanoparticles with Reduced GAC on the Removal Efficiency

Preliminary batch tests were conducted to investigate the capability of coupling reduced GAC with magnetite nanoparticles for COD removal from pretreated OMW. 5% reduced GAC with particle size range of 125-150 μm was coupled either with 1% or 0% magnetite nanoparticles and used to remove COD from pretreated OMW whose pH was 5.3 and contacted for 24 hr. As shown in Table 14, COD removal percentages were 72% and 63% for media with and without magnetite nanoparticles respectively. It's obvious that magnetite nanoparticles increases the COD removal percentage due to its vast surface area available for adsorption.

3.4.11 The Effect of Reduced GAC Particle Size on the Removal Efficiency

Reduced GAC with different particle size ranges of 125-150 μm and 38-45 μm were coupled with 1% magnetite nanoparticles and used to remove COD from pretreated water whose pH was 5.3 and left on the shaker for 24 hr. The result was consistent with our expectations that the GAC with smaller particle size has higher capability to remove COD with 88 and 72 removal percentage for the lower and higher particle size respectively (Table 14) since the surface area increased with decreasing the particle size thus increasing the ability for adsorption. Figure 47 shows the effect of the using different particle size ranges of the media and the effect of coupling the media with magnetite nanoparticles on the color of OMW.

Table 14: COD removal% for GAC samples modified chemically by base impregnation

Sample	Particle size range (µm)	Magnetite dose	pH of pretreated OMW	Contact time (hr.)	COD Removal%
GAC	125-150	1% by weight	5.3	24	72
GAC	125-150	0% by weight	5.3	24	63
GAC	38-45	1% by weight	5.3	24	88

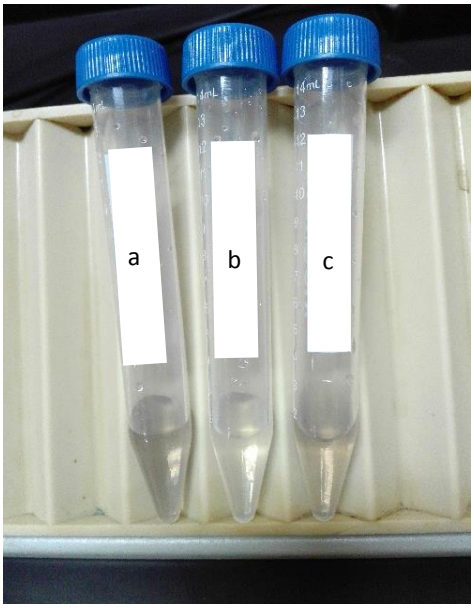

Figure 47: The effect of GAC treatment on the color of the OMW (a) GAC (125-150 µm) and 1% magnetite nanoparticles, (b) GAC (38-45 µm) with 1% magnetite nanoparticles, (c) GAC (125-150 µm) without magnetite nanoparticles

3.5 Adsorption Evaluation via Column Experiments

3.5.1 The Effect of Coupling VT with Magnetite Nanoparticles through Mixing and Nanocomposites Scenarios

The real scenario of the adsorption efficiency of each adsorbent was investigated through column experiments, with the same bed mass of 6 g, particle size < 45μm and OMW flow rate of 0.9 ml/ min. The magnetite nanoparticles dose and pH of the pretreated OMW were adjusted to the best values obtained from batch tests for each adsorbent. As shown in Figure 48, it is obvious that activation of VT doesn't increase the breakthrough time. However a significant decrease in the COD concentration was observed with VTA24C as the best adsorbent followed by VTA48C, VTA2C, VTA72C and VTC respectively. On the other hand, VTA24C/magnetite nanocomposites exhibited high efficiency at the beginning but after break through volume, its efficiency was decreased greatly. It's worth noting that this results are similar to those obtained by Nassar et al for iron oxide nanoparticles (γ-Fe_2O_3) coupled with sand (Nassar et al., 2014).

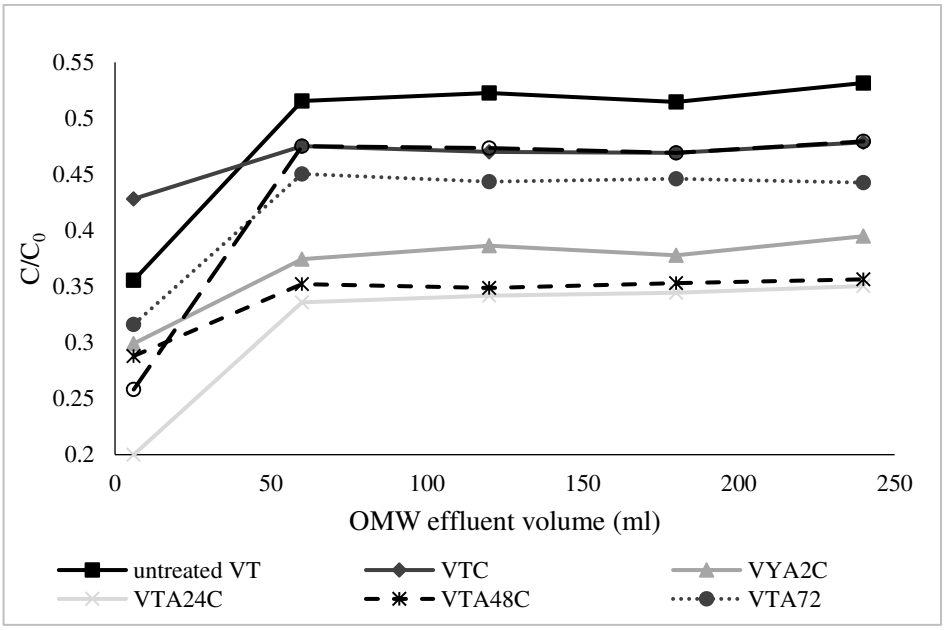

Figure 48: Breakthrough curves for all VT samples using mixing and nanocomposites scenarios

3.5.2 The Effect of Coupling GAC with VT and Magnetite Nanoparticles Through Layers Scenario

Preliminary column experiments were conducted to test the adsorption capability of reduced GAC coupled with VTA24C and magnetite nanoparticles using layers scenario. 6 g bed mass of 1:1:0.01 GAC: VTA24C: magnetite nanoparticles ratio was tested with VTA24C being in the bottom, magnetite nanoparticles in the middle and reduced GAC at the top of the column. The particle size for VTA24C and GAC was less than 45 μm, OMW flow rate was 0.9 ml/ min and the pretreated OMW pH was adjusted to 8 to optimize the adsorption of COD. Figure 49 represents the breakthrough curves obtained from the three adsorbent layers of VTA24C, magnetite nanoparticles and reduced GAC in comparison with the breakthrough curve of VTA24C mixed with magnetite nanoparticles. It's obvious from the breakthrough curves that exchange 50% of VTA24C with reduced GAC and order them in layers increased the breakthrough time and decreased in the COD concentration of OMW. Figure 50 shows the effect of using layers scenario on the color of the treated water at different effluent volumes. Further research is needed to determine the best media and conditions for OMW treatment.

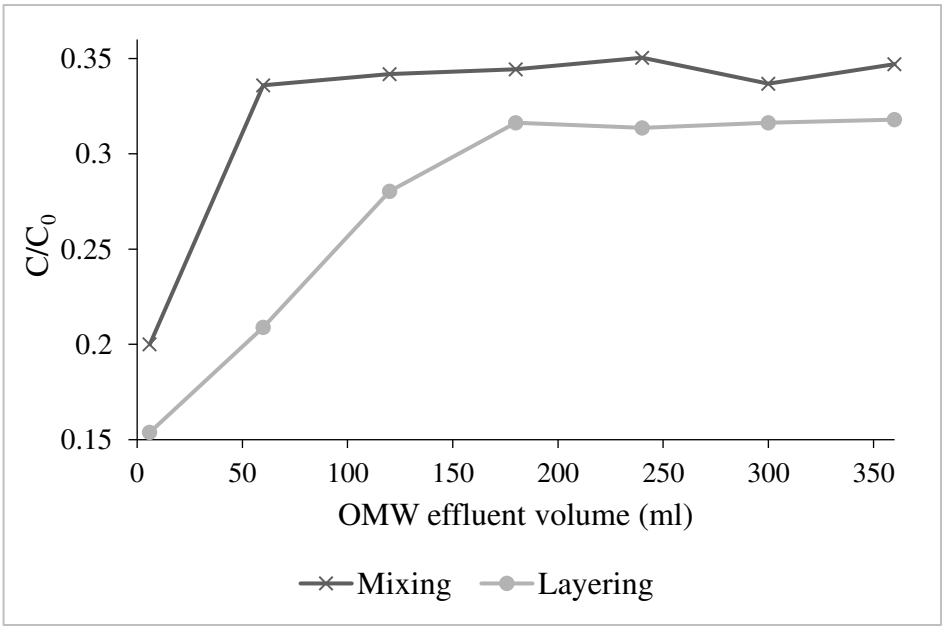

Figure 49: Breakthrough curves for mixing and layers scenarios

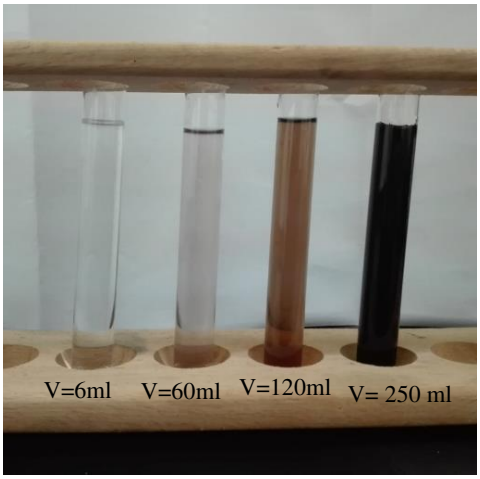

Figure 50: The effect of using layers scenario on the color of the treated water at different effluent volumes

Conclusions and Recommendations

- Pretreatment of OMW by coagulation flocculation and sedimentation processes is very important step that approximately remove all suspended solids present in OMW and approximately 50% of the organic compounds thus enhance the adsorption process.
- Activation of the VT with acid impregnation followed by calcination enhanced the adsorption properties by increasing the hydrophobicity and the surface area of the samples.
- VTA48C and VTA24C were the best adsorbents and had approximately comparable efficiency for COD removal. However, VTA48C required higher impregnation period with acid for activation thus VTA24C can considered as the most efficient and cost effective media for COD removal.
- Calcination of VT extremely enhanced the efficiency of the media for TPC removal although it required adjustment of the pH to high value of 10 and relatively long contact time of 48 hr.
- Coupling 0.5% by weight of magnetite nanoparticles with activated VT media through mixing scenario enhanced the adsorption and improve the efficiency of the media, while using nanocomposites scenario proved its ineffectiveness in the removal efficiency comparing to the mixing scenario.
- GAC had higher efficiency than VT in COD and TPC removal.

More examinations are still required and recommended for future work such as:

- Investigation of the sulfuric acid concentration effect on COD and TPC adsorption.
- Investigation of VT activation through acid impregnation using different acids i.e. nitric acid, phosphoric acid, perchloric acid…. etc.

- Optimization and investigations of the GAC modified chemically by base impregnation through batch and column i.e. coupling with VT and magnetite nanoparticles with different rations at different pH values and different contact times.
- Utilization of olive cake after chemical modifications in the treatment of OMW in order to find an integrated solution for the olive mill factories owners.
- Investigation of the capability of treating OMW using natural media under pilot scale that resemble the circumstances found in olive mill factories

References:

AbuDalo, M., Nevostrueva, S., Hernandez, M. (2013). Enhanced Copper (II) Removal from Acidic Water by Granular Activated Carbon Impregnated with Carboxybenzotriazole. *APCBEE Procedia*, 5, 64–68.

Achak, M., Elayadi, F., Boumya, W. (2019). Chemical Coagulation/Flocculation Processes for Removal of Phenolic Compounds from Olive Mill Wastewater: A Comprehensive Review. *American Journal of Applied Sciences*, 16(3), 59–91.

Aguilar, M., Saez, J., Llorens. M., Soler. A., Ortuno. J., Meseguer. V., Fuentes. A. (2005). Improvement of coagulation-flocculation process using anionic polyacrylamide as coagulant aid. *Chemosphere*, 58, 47–56.

Ahribesh, A. (2016). Synthesis, characterization and application of magnetic adsorbents based on sepiolite and zeolite. Ph.D. thesis. *University of Belgrade. Serbia.*

Al Dwairi, R. (1987). A chemical study of the palagonitic tufts of the Aritain area of Jordan, with special reference to nature, origin and industrial potential of the associated zeolite deposits. Ph.D. Thesis, *Hull University UK*.

Al Dwairi, R. (2014). Characterization of Pozzolana from Tafila area and its potential use as soil amendment for plant growth. *Jordan Journal of Earth and Environmental Sciences,* 6(3), 35-40.

Al Dwairi, R., Khoury, H., Ibrahim, K. (2009). Mineralogy and Authigenesis of Zeolitic Tuff from Tall-Juhira and Tall Amir, South Jordan. *Jordan Journal of Earth and Environmental Sciences,* 2(1), 72-83.

Alburquerque, J., Gonzalvez, J., Gracia, D., Cegrra, J. (2004). Agrochemical characterization of alprejo, a solid by product, of the two phase centrifugation method for olive oil extraction. *Bioresource Technology*, 91(2), 195-200.

Al-Malah, K., Azzam, M., Abulail, N. (2000). Olive mills effluent (OME) wastewater post-treatment using activated clay. *Separation and Purification Technology*, 20, 225–234.

Al-Tabbal, J., Ammary, B., Al-Zboon, K., Al-Zou'by J. (2015). Effect of treated industrial wastewater reuse on the germination and seedling growth of leucaena leucocephala. Proceedings of the 14th International Conference on Environmental Science and Technology Rhodes, Greece, 3-5 September 2015.

Aly, A., Hasan, Y., Al-Farraj, A. (2014). Olive mill wastewater treatment using a simple zeolite- based low- cost method. *Journal of environmental management*, 145, 341-348.

Anirudhan, T., Suchithra, P., Rijith, S. (2008). Amine–modified polyacrylamide–bentonite composite for the adsorption of humic acid in aqueous solutions. Colloids and Surfaces A: Physicochemical and Engineering Aspects, 326(3), 147–156.

Ates, A., Akgül, G. (2016). Modification of natural zeolite with NaOH for removal of manganese in drinking water. *Powder Technology*, 287, 285–291.

Ayoub, S. (2017). Management of olive by-products in Jordan. Proceeding the conference of ensuring sustainability of Jordanian olive sector. 24 April, 2017. Jordan.

Azzam, M. (2018). Olive mills wastewater treatment using mixed adsorbents of volcanic tuff, natural clay and charcoal. *Journal of Environmental Chemical Engineering*, 6(2), 2126–2136.

Azzam, M., Al-Gharabli, S., Al-Harahsheh, M., (2015). Olive mills wastewater treatment using local natural Jordanian clay. *Desalination and Water Treatment*. 53, 627–636.

Azzam, M., Al-Malah, K., Abu-Lail, N. (2004). Dynamic Post-treatment Response of Olive Mill Effluent Wastewater Using Activated Carbon. *Journal of Environmental Science and Health, Part A*, 39(1), 269–280.

Azzam, M., Al-Malah, K., Al-Gazzawi, Z., Al-Omari, S. (2010). Dynamic Treatment Response of Olive Mills Wastewater Using Series of Adsorption Steps. CLEAN - Soil, Air, Water, 38(9), 822–830.

Blatchly, R., Nircan, Z., O`Hara, P. (2017). The chemical story of olive oil from grove to table. UK: Royal society of chemistry.

Bradley, R., Baruchello, L. (1980). Primary wastes in the olive oil industry. *Effluent Water Treatment Journal*, 20(4), 176–177.

Brunauer, S., Emmett, P., Teller, E. (1938). Adsorption of Gases in Multimolecular Layers. *Journal of the American Chemical Society*, 60, 309-319.

Channei, D., Phanichphant, S., Nakaruk, A., Mofarah, S., Koshy, P., Sorrell, C. (2017). Aqueous and Surface Chemistries of Photocatalytic Fe-Doped CeO2 Nanoparticles. Catalysts, 7(12), 45.

Chen, J., Wu, S., Chong, K. (2003). Surface modification of a granular activated carbon by citric acid for enhancement of copper adsorption. Carbon, 41(10), 1979–1986.

Claudia, X., Rojas-Pavón, M., Olguín, T., Jiménez-Cedillo, M., Maubert, A. (2015). Sorption properties of modified clinoptilolite-and mordenite-rich tuffs for manganese removal from aqueous systems. *Research and Reviews in Materials Science and Chemistry,* 5(1), 29-61.

Damjanovic, L., Rakic, V., Rac, V., Stosic, D., Aurouxc, A. (2010). The investigation of phenol removal from aqueous solutions by zeolites as solid adsorbents. *Journal of Hazardous Materials*, 184, 477–484.

De'Gennaro, M., Cappelletti, P., Langella, A., Perrotta, A., Scarpati, C. (2000). Genesis of zeolites in the Neapolitan Yellow Tuff: geological, volcanological and mineralogical evidence. *Contributions to Mineralogy and Petrology*, 139, 17 –35.

Di Giacomo, G., Brandani, V., Del Re, G. (1991). Evaporation of olive oil mill vegetation waters. Proceedings of the 12th International Symposium on Desalination and Water Re use. Malta, 15–18 April 1991.

Djaeni, M., Kurniasari, L., Purbasari, A., Sasongko, S. (2010). Activation of Natural Zeolite as Water Adsorbent for Mixed-Adsorption Drying. Proceeding of the 1st International Conference on Materials Engineering. Yogyakarta Indonesia, 25-26 November 2010.

Djobo, Y. (2017). Synthesis factors, characteristics and durability of volcanic ash-based geopolymer cement. Ph.D. thesis, University of Yaoundé, Cameroon.

Drachmann, A. (1932). Ancient oil mills and presses. UK: Cambridge University Press.

Dufour, J., Marron, J., Negro, C., Latorre, R., Formoso, A., Lopez-Mateos, F. (1997). Mechanism and kinetic control of the oxyprecipitation of sulphuric liquors from steel pickling, *Chemical Engineering Journal*, 68, 173-187.

Dumitriu, E., Cobzaru, C., Hulea, V., Rotariu, A., Oprea, S., (2009). Dealuminated Natural Zeolites for Applications in Catalytic Processes with Formation of C-C Bonds. *Revista de Chimie Journal*, 60(3), 296-300.

El-Geundi, M. (1997). Adsorbents for Industrial Pollution Control. *Adsorption Science and Technology,* 15(10), 777-787.

Fiestas De Ursinos, J., Padilla, R. (1992). Use and treatment of olive mill wastewater – current situation and prospects in Spain. *Grasas Aceites Journal*, 43, 101–106.

Food and Agriculture organization of the United Nations. (2018). FAOSTAT database, Cropland (Emissions - Land Use). December 20, 2018.

Food and Agriculture organization of the United Nations. (2019). FAOSTATE database, Crops (production). January 18, 2019.

Georgacakis, D., Andreadi, E., Christopoulou, N. (2002). Exploitation of cost efficient biogas production and utilization from Greek pig farms and olive oil mill wastes. Research program report. Laboratory of Agricultural Structures, Agricultural University of Athens, Greek.

Gharaibeh, S., Rababah, A., Nishino, H. (2008). Low cost treatment and disposal of olive mill wastewater. Pollution solutions,1-2.

Ghernaout, D., Ghernaout, B. (2012). Sweep flocculation as a second form of charge neutralisation—a review. *Desalination and Water Treatment*, 44(1-3), 15–28.

Greenwood, R., Kendall, K. (1999). Electroacoustic studies of moderately concentrated colloidal suspensions. *Journal of the European Ceramic Society*. 19(4), 479–488.

Gregg S., Sing, K. (1967). Adsorption, Surface Area, and Porosity. UK: Academic Press.

Haddad, K., Jeguirim, M., Jerbi, B., Chouchene, A., Detouring, P., Thevenin, N., Ruidavets, L., Jellali, S., Limousy, L. (2017). Olive Mill Wastewater: From a Pollutant to Green Fuels, Agricultural Water Source and Biofertilizer. *ACS Sustainable Chemistry and Engineering*, 5, 8988−8996.

Hadjisavvas, S. (1992). Olive oil processing in Cyprus: From the bronze age to the Byzantine period (Studies in Mediterranean Archaeology). Cyprus: Astroms.

Hanaor, D., Michelazzi, M., Leonelli, C., Sorrell, C. (2012). The effects of carboxylic acids on the aqueous dispersion and electrophoretic deposition of ZrO_2. *Journal of the European Ceramic Society*, 32(1), 235–244.

Hariani, P., Faizal, M., Ridwan. M., Setiabudidya, D. (2013). Synthesis and properties of Fe_3O_4 nanoparticles by Co-precipitation method to removal procion dye. *International Journal of environmental science and development,* 4(3), 336-340.

Harpel, C., Kyle, P., Dunbar, N. (2008). Englacial tephrostratigraphy of Erebus volcano, Antarctica. *Journal of Volcanology and Geothermal Research*, 177, 549 –568.

Hattaab, A., Bagane, M. (2016). Removal of COD, polyphenols and color from olive mill wastewater using activated carbon. Proceedings of 3rd International Conference on Green energy and environmental engineering, *Tunisia*, 23-25 April 2016.

Hodaifa, G., Páez, J., Agabo, C., Ramos, E., Gutiérrez, J., Rosal, A. (2015). Flocculation on the treatment of olive oil mill wastewater: pretreatment. *International Journal of Chemical and Molecular Engineering,* 9(5), 645- 650.

Ibrahim, K. (1996). Geology, mineralogy, chemistry, origin and uses of the zeolites associated with quaternary tuffs of northeast Jordan. Ph.D. thesis. University of London, England.

Ibrahim, K., Hall, A. (1995). New occurrences of diagenetic faujasite in the quaternary tuffs of northeast Jordan. *European Journal of Mineralogy*, 7, 1129-1135.

Ibrahim, K., Moh'd, B., Masri, A., Al-Taj, M., Musleh, S., Alzughoul, K. (2014). Volcanotectonic evolution of central Jordan: Evidence from the Shihan. *Journal of African Earth Sciences*. 100, 541–553.

Iniotakis, N., Keutmann, W., Decken, C. (1993). Membrane filter for sepn. of poly-dispersions into continuous and dispersed phases - is a bonded powder mass on a carrier support grid providing high mechanical strength etc., useful for sepg. fluids contg. particle or oil matter. Patent DE 4210413.

Jenkins, R., De Vries, J. (1973). Practical X-ray Spectrometry, Germany; Springer-Verlag.

John, B., Sulaiman, C., George, S., Reddy, V. (2014). Total phenolics and flavonoids in selected medicinal plants from kerala. *International journal of pharmaceutical sciences,* 6(1), 406-408.

Kannan, H. (2017). Coupling activated carbon with surface active materials for olive mill wastewater treatment. MSc. *Thesis, Jordan University of Science and Technology, Jordan.*

Kapellakis, I., Tsagarakis, K., Crowther, J. (2008). Olive oil history, production and by-product management. Reviews. *Environmental Science and Biotechnology*, 7,1–6.

Kasirga, E. (1988). Treatment of olive oil industry wastewaters by anaerobic stabilization method and development of kinetic model. Ph.D. Thesis. Dokuz Eylul University, Turkey.

Khoury, H., Ibrahim, K., Al Dwairi, R. (2015) Wide spread zeolitization of the Neogene - quaternary volcanic tuff in Jordan. *Journal of African Earth Sciences*, 101, 420-429.

Khoury, H., Ibrahim, K., Ghrir, A., Ed-Deen, T. (2003). Zeolite and zeolitic tuff in Jordan. Amman: University of Jordan.

Koyama, T. (1963). Gaseous metabolism in lake sediments and paddy soils and the production of atmospheric methane and hydrogen. *Journal of Geophysical Research.* 68(13). 3971–3973.

Krug, H. (2008). Nanotechnology. (2nd Ed.). Germany: WILLY-VCH.

Lakshmanan, R. (2013). Application of magnetic nanoparticles and reactive filter materials for wastewater treatment. Ph.D. thesis, Royal institute of technology, Stockholm.

Lazarević, S., Janković-Častvan, I., Jovanović, D., Milonjić, S., Janaćković, D., Petrović, R. (2007). Adsorption of Pb^{2+}, Cd^{2+} and Sr^{2+} ions onto natural and acid-activated sepiolites. *Applied Clay Science*, 37, 47–57.

Lee, C., Robinson, J., Chong, M. (2014). A review on application of flocculants in wastewater treatment. *Process Safety and Environmental Protection*, 92(6), 489–508.

León-Félix, L., Chaker, J., Parise, M., Coaquira, J., De Los Santos Valladares, L., Bustamante, A., Morais, P. (2013). Synthesis and characterization of uncoated and gold-coated magnetite nanoparticles. *Hyperfine Interactions*, 224(1-3), 179–188.

Leouifoudi, I., Harnafi, H., Zyad, A. (2015). Olive Mill Waste Extracts: Polyphenols Content, Antioxidant, and Antimicrobial Activities. *Advances in Pharmacological Sciences*. 2015, 1-11.

Li, L., Liu, S., Junxin, L. (2011). Surface modification of coconut shell based activated carbon for the improvement hydrophobic VOC removal. *Journal of Hazardous Materials*, 192, 683-690.

Li, S., Wang, T. (1981). Volcanic Rocks. Geological Publishing House: China.

Ministry of Agriculture. (2017). Annual Report, Department of Agricultural Economy, The Hashemite Kingdom of Jordan.

Ministry of energy and mineral resources. (2015). Mineral Status and Future Opportunity, Zeolitic Tuff. The Hashemite Kingdom of Jordan.

Mitrakas, M., Papageorgiou, G., Docoslis, A., Sakellaropoulos, G. (1996). Evaluation of various pretreatment methods for olive oil mill wastewaters. *European water pollution control*, 6(6), 10–16.

Mkadem, H. Kaanane, A. Sadek, A. Altimimi, S. Crolla, A. Kinsley, C. (2014). Treatment of olive mill wastewater from traditional presses (Maâsra) using filtration and adsorption processes. *Applied Engineering in Agriculture*, 29(6), 935–941.

Moshoeshoe, M., Nadiye-Tabbiruka, M. Obuseng, V. (2017). A review of the chemistry, structure, properties and applications of zeolites. *American Journal of Materials Science*, 7(5), 196-221.

Mskay J. and Calvert R. (1990) Adsorption behavior of copper and zinc in soil: influence of pH on adsorption characteristics. *Soil Science*. l50, 513-521.

Nassar, N., Arar, L., Marie, N., Abu Ghanam, M., Dwekat, M., Sawalha, S. (2014). Treatment of olive mill based waste water by means of magnetic nanoparticles: decolourization, dephenolization and COD removal. *Environmental Nanotechnology, Monitoring & Manaement.*1-2, 14-23.

Niaounakis, M., Halvandakis, C. (2006). Olive processing waste management: Literature review and patent survey, (2nd Ed.). UK: Elsevier Ltd.

Njoum, M. (2014). Removal of total phenols compounds from Olive Mill Wastewater by using Phillipsite natural Zeolite. M.Sc. Thesis, Al-Quds University: Palestine.

Ozan Eskikaya, B., Kozak, M., Göçer, S., Akgul, V., Duyar, A., Akman, D., Cirik, K. (2017). Treatment of Olive Mill Wastewater with Coagulation Process using Different Concentrations of Iron Sulfate Treatment of Olive Mill Wastewater using Coagulation Process. *International Journal of Advances in Science Engineering and Technology*, 5(3), 4-7.

Papaphilippou, P., Yiannapas, C., Politi, M., Daskalaki, V., Michael, C., Kalogerakis, N., Fatta-Kassinos, D. (2013). Sequential coagulation–flocculation, solvent extraction and photo-Fenton oxidation for the valorization and treatment of olive mill effluent. *Chemical Engineering Journal*, 224, 82–88.

Paraskeva, P., Diamadopoulos, E. (2006). Technologies for olive mill wastewater (OMW) treatment: a review. *Journal of Chemical Technology & Biotechnology*, 81(9), 1475–1485.

Pelendridou, K., Michailides, M., Zagklis, D., Tekerlekopoulou, A., Paraskeva, C., Vayenas, D. (2014). Treatment of olive mill wastewater using a coagulation–flocculation process either as a single step or as post-treatment after aerobic biological treatment. *Journal of Chemical Technology and Biotechnology*, 49(12), 1866-1874.

Person, G. (1979). Review of the folin phenol protein quantitation method of lowry, rosebrough, farr and randall. *Analytical biochemistry*, 100, 201-220.

Petarca, L., Vitolo, S., Bresci, B. (1997). Pyrolysis of concentrated olive mill vegetation waters. Proceeding the International Conference on Biomass Gasification and Pyrolysis. UK: CPL Press.

Pliny the Elder. (1971). Natural History. Translated by H. Rackham. Heinemann Ltd.: London.

Pongchalermporn, M. (2002). Experimental investigation on ferric chloride as coagulant in water treatment process. Ph.D. *Thesis, Asian Institute of Technology, Thailand*.

Rashed, M. (2013). Adsorption Technique for the Removal of Organic Pollutants from Water and Wastewater. In: Rashed, M. Organic Pollutants-Monitoring, Risk and Treatment. Published under CC By 3.0 License.

Reddy, M., Claassen, H. (1994). Specific surface area of a crushed welded tuff before and after aqueous dissolution. *Applied Geochemistry*, 9(2), 223–233.

Rice, E., Baird, R., Eaton, A., Clesceri, L. (2012). Standard methods for the examination of water and wastewater, (22nd Ed.). USA: American public health association.

Rui, L., Daud, Z., Abdul-Aziz, A., Abdul Latiff, A. (2012). Treatment of Leachate by Coagulation-Flocculation using different Coagulants and Polymer: A Review. UK: Elsevier.

Ruiz-Méndez, M., Romero, C., Medina, E., Garcia, A., De Castro, A., Brenes, M. (2012). Acidification of Alperujo Paste Prevents Off-Odors During Their Storage in Open Air. *Journal of the American Oil Chemists' Society*. 90(3), 401-406.

Rusan, M., Albalasmeh, A., Zuraiqi, S. et al. (2015). Evaluation of phytotoxicity effect of olive mill wastewater treated by different technologies on seed germination of barley (Hordeum vulgare L.). *Environmental Science and Pollution Research*, 12(22), 9127-9135.

Ruzmanova, I. Stoller, M., Chianese, A. (2013). Photocatalytic treatment of olive mill wastewater by magnetic core titanium dioxide nanoparticles. *Chemical Engineering Transactions*, 32, 2269-2274.

Saravanakumar, K., Kumar, A. (2013). Removal of phenol from aqueous solution by adsorption using zeolite. *Academic Journals*, 8(23), 2965-2969.

Schwoyer, W. (1981). Polyelectrolytes for Water and Wastewater Treatment. UK: CRC Press, Inc.

Searle, E. (1961). The petrology of the Auckland Basalts. *New Zealand Journal of Geology and Geophysics*, 4(2), 165–204.

Shaarani, F. and Hameed, B. (2011). Ammonia-modified activated carbon for the adsorption of 2,4-dichlorophenol. *The Chemical Engineering Journal,* 169(1),180-185.

Shammas, N. (2005). Coagulation and Flocculation. In: Wang L., Hung Y., Shammas N. Physicochemical Treatment Processes. Handbook of Environmental Engineering, (3rd Ed.). UK: Humana Press.

Singleton, V., Orthofer, R., Lamuela-Raventos, R. (1999). Analysis of Total Phenols and Other Oxidation Substrates and Antioxidants by Means of Folin-Ciocalteu Reagent. *Methods in Enzymology*, 299, 152-178.

Souilem, S., El Abbassi, A., Kiai, H., Hafidi, A., Sayadi, S. Galanakis, C. (2017). Olive oil production sector: Environmental effects and sustainability challenges. In: Olive Mill Waste. Recent Advances for Sustainable Management. UK: Elsevier.

Speltini, A., Maraschi, F., Sturini, M., Caratto, V., Ferretti, M., Profumo, A. (2016). Sorbents coupled to solar light TiO_2- based photocatalysts for olive mill wastewater treatment. *International journal of photoenergy*, 2016, 1-8.

Sponza, D., Balaban, M. (2018). Treatment of Olive Mill Effluent by Nano-Zinc Oxide Magnetite. *American Journal of Nanotechnology and Nanomedicine*. 1(1), 028-042.

Steinmetz, C., (1917). Theory and Calculation of Electric Circuits. London: McGraw-Hill.

Suárez, R., Suárez-Lepe, J., Morata, A., Calderón, F. (2007). The production of ethylphenols in wine by yeasts of the genera Brettanomyces and Dekkera: A review. Food chemistry. 102(1), 10-21.

Susilawati, Nasruddin, M., Kurniawan, C., Nainggolan, I., Sihombing, Y., (2018). Ethanol Purification Using Active Natural Pahae Zeolite by Adsorption Distillation Method. *Journal of Physics: Conference Series*, 1116, 032037.

Tasdemir, A., Tasdemir, T. (2016). Determination of the Effects of Operating Parameters on the Residual Turbidity of Quartz Suspensions by Design of Experiments. *European Journal of Engineering and Natural Sciences*, 1(1), 23-32.

TDC-OLIVE project. (2004). Processing technology in olive oil and table olive. European Commission, Priority 5 on Food Quality and Safety (Contract number FOOD-CT-2004-505524 Specific Targeted Project.

Warren, B. (1969). X-ray diffraction. USA: Reading, Mass, Addison-Wesley Pub. Co.

Weckhuysen, B., Yu, J. (5015). Recent advances in zeolite chemistry and catalysis. *Chemical Society Reviews*. 44, 7022 – 7024.

Wei, Y., Han, B., Hu, X., Lin, Y., Wang, X., Deng, X. (2012). Synthesis of Fe_3O_4 nanoparticles and their magnetic properties. *Procedia Engineering Journal*. 27, 632–637.

Williams, D., Carter, C. (1996). Transmission electron microscopy: a textbook for materials science. (18^{th} Ed). New York: Plenum Press.

Yazdanbakhsh, A., Mehdipour, F., Eslami, A., Maleksari, H., Ghanbari, F. (2015). The combination of coagulation, acid cracking and Fenton-like processes for olive oil mill wastewater treatment: phytotoxicity reduction and biodegradability augmentation. *Water Science and Technology*. 71(7), 1097–1105.

Yean, S., Cong, L., Yavuz, C., Mayo, J., Yu, W., Kan, A., Tomson, M. (2005). Effect of magnetite particle size on adsorption and desorption of arsenite and arsenate. *Journal of Materials Research,* 20(12), 3255–3264.

Yousef, R., El-Eswed, B. (2009). The effect of pH on the adsorption of phenol and chlorophenols onto natural zeolite. Colloids and Surfaces A: Physicochemical and Engineering Aspects, 334(1-3), 92–99.

Zdravkov, B., Čermák, J., Šefara, M., Janků, J. (2007). Pore classification in the characterization of porous materials: A perspective. *Central European Journal of Chemistry*, 5(2), 385-395.

Appendices

Appendix (A)

Calibration curve used to estimate TPC

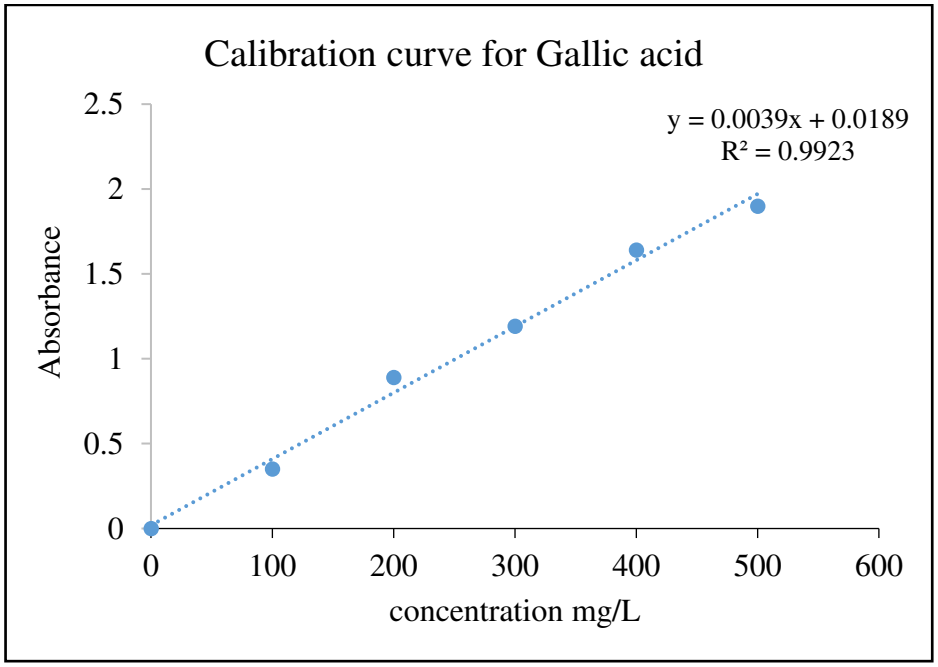

Figure A.1: Calibration curve for Gallic acid

اقتران جزيئات المغنتيت النانويه مع المواد الماصه لمعالجه مخلفات مياه معاصر الزيتون

إعداد: جهاد وليد عبد النبي

الملخص

تعتبر المياه العادمة الناتجة من معاصرالزيتون (مياه الزيبار) مشكلة بيئية حرجة في منطقة البحر الأبيض المتوسط بسبب احتوائها على تراكيز عالية من المركبات العضوية الضارة مثل الفينول ومشتقاته، حيث يتم إنتاج كميات هائلة من من مياه الزيبار سنويًا في فترة قصيرة جدًا (من تشرين اول إلى كانون اول)، التخلص منها بطرق غير مناسبة او تخزينها في المعاصر يؤدي الى مشكلة بيئية غاية بالأهمية من تلوث موارد المياه الجوفية، بالإضافة الى تاثيراتها السلبية على صحة الإنسان والحيوان عند التعرض المباشر لها، لذلك يعد التوصل لطريقة اقتصادية وفعالة لمعالجة مياه الزيبار ضرورة محلية أساسية، حيث يواجه الأردن مشكلة حرجة تتعلق بالموارد المائية وجودتها، في هذه الدراسة، تم العمل على تصنيع وتطويرمواد لامتصاص مركبات الفينول من مياه الزيبار باستخدام الطف البركاني والكربون المنشط حيث تم تنشيط هذه المواد كيميائيا، وتمت دراسة خصائص السطح لهذه العينات عن طريق قياس نقطة الشحن الصفريpH_{pzc}، مساحه ومورفولوجية السطح بالاضافه الى مكوناتها الكيميائيه باستخدام الأجهزه التالية SEM، XRD، XRF، BET، وتم ايضا تحضير جسيمات الماغنتيت النانوية بطريقة الترسيب المشترك وتشخيصها (نقطه الشحن الصفري، التمغنط، القطر الهيدروديناميكي، جهد زيتا، مورفولوجية السطح والمعادن الموجوده في الجسيمات النانويه)، لفحص كفاءة هذه المواد المصنعة في إزالة المواد القابله للاكسدة (COD) و المركبات الفينوليه (TPC)، تم معالجة المياه اوليا بعمليات التخثر / التلبد / الترسيب بهدف إزالة المواد الصلبة العالقة التي قد تعيق عمليه الامتصاص، ثم تم دمج المواد الماصه (الكربون المنشط او الطف البركاني) المعالجة وغير المعالجة مع جسيمات الماغنتيت النانوية ودراسة فعاليتها بطريقتي الخلط والعمود، كشفت النتائج التي تم الحصول عليها من هذه الدراسة أن الطف البركاني المنشط بواسطة التشريب الحمضي لمدة 48 ساعة متبوعًا بالكلسنه والمخلوط مع 0.5% من جسيمات الماغنتيت النانويه كان أفضل عينه طف بركاني لازاله COD، حيث وصلت أقصى نسبه ازالة COD الى 76٪ بعد 24 ساعة عند درجه حموضه تساوي 8، من ناحية أخرى، فإن الطف البركاني المنشَّط بالكلسنه والمخلوط مع 0.5٪ من جسيمات الماغنتيت النانوية كان أفضل مادة ماصة لمعالجة TPC بكفاءة 73٪ بعد 48 ساعة وعند درجه حموضه 10، وأظهرت النتائج الأولية كفاءة عالية للكربون المنشط المعالج كيميائيا في معالجة COD و TPC حيث حقق نسب إزالة 88٪ و 82٪، على التوالي بعد 24 ساعه وعند درجة حموضة تساوي 5.3.